NASA Tech Briefs

Official Publication of
National Aeronautics and
Space Administration
Volume 14 Number 2

Transferring Technology to
American Industry
and Government
February 1990

NASA's MSAT-X Project: Pioneering Mobile Satellite Communications

This Multimeter Actually Talks!

and Tells You What's on the Display in English •French •Spanish •Italian •German •Russian •Japanese •Chinese

**Supplied with English Voice Chip—
Other Chips Available at Extra Cost**

Thermocouple probe, model KMQSS-125G-6, $24

OMEGA's patented universal connector handle accepts standard and miniature probes. Model SDX-HHM1, $3

$349

Model HHM1 comes complete with custom DMM test leads, English voice chip, earphone, soft carrying case, 9V lithium battery, 110 Vac adaptor, fuses, two beaded wire thermocouple probes, std-to-mini transition adaptor and user's manual.

Shown Actual Size

For More Information,
Dial **(203) 359-1660**

As Shown in the Vol. 27 Temperature Handbook!

There is no meter like this meter anywhere… It talks in 8 different languages.

We Take Great Ideas . . .
& Make Them Even Better™

NEW! FREE! NOW HARDBOUND!

For Your Technical Library!

- Over 1000 Full Color Pages
- All Prices Included
- Thousands of Products
- Complete with Technical Data
- Fast Off-The-Shelf Delivery

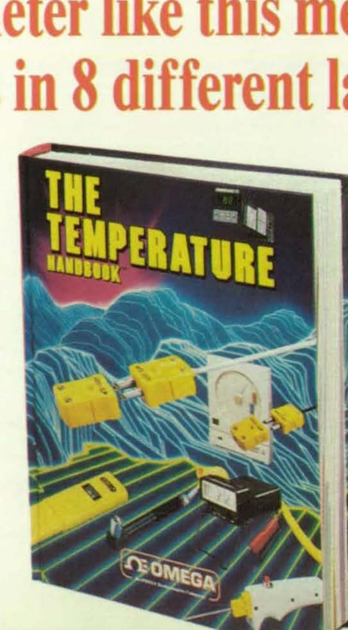

In a Hurry for Your Handbooks?
Dial **(203) 359-RUSH**
(203) 359-7874

Or Circle the Reader Service No. for your Handbook Qualification Form. (OMEGA offers 6 Technical Handbooks, with over 3500 pages.)

Temperature • Pressure • Flow and Level • pH and Conductivity • Data Acquisition Systems • Electric Heaters

OMEGA®

An OMEGA Technologies Company

One Omega Drive, Box 4047, Stamford, CT 06907
Telex 996404 Cable OMEGA FAX (203) 359-7700

Circle Reader Action No. 617

Need a Pump?

PHP-70 Series
From $179
Chemical Meter Pumps
For On/Off or Proportional Control

Pumps Come Complete with Tubing, Filter, Valves and Other Accessories.

PHP-80 Series
From $270
Heavy Duty
Chemical Metering Pumps

As Shown in the Vol. 27 Flow and pH Handbooks!

PHP-200 Series
From $512
Microprocessor Based
Chemical Metering Pumps

For More Information,
Dial **(203) 359-1660**

You'll Find it in this Handbook!

We Take Great Ideas . . .
& Make Them Even Better™

NEW! FREE! NOW HARDBOUND!

For Your Technical Library!

- Over 400 Full Color Pages
- All Prices Included
- Thousands of Products
- Complete with Technical Data
- Fast Off-The-Shelf Delivery

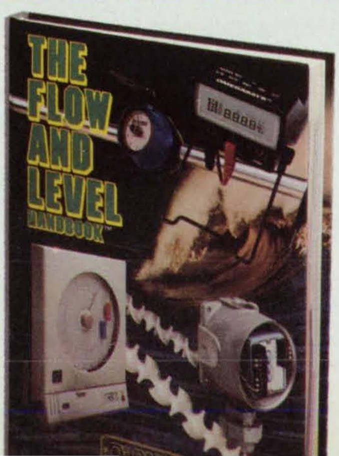

In a Hurry for Your Handbooks?
Dial **(203) 359-RUSH**
(203) 359-7874

Or Circle the Reader Service No. for your Handbook Qualification Form. (OMEGA offers 6 Technical Handbooks, with over 3500 pages.)

Temperature • Pressure • Flow and Level • pH and Conductivity
Data Acquisition Systems • Electric Heaters

OMEGA®
An OMEGA Technologies Company
One Omega Drive, Box 4047, Stamford, CT 06907
Telex 996404 Cable OMEGA FAX (203) 359-7700

Circle Reader Action No. 619

AEROSTRENGTH

OUR COMPOSITES MAKE LIGHT WORK OF STIFF REQUIREMENTS.

Major airframe manufacturers rely on the superior strength and stiffness of lightweight Hercules® graphite materials to get primary structural designs off the ground.

Consider the wing assemblies of Bell Boeing's V-22 *Osprey*. They're constructed with our high-stiffness IM6 graphite fiber and applied unidirectionally to give *Osprey* wings a greater aerodynamic shape. End result: vertical lift capability of 47,000 lbs.—three times the structural weight of the aircraft itself. IM6 fiber has also been selected for C-17 transport and A-6 fighter applications that are stiffness- and strength-critical.

Virtually the entire V-22 airframe is fabricated with Hercules composites, saving 25% in weight over metal equivalents to produce greater range, speed and payload.

Fuselage and empennage structures also incorporate our AS4 graphite fiber, formulated for high strength and delivering superior performance benefits—from increased fatigue- and corrosion-resistance to improved ballistic tolerance and enhanced crashworthiness.

If you want to get innovative structural designs off the ground and into the air, go with the strength of Hercules. We're the world's leading producer of advanced composites and can meet the stiffest challenges.

Contact: Hercules Aerospace Company, Composite Products Group, P.O. Box 98, Magna, UT 84044 U.S.A. (801) 251-5372, FAX: (801) 251-3268, Telex: 289972 Hercules SLC.

In Europe: Hercules Aerospace—Europe, Composite Products Group, 3, Rue Eugene & Armand Peugeot, 92508 Rueil-Malmaison Cedex, France (1) 47-51-29-19 Fax: (1) 47-08-50-75

HERCULES

Circle Reader Action No. 488

A Hercules Incorporated Company

NASA Tech Briefs
Transferring Technology to
American Industry and Government

FEBRUARY 1990
Volume 14 Number 2

ABP BPA

SPECIAL FEATURES

Photo Courtesy NASA

Under NASA's Mobile Satellite Experiment (MSAT-X) program, Jet Propulsion Laboratory is developing directional vehicle antennas, mobile radios, and other ground segment equipment for mobile satellite systems. The above photo shows an MSAT-X electronically-steered antenna mounted on a demonstration vehicle. The antenna is designed to track a geostationary satellite while the vehicle moves about, changes direction, and experiences signal fading. See page 12.

TECHNICAL SECTION

DEPARTMENTS

On The Cover: Conceptual drawing of a mobile satellite antenna undergoing flight tests on the space shuttle. Future mobile communications satellites will have large multiple-beam antenna systems capable of providing blanket coverage of an entire continent.
(Illustration courtesy NASA)

Illustration courtesy NASA

The next generation of communications satellites will extend mobile telephone services to remote ground users and to users in the air and at sea who cannot be served by cellular telephone systems. Turn to page 12.

NASA Tech Briefs, ISSN 0145-319X, USPS 750-070, copyright © 1990 in U.S., is published monthly by Associated Business Publications Co., Ltd. 41 E. 42nd St., New York, NY 10017-5391. The copyrighted information does not include the individual Tech Briefs which are supplied by NASA. Editorial, sales, production and circulation offices at 41 E. 42nd Street, New York, NY 10017-5391. Subscriptions for non-qualified subscribers in the U.S., Panama Canal Zone, and Puerto Rico, $75.00 for 1 year; $125.00 for 2 years; $200 for 3 years. Single copies $10.00. Remit by check, draft, postal or express orders. Other remittances at sender's risk. Address all communications for subscriptions or circulation to NASA Tech Briefs, 41 E. 42nd Street, New York, NY 10017-5391. Second-class postage paid at New York, NY and additional mailing offices.

POSTMASTER: please send address changes to NASA Tech Briefs, 41 E. 42nd Street, Suite 921, New York, NY 10017-5391.

PHILIPS

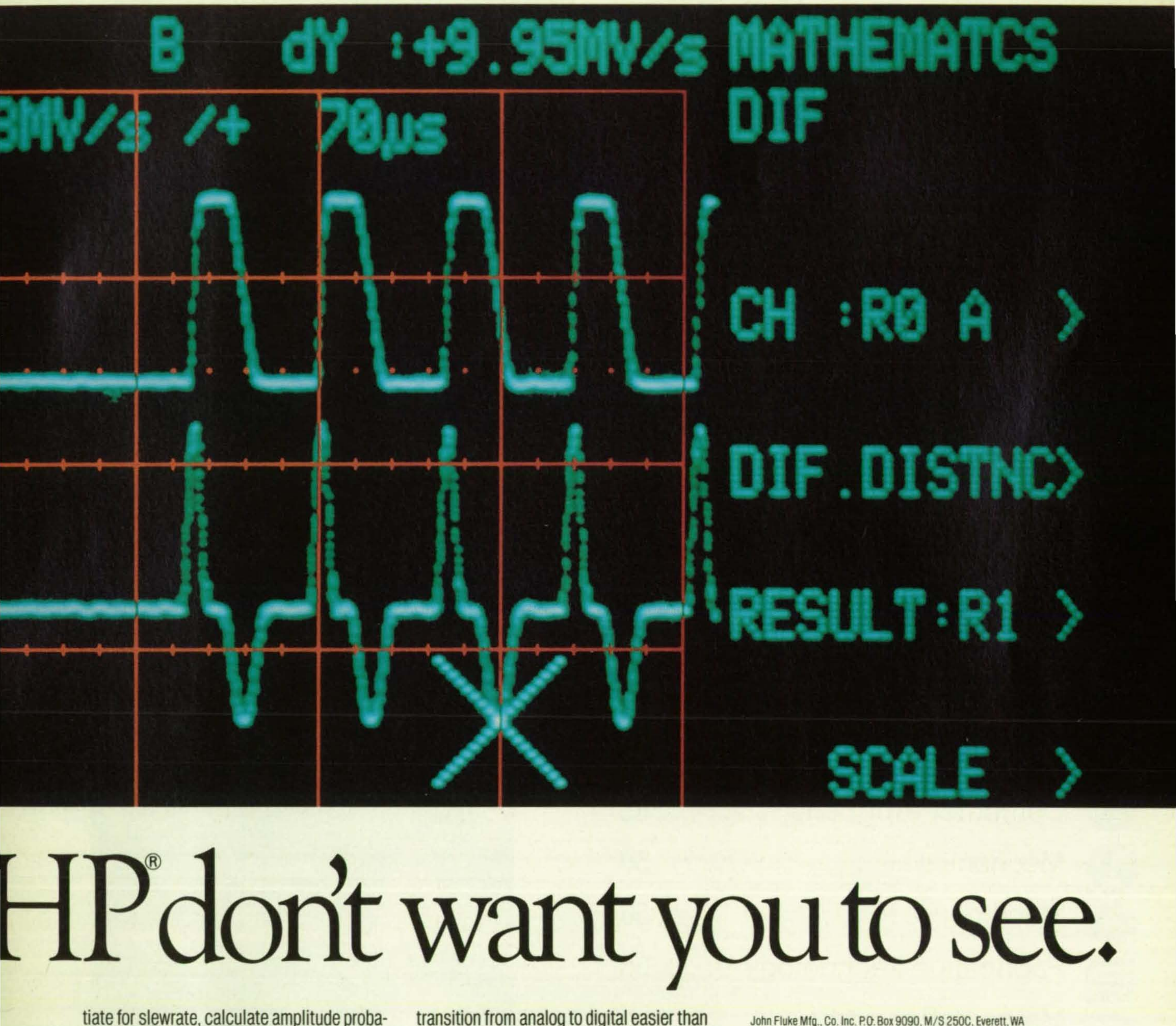

HP® don't want you to see.

tiate for slewrate, calculate amplitude probability, even FFTs to show frequency domain. And there's no need for an external computer.

Plus, memory sufficient for 251 front panel setups makes automation easy.

See the difference. Only from Fluke.

At only $7,750, the PM 3323 is just one of the talented DSOs from Fluke offering superior specs for unparalleled performance and value.

See them all, including our medium frequency combination digital/analog scopes which make the transition from analog to digital easier than ever, by sending for our free video titled "DSOs With a Difference: Chapter II." Just fill out and mail the postage paid card provided, or call **1-800-44-FLUKE, ext. 77.**

Features	Fluke PM 3323	Tek® 2440	HP® 54502A
Speed	300 MHz 500 MS/s	300 MHz 500 MS/s	100 MHz real time, 400 MHz repetitive 400 MS/s
Vertical Resolution	10 bits	8 bits	6 bits
Glitch Capture	Yes	Yes	No
Stop/Save on Difference	Yes	Yes	No
Analysis Functions (Int., Diff., Hist., Filter, FFT)	Yes	No	No
Math Functions (add, subtract, multiply, divide)	Yes	Multiply only	Yes
Measurement Functions (RMS, Freq., etc.)	Yes	Yes	Yes

FLUKE

Circle Reader Action No. 668

NASA Tech Briefs

Official Publication of
National Aeronautics and
Space Administration

ABP BPA

NASA Tech Briefs:

Published by .... **Associated Business Publications**
Editor-in-Chief/Publisher .... **Bill Schnirring**
Associate Publisher .... **Frank Nothaft**
Editor .... **Joseph T. Pramberger**
Managing Editor .... **R. J. Laer**
Assistant Editor .... **Theresa M. Detko**
Technical Advisor .... **Dr. Robert E. Waterman**
Production Manager .... **Rita Nothaft**
Traffic Manager .... **James E. Cobb**
Circulation Director .... **Anita Weissman**
Advertising Coordination Manager .... **Maya Falek**
Telecommunications Specialist .... **Evelyn Mars**
Reader Service Manager .... **Sylvia Valentin**

Briefs & Supporting Literature:
Provided to National Aeronautics and Space Administration by **International Computers & Telecommunications, Inc.,** NY, NY with assistance from **Logical Technical Services,** NY, NY
Technical/Managing Editor .... **Ted Selinsky**
Art Director .... **Ernest Gillespie**
Administrator .... **Elizabeth Texeira**
Chief Copy Editor .... **Lorne Bullen**
Staff Writers/Editors .... **Dr. James Boyd, Dr. Larry Grunberger, Dr. Theron Cole, Jordan Randjelovich, George Watson, Oden Browne**
Graphics .... **Luis Martinez, Vernald Gillman, Charles Sammartano**
Editorial & Production .... **Bill Little, Ivonne Valdes, Frank Ponce, Susan Finelli**

NASA:
NASA Tech Briefs are provided by the National Aeronautics and Space Administration, Technology Utilization Division, Washington, DC:
Administrator .... **Richard H. Truly**
Assistant Administrator for Commercial Programs ..... **James T. Rose**
Deputy Assistant Administrator (Programs) .... **Henry J. Clarks**
Deputy Director TU Division (Publications Manager) ... **Leonard A. Ault**
Manager, Technology Utilization Office, NASA Scientific and Technology Information Facility .... **Walter M. Heiland**

Associated Business Publications
41 East 42nd Street, Suite 921, New York, NY 10017-5391
(212) 490-3999 FAX (212) 986-7864
President .... **Bill Schnirring**
Executive Vice President .... **Frank Nothaft**
Vice President .... **Domenic A. Mucchetti**
Operations Manager .... **Rita Nothaft**
Controller .... **Felecia Lahey**

Advertising:
New York Office: (212) 490-3999 FAX (212) 986-7864
National Sales Manager .... **James G. McGarry**
Regional Sales Manager (Mid-Atlantic) .... **Michelle Larsen**
Account Executive .... **Debby Crane** at (201) 967-9838
Account Executive (Midwest, Northwest) .... **Paul Lesher, C.B.C.** at (708) 501-4140
Account Executive (South-Central) .... **Douglas Shaller** at (212) 490-3999
Account Executives (Eastern MA, NH, ME, RI) .... **Paul Gillespie** at (508) 429-8907; **Bill Doucette** at (508) 429-9861
Account Executives (Western MA, CT, VT) .... **George Watts** or **David Haggett** at (413) 253-9881
Account Executives (Southeast) .... **Newton Collinson** or **Jonathan Kiger** or **Lawrence Mischik** at (404) 939-8391
Account Executives (Calif., AZ, NV, NM) ....
for Area Codes 818/213/805 —**Thomas Stillman**
for Area Codes 408/415/916/209 —**Elizabeth Cooper**
and for Area Codes 619/714 —**Karen Mock** at (213) 372-2744

NTBM-Research Center
Account Supervisor .... **Lourdes Del Valle**

After centuries of practice, mankind perfects engineering calculations: MathCAD.

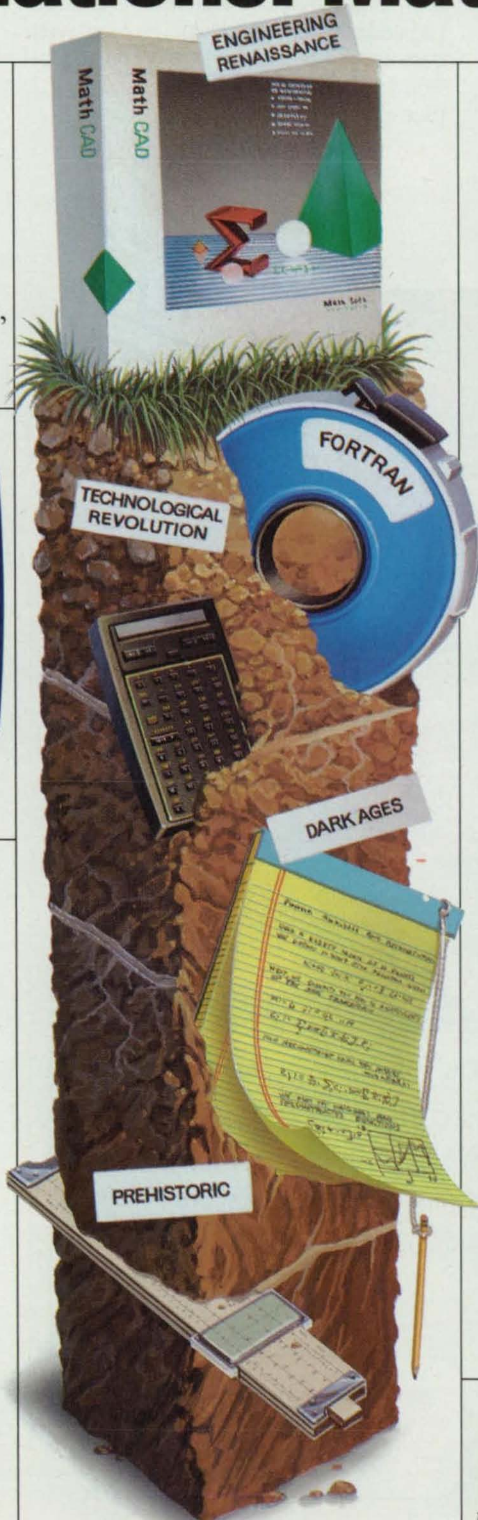

Announcing MathCAD 2.5: The Dawn of a New Age.

What the historians will call it, only time will tell.

Perhaps the Century of Speed, or the Era of Ease. But whatever the name, this is the age of MathCAD 2.5, the only math package that looks and works the way you think.

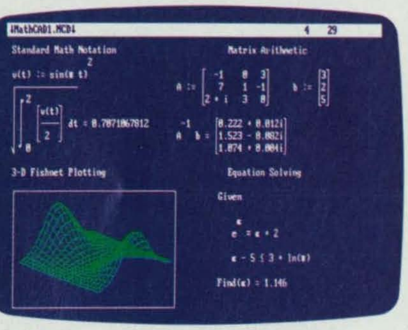

MathCAD 2.5 includes 3-D plotting, HPGL sketch import, and PostScript output.

MathCAD is far and away the best-selling math package in the world. Because it lets you perform engineering and scientific calculations in a way that's faster, more natural and less error-prone than the way you're doing them now—whether you're using a scratchpad, calculator, spreadsheet or program that you wrote yourself.

And now we've made the best even better. MathCAD 2.5 is a dramatically improved version that includes three-dimensional plotting, enhanced numerical analysis, and the ability to import HPGL files from most popular CAD programs, including AutoCAD.® And now you can print on PostScript® compatible printers.

And like before, MathCAD's live document interface™ lets you enter equations anywhere on the screen, add text to support your work, and graph the results. Then print your analysis in presentation-quality documents.

It has over 120 commonly used functions built right in, for handling equations and formulas, as well as exponentials, differentials, cubic splines, FFTs and matrices.

No matter what kind of math you do, MathCAD 2.5 has a solution for you. In fact, it's used by over 60,000 engineers and scientists, including electrical, industrial, and mechanical engineers, physicists, biologists, and economists.

But don't take our word for it; just ask the experts. PC Magazine recently described MathCAD as "everything you have ever dreamed of in a mathematical toolbox."

PC MAGAZINE EDITOR'S CHOICE
March 14, 1989 issue.
Best of '88
Best of '87

And for Macintosh® users, we present MathCAD 2.0, rewritten to take full advantage of the Macintosh interface. Entering operators and Greek letters into equations is pure simplicity!

Look for MathCAD 2.5 at your local software dealer, or give us a call. For more information, a free demo disk, or upgrade information, dial 1-800-MATHCAD (in MA, 617-577-1017).

Available for IBM® compatibles and Macintosh computers.

TM and ® signify manufacturer's trademark or manufacturer's registered trademark respectively.

MathCAD®

MathSoft, Inc. One Kendall Square, Cambridge, MA 02139

22

U.K.: Adept Scientific 0462-480055; **France:** ISE CEGOS 1-46092768; **Germany:** Softline 07802-4036; **Japan:** CRC 03-665-9768. *PE*

Circle Reader Action No. 628

New Product Ideas

New Product Ideas are just a few of the many innovations described in this issue of *NASA Tech Briefs* and having promising commercial applications. Each is discussed further on the referenced page in the appropriate section in this issue. If you are interested in developing a product from these or other NASA innovations, you can receive further technical information by requesting the TSP referenced at the end of the full-length article or by writing the Technology Utilization Office of the sponsoring NASA center (see page 16). NASA's patent-licensing program to encourage commercial development is described on page 16.

Shape Gauge Measures Surfaces

Roundness, perpendicular deviation, or slope of the surface can be determined by an optical/mechanical/electronic system that acts as a shape gauge by taking measurements of machine-tool motions or complicated contours of objects. The measured data can be processed into maps or profiles indicative of the shapes.
(See page 52)

Graphite/Thermoplastic-Pultrusion Die

A thermoplastic-pultrusion die produces a hot-melt thermoplastic-impregnated graphite prepreg tape for subsequent use in lamination or molding. This simple attachment to a commercial extruder should enable developers of composites to begin experimenting with large numbers of proprietary resins, fibers, and hybrid composite structures.
(See page 59)

Mechanically-Steered, Mobile Satellite-Tracking Antenna

An L-band, mechanically-steered, medium-gain antenna is part of the prototype radio equipment mounted in a vehicle to demonstrate the concept of a land-mobile/satellite communication system. The system will provide such services as mobile telephone, voice or alphanumeric dispatch, paging, position-location information, and low-rate data transmission.
(See page 24)

Integrated Optoelectronic Interface

A proposed integrated optoelectronic interface would be made as a "master" integrated-circuit chip. The interconnections between the component circuits on the chip could be selected to choose any of the operating modes and configurations such as simplex transmitter or receiver, duplex transceiver, digital repeater, or analog repeater.
(See page 33)

Printed-Circuit Cross-Slot Antenna

A balanced feed configuration minimizes the coupling between the slots of a printed-circuit cross-slot antenna unit. Units of this type could be elements of phased-array antennas for radar, mobile/satellite communications, and other applications that require flush mounting and/or rapid steering of beams with circular polarization.
(See page 26)

Aerospace Food Tray

A tray provides restraint and thermal insulation for modular packages of food. This tray may become useful for serving meals in airplanes, boats, hospitals, and facilities that care for children.
(See page 72)

ANOTHER ASTRO-MED FIRST IN 8-CHANNEL RECORDERS

LASER PRINTER RESOLUTION!

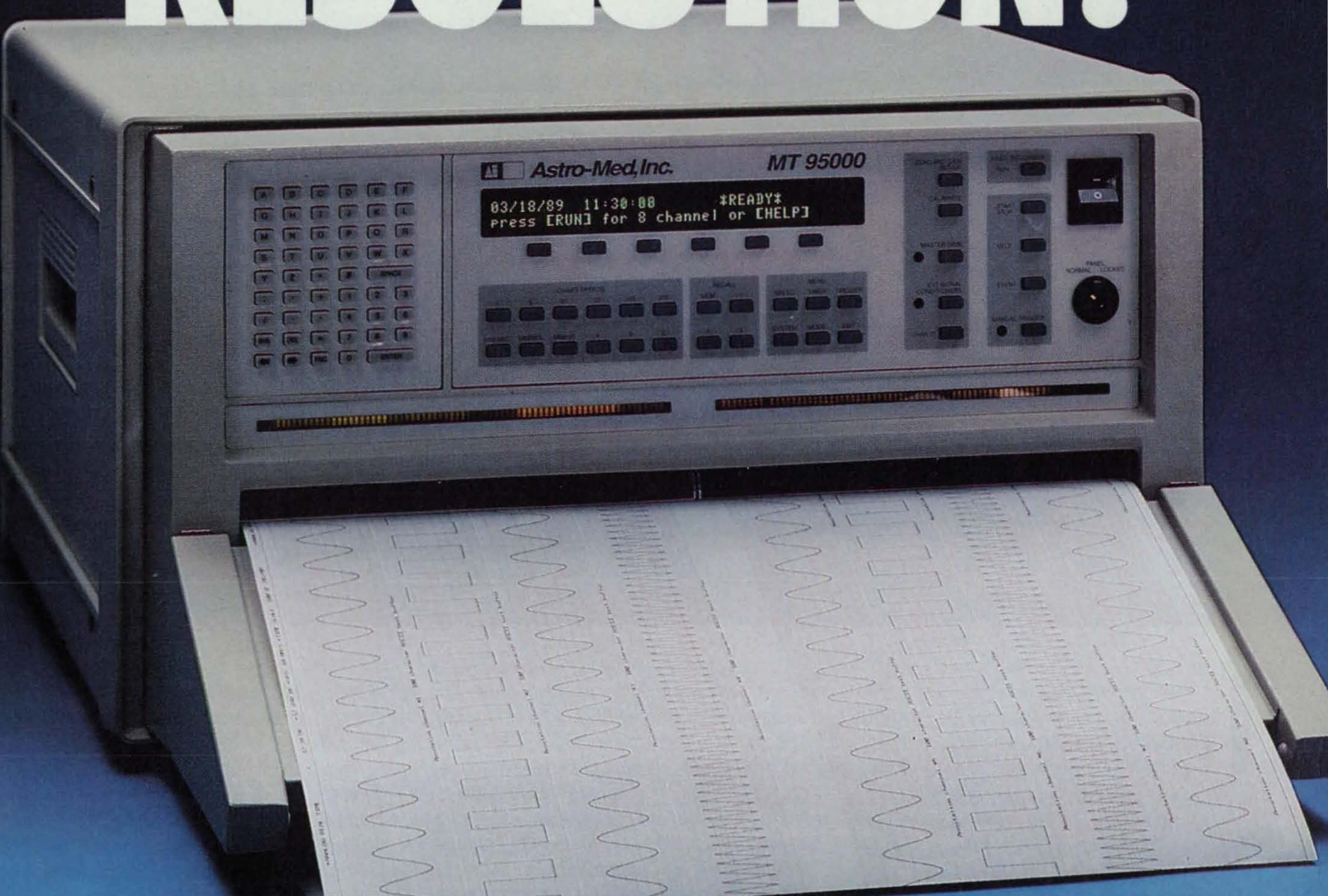

- **Laser Quality Writing–300 dpi**
- **20 kHz Frequency Response**
- **Automatic Self-Calibration–Traceable to NBS**
- **Expandable to 16 Channels**
- **Data Capture with 200 kHz Sample Rate Per Channel**
- **Built-In Programmable Signal Conditioners**

From its laser-sharp charts to its unparalleled frequency response, this remarkable new 8-channel recorder brings you the technology of the Twenty-First Century today! It outperforms even Astro-Med's MT-9500, which in 1987 was heralded as the first breakthrough in 8-channel recorders in 20 years. It has 50% more resolution, 4 times higher frequency response, and 8 times more memory than the MT-9500. With automatic self-calibration traceable to NBS, expandability to 16 channels, and a host of other important features. We call it the MT-95000, a product so unique that it is protected by U.S. Patent No. 4,739,344.

Phone, Fax or Write for details!

Astro-Med, Inc.®

Astro-Med Industrial Park, West Warwick Rhode Island 02893
Telephone (401) 828-4000 • Toll Free 800-343-4039
Telex No. 710-382-6409 • Fax (401) 822-2430

Circle Reader Action No. 405

The MSAT-X Project: NASA Explores Advanced Communications Technologies

JPL researchers are developing advanced ground segment technologies and techniques for mobile communications via satellite.

Illustration courtesy NASA

In the coming decade, a new generation of communications satellites will bring people and businesses together as never before. Mobile satellite service (MSS) will enable mobile users to transmit and receive digitized voice and data from their cars, airplanes, or ships anywhere in the continental United States (CONUS). And the ground equipment will be small and inexpensive.

While similar to terrestrial mobile systems in which users can make calls while within line of sight of relay towers, the satellite system, with its "relay tower" at an altitude of 22,300 miles (36,000 km), will provide uninterrupted blanket coverage of CONUS. In addition to planes in flight and ships at sea, the system could serve private drivers, cross-country trucks, forestry personnel, and law-enforcement agents.

NASA, through its Mobile Satellite Experiment (MSAT-X) program, is paving the way for the introduction and future growth of this new communications network. In cooperation with US industry and universities, NASA's Jet Propulsion Laboratory (JPL) is developing advanced ground segment technologies that will make efficient use of precious spectrum resources and satellite power. Areas of research include directional vehicle antennas, speech compression techniques, digital modems, network architecture, and multiple-access schemes.

Satellite-Tracking Antennas

JPL and its contractors have developed L-band medium-gain (10-12 dB) directional vehicle antennas that will alleviate the spacecraft power burden by providing higher gain than broad-beam omnidirectional antennas and enable two regional satellites to operate in the same frequency band, effectively doubling the available spectrum. They have created highly accurate and robust beam pointing systems that can acquire and maintain pointing towards the satellite while the vehicle moves about, changes direction, and experiences signal degradations due to multipath fading and foliage shadowing. In order to track the satellite as the vehicle moves, the antenna beam must be capable of azimuth rotation, either mechanically by antenna rotation or electronically by adjusting the phases in a phased antenna array.

Prototype antennas developed under MSAT-X include two electronically-steered planar phased arrays built by Ball Aerospace Corp. and Teledyne Ryan Electronics, a mechanically-steered tilted array antenna developed in-house at JPL, and a hybrid mechanically/electronically-steered planar array, also built by Teledyne. The electronically-steered antennas offer the advantages of low profile (1" height) and excellent beam-scan agility at the expense of higher production costs, which are mainly due to the cost of parts and labor needed to assemble and test the antenna phase shifters and associated driver circuits. JPL's mechanically-steered antenna

would be less costly to manufacture, but its 6" height makes it impractical for mounting on passenger cars. The hybrid model "offers a middle ground," according to Richard Emerson, JPL's deputy task manager for MSAT-X. "The production costs are moderate and it has a low profile like the phased arrays," he explained.

Telephone-Quality Speech

A major goal of the MSAT-X program is the attainment of near-toll-quality speech at a 4800 bits-per-second (bps) speech compression rate. Under contract to JPL, the Georgia Institute of Technology and the University of California at Santa Barbara have developed inexpensive, compact speech coders which, in flight and ground-based tests, have demonstrated "naturalness and good speaker identification," according to Emerson. Although the basic coder performance approaches the near-toll-quality goal, Emerson said refinements are still needed in intelligibility and in the rejection of background noise.

A companion effort to the voice compression experiments looks to develop advanced modulation techniques capable of transmitting 4800 bps in a narrow 5-kHz fading channel. JPL researchers have constructed a 4800-baud digital modem that processes octuple differential-phase-shift-keyed (8-DPSK) trellis-coded modulation. In conjunction with the multi-level signaling, pulse shaping is employed to achieve spectral efficiency.

The modem's processing algorithms enable it to freewheel through long, deep fades and recover rapidly. In one experiment using a fading channel simulator, JPL researchers disconnected the signal for five seconds during the middle of a long data transmission. The modem symbol timing stayed in lock and the correct number of symbols were received. Moreover, throughout the entire experiment hundreds of millions of symbols were sent and received and the modem recovered all symbols, with few errors.

The Network Architecture

One of JPL's most challenging assignments has been to design a network architecture and multiple-access scheme for mobile satellite communications. The network design is complicated by the uncertainty about the locations of subscribers roaming over a vast geographical area, the multipath fading that constantly works against the reliability of transmission, and the propagation delay of satellite systems. Furthermore, the traffic in such a system will not be homogeneous. Some users will need short-burst transmissions typical of interactive data transactions, while others will want open-end channel assignments for conversations.

JPL's network design is partially based on the seven-layer open-system-interconnection model suggested by the International Standards Organization. In this model, each layer performs a specific set of functions that enhances those performed by the lower layers. The layered structure allows for modular designs of communications networks so that a technological improvement in one layer will not necessitate redesigning the entire network. This flexibility is crutial in the design of a large-scale, evolving mobile satellite network.

While higher-level protocols are application-dependent, the lowest three layers — the physical, data-link, and network layers — form the skeleton of any network. The physical layer is concerned with transmitting and receiving coded information symbols and includes link hardware such as modems and codecs. The data-link layer accommodates the multiple-access protocol; all channel requests and assignments are handled here. While the data-link layer provides a communications path between two network elements in a single satellite hop, the network layer handles communications requiring multiple satellite hops, such as for conversations between two mobile users.

JPL's Integrated Adaptive Multiple-Access Protocol (I-AMAP) represents one design of the second-layer protocol. It defines the interactions between various network elements and the network management center (NMC), which dynamically allocates network resources among its elements. The NMC maintains a pool of channels; a subscriber who wants access to the network forwards a request through designated signaling channels to the management center, which will then assign an information channel for the user to transmit and receive voice or data. Once the user has finished the information transfer, the channel is returned to the pool for reassignment.

A modified ALOHA random-access scheme has been used to make connection requests during MSAT-X field experiments. In the pure ALOHA protocol, a land station transmits a message as soon as it is generated. If the station does not receive a positive acknowledgment during a specified time, it waits a random interval and then attempts transmission again. The modified ALOHA protocol is based on the assumption that it will be necessary in a fading channel to repeat during many transmission attempts. Rather than waste the timeout and waiting periods, the modified ALOHA specifies that at each transmission attempt the message is to be repeated a fixed number of times without interruption. The aim is to reduce message delay and increase channel throughput. JPL is also investigating a collision-resolution-based free-access protocol that promises a 40-percent increase in throughput over the ALOHA protocol for three or more request channels.

The channel assignment process is different for data and voice users. Data connections are made on a queued basis. Upon receiving a connection request, the NMC selects the data channel with the smallest backlog. It then assigns that channel to the subscriber for a specific period of time in the future. Since the data need not be delivered in real time, Automatic Repeat Request error-control techniques can be applied to improve the connection's fidelity.

Voice connections are open-ended; the duration of the connection is not specified at the time the call is initiated. In addition, voice connections are in real time so that only a fixed delay equal to the propagation time occurs between a transmission and its delivery. This real-time requirement limits error control to either improvement of the physical link or forward error correction.

Testing The Technology

The first field test of MSAT-X equipment in a true satellite land-mobile environment was conducted last summer in Southeastern Australia. The joint experiment between JPL and AUSSAT, the Australian national satellite system, used the Japanese Experimental Technologies Satellite (ETS-V) to demonstrate MSAT-X data and voice links and characterize their performance over the land-mobile satellite link. The experiments involved communications between a base station at AUSSAT Headquarters in Sydney and a mobile terminal mounted in a van traveling between Sydney and Brisbane. The terminal communicated principally through the ETS-V using either the JPL mechanically-steered antenna or the Teledyne electronically-steered antenna. Routes followed by the mobile unit took it behind trees, under bridges, and around other

The transmit antenna used for MSAT-X/ AUSSAT land-mobile satellite experiments in Australia

Photo courtesy NASA

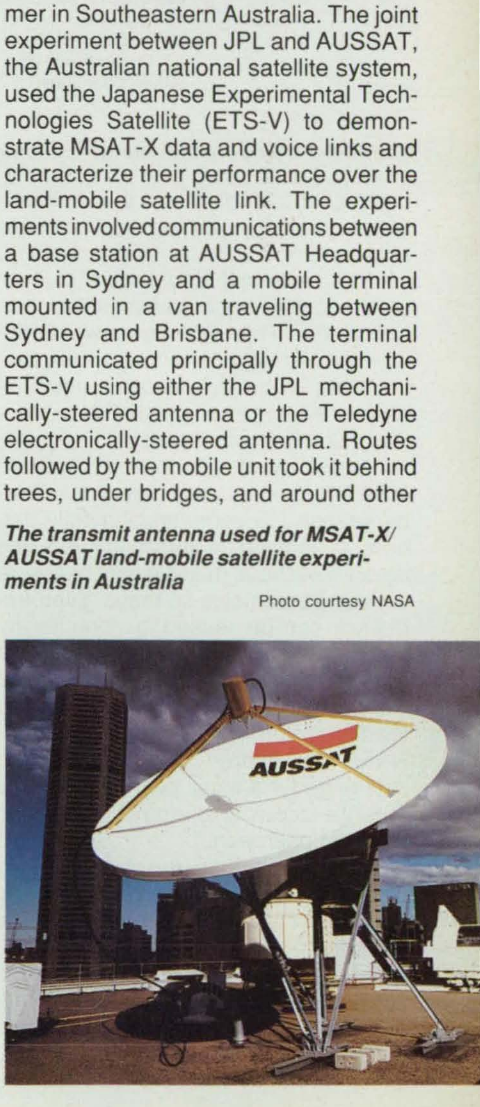

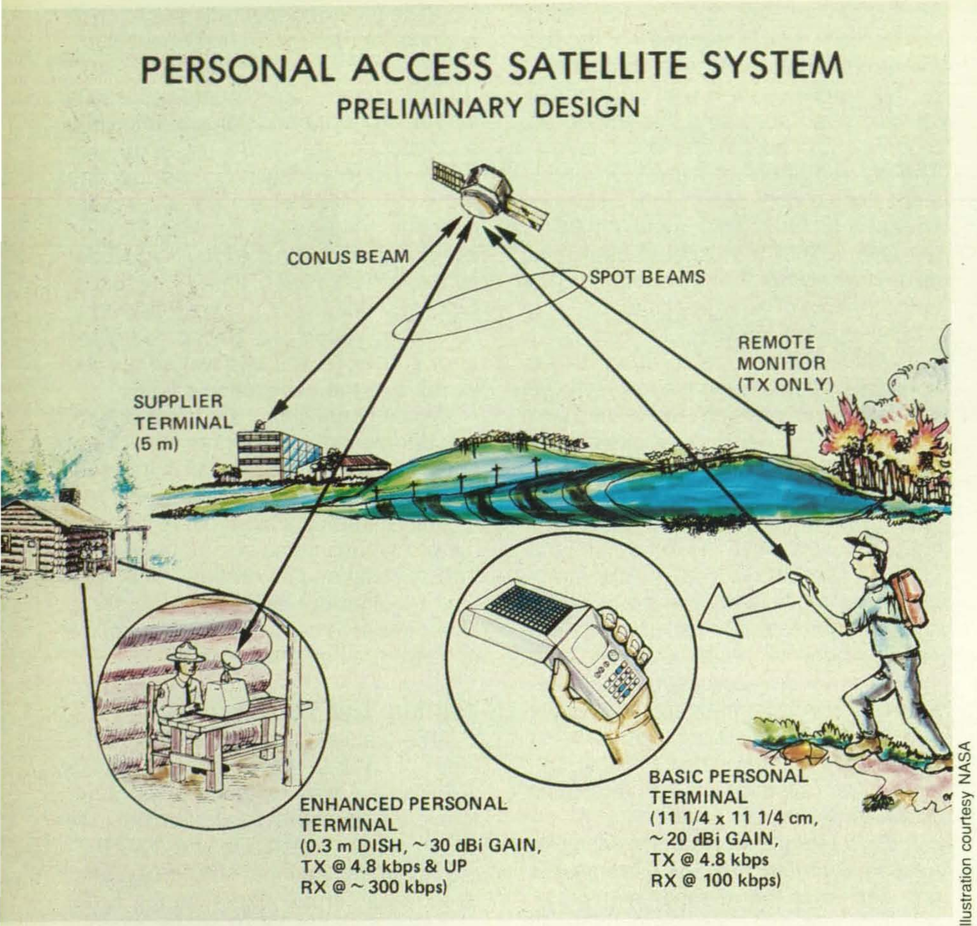

The PASS would enable emergency communications in remote locations.

obstructions, with no loss of synchronization during calls lasting more than two hours each.

The tests included secure calls in which digital voice transmission was encrypted. This technique would be important to government agencies participating in the US national communications system such as the FBI and the Drug Enforcement Agency.

NASA wants to further evaluate MSAT-X technologies using the first-generation US commercial mobile satellite, scheduled for launch in 1993. The satellite will have multiple spot beams at various frequencies so that a given frequency can be reused in nonadjacent beams, thereby conserving spectrum resources. Through a barter agreement with the American Mobile Satellite Corp., the designated provider of domestic MSS, NASA has offered launch services in exchange for a small percentage of the satellite capacity during the first two years of operation.

In the meantime, the space agency is refining MSAT-X components and exploring new applications for mobile satellite communications. One idea on the drawing board is a personal access satellite system (PASS) that would provide low bit rate voice and data services to CONUS using the Ka band (20/30 GHz), a virtually untapped portion of the frequency spectrum. The system would feature a lightweight handheld terminal "about the size of a cordless telephone," according to Dr. William Rafferty, manager of JPL's Communications Section, and would offer the user "unrestricted freedom of access and mobility." In addition to voice communications, potential applications include paging, low-rate broadcasting, video, data distribution nets, remote monitoring and control, and emergency communications.

The development of miniature terminals and antennas presents a major technological challenge, Rafferty said, requiring advances in monolithic microwave integrated circuits and Ka band components such as solid-state power amplifiers and low noise amplifiers.

NASA plans to test the PASS hardware and system architecture using the Advanced Communications Technology Satellite (ACTS) and the European Space Agency's OLYMPUS-1 satellite — both of which are designed to operate in the Ka band. Rafferty said a production version of the PASS terminal could be ready by the turn of the century. ❑

For more on the MSAT-X program, see the related technical briefs in this issue on pages 24 and 26.

HOW YOU CAN BENEFIT FROM NASA's TECHNOLOGY UTILIZATION SERVICES

If you're a regular reader of TECH BRIEFS, then you're already making use of one of the low- and no-cost services provided by NASA's Technology Utilization (TU) Network. But a TECH BRIEFS subscription represents only a fraction of the technical information and applications/engineering services offered by the TU Network as a whole. In fact, when all of the components of NASA's Technology Utilization Network are considered, TECH BRIEFS represents the proverbial tip of the iceberg.

We've outlined below NASA's TU Network—named the participants, described their services, and listed the individuals you can contact for more information relating to your specific needs. We encourage you to make use of the information, access, and applications services offered by NASA's Technology Utilization Network.

How You Can Utilize **NASA's Industrial Applications Centers**—A nationwide network offering a broad range of technical services, including computerized access to over 100 million documents worldwide.

You can contact NASA's network of Industrial Applications Centers (IACs) for assistance in solving a specific technical problem or meeting your information needs. The "user friendly" IACs are staffed by technology transfer experts who provide computerized information retrieval from one of the world's largest banks of technical data. Nearly 500 computerized data bases, ranging from NASA's own data base to Chemical Abstracts and INSPEC, are accessible through the ten IACs located throughout the nation. The IACs also offer technical consultation services and/or linkage with other experts in the field. You can obtain more information about these services by calling or writing the nearest IAC. User fees are charged for IAC information services.

Aerospace Research Applications Center (ARAC)
Indianapolis Center for Advanced Research
611 N. Capitol Avenue
Indianapolis, IN 46204
Dr. F. Timothy Janis, Director
(317) 262-5036

Central Industrial Applications Center/NASA (CIAC)
Rural Enterprises, Inc.
P.O. Box 1335
Durant, OK 74702
Dickie Deel, Director
(405) 924-5094

Science and Technology Research Center (STRC)
Post Office Box 12235
Research Triangle Park, NC 27709-2235
H.L. (Lynn) Reese, Director
(919) 549-0671

NASA Industrial Applications Ctr. 823 William Pitt Union
University of Pittsburgh
Pittsburgh, PA 15260
Dr. Paul A. McWilliams, Exec. Director
(412) 648-7000

NASA/Southern Technology Applications Center
Box 24
Progress Ctr., One Progress Blvd.
Alachua, FL 32615
J. Ronald Thornton, Director
(904) 462-3913
(800) 354-4832 (FL only)
(800) 225-0308 (toll-free US)

NASA/UK Technology Applications Program
University of Kentucky
109 Kinkead Hall
Lexington, KY 40506-0057
William R. Strong, Director
(606) 257-6322

NERAC, Inc.
One Technology Drive
Tolland, CT 06084
Dr. Daniel U. Wilde, President
(203) 872-7000

Technology Application Center (TAC)
University of New Mexico
Albuquerque, NM 87131
Dr. Stanley A. Morain, Director
(505) 277-3622

NASA Industrial Applications Center
University of Southern California
Research Annex
3716 South Hope Street
Los Angeles, CA 90007-4344
Robert Stark, Director
(213) 743-6132
(800) 642-2872 (CA only)
(800) 872-7477 (toll-free US)

NASA/SU Industrial Applications Center
Southern University Department of Computer Science
P.O. Box 9737
Baton Rouge, LA 70813-9737
Dr. John Hubbell, Director
(504) 771-6272

If you represent a public sector organization with a particular need, you can contact NASA's Application Team for technology matching and problem solving assistance. Staffed by professional engineers from a variety of disciplines, the Application Team works with public sector organizations to identify and solve critical problems with existing NASA technology. **Technology Application Team, Research Triangle Institute, P.O. Box 12194, Research Triangle Park, NC 27709. *Doris Rouse, Director,* (919) 541-6980**

How You Can Access Technology Transfer Services At NASA Field Centers: **Technology Utilization Officers & Patent Counsels**—Each NASA Field Center has a Technology Utilization Officer (TUO) and a Patent Counsel to facilitate technology transfer between NASA and the private sector.

If you need further information about new technologies presented in *NASA Tech Briefs,* request the Technical Support Package (TSP). If a TSP is not available, you can contact the Technology Utilization Officer at the NASA Field Center that sponsored the research. He can arrange for assistance in applying the technology by putting you in touch with the people who developed it. If you want information about the patent status of a technology or are interested in licensing a NASA invention, contact the Patent Counsel at the NASA Field Center that sponsored the research. Refer to the NASA reference number at the end of the Tech Brief.

Ames Research Ctr.
Technology Utilization Officer: Laurance Milov
Mail Code 223-3
Moffett Field, CA 94035
(415) 694-4044
Patent Counsel: Darrell G. Brekke
Mail Code 200-11
Moffett Field, CA 94035
(415) 694-5104

Lewis Research Center
Technology Utilization Officer: Anthony F. Ratajczak
Mail Stop 7-3
21000 Brookpark Road
Cleveland, OH 44135
(216) 433-5568
Patent Counsel: Gene E. Shook
Mail Code 301-6
21000 Brookpark Road
Cleveland, OH 44135
(216) 433-5753

John C. Stennis Space Center
Technology Utilization Officer: Robert M. Barlow
Code GA-00
Stennis Space Center, MS 39529
(601) 688-1929

John F. Kennedy Space Center
Technology Utilization Officer: Thomas M. Hammond
Mail Stop PT-PMO-A
Kennedy Space Center, FL 32899
(407) 867-3017
Patent Counsel: James O. Harrell
Mail Code PT-PAT
Kennedy Space Center, FL 32899
(407) 867-2544

Langley Research Ctr.
Technology Utilization Officer: John Samos
Mail Stop 139A
Hampton, VA 23665
(804) 864-2484
Patent Counsel: George F. Helfrich
Mail Code 279
Hampton, VA 23665
(804) 864-3523

Goddard Space Flight Center
Technology Utilization Officer: Donald S. Friedman
Mail Code 702.1
Greenbelt, MD 20771
(301) 286-6242
Patent Counsel: R. Dennis Marchant
Mail Code 204
Greenbelt, MD 20771
(301) 286-7351

Jet Propulsion Lab.
NASA Resident Office
Technology Utilization Officer: Gordon S. Chapman
Mail Stop 180-801
4800 Oak Grove Drive
Pasadena, CA 91109
(818) 354-4849
Patent Counsel: Paul F. McCaul
Mail Code 180-801
4800 Oak Grove Drive
Pasadena, CA 91109
(818) 354-2734
Technology Utilization Mgr. for JPL: Dr. Norman L. Chalfin
Mail Stop 156-211
4800 Oak Grove Drive
Pasadena, CA 91109
(818) 354-2240

George C. Marshall Space Flight Center
Technology Utilization Officer: Ismail Akbay
Code AT01
Marshall Space Flight Center, AL 35812
(205) 544-2223
Fax (205) 544-3151
Patent Counsel: Bill Sheehan
Mail Code CC01
Marshall Space Flight Center, AL 35812
(205) 544-0021

Lyndon B. Johnson Space Center
Technology Utilization Officer: Dean C. Glenn
Mail Code IC-4
Houston, TX 77058
(713) 483-3809
Patent Counsel: Edward K. Fein
Mail Code AL3
Houston, TX 77058
(713) 483-4871

NASA Headquarters
Technology Utilization Officer: Leonard A. Ault
Code CU
Washington, DC 20546
(202) 453-8377
Assistant General Counsel for Patent Matters: Robert F. Kempf, Code GP
Washington, DC 20546
(202) 453-2424

A Shortcut To Software: **COSMIC®**—For software developed with NASA funding, contact COSMIC, NASA's Computer Software Management and Information Center. New and updated programs are announced in the Computer Programs section. COSMIC publishes an annual software catalog. For more information call or write: **COSMIC®** 382 East Broad Street, Athens, GA 30602 *John A. Gibson, Dir.,* (404) 542-3265

If You Have a Question... **NASA Scientific & Technical Information Facility** can answer questions about NASA's Technology Utilization Network and its services and documents. The STI staff supplies documents and provides referrals. Call, write or use the feedback card in this issue to contact: **NASA Scientific and Technical Information Facility,** Technology Utilization Office, P.O. Box 8757, Baltimore, MD 21240-0757. *Walter M. Heiland, Manager,* (301) 859-5300, Ext. 242, 243

Electronic Components and Circuits

Hardware, Techniques, and Processes

Programmable Analog Memory Resistors for Electronic Neural Networks

Potential uses include nonvolatile, erasable, electronically programmable read-only memories.

NASA's Jet Propulsion Laboratory, Pasadena, California

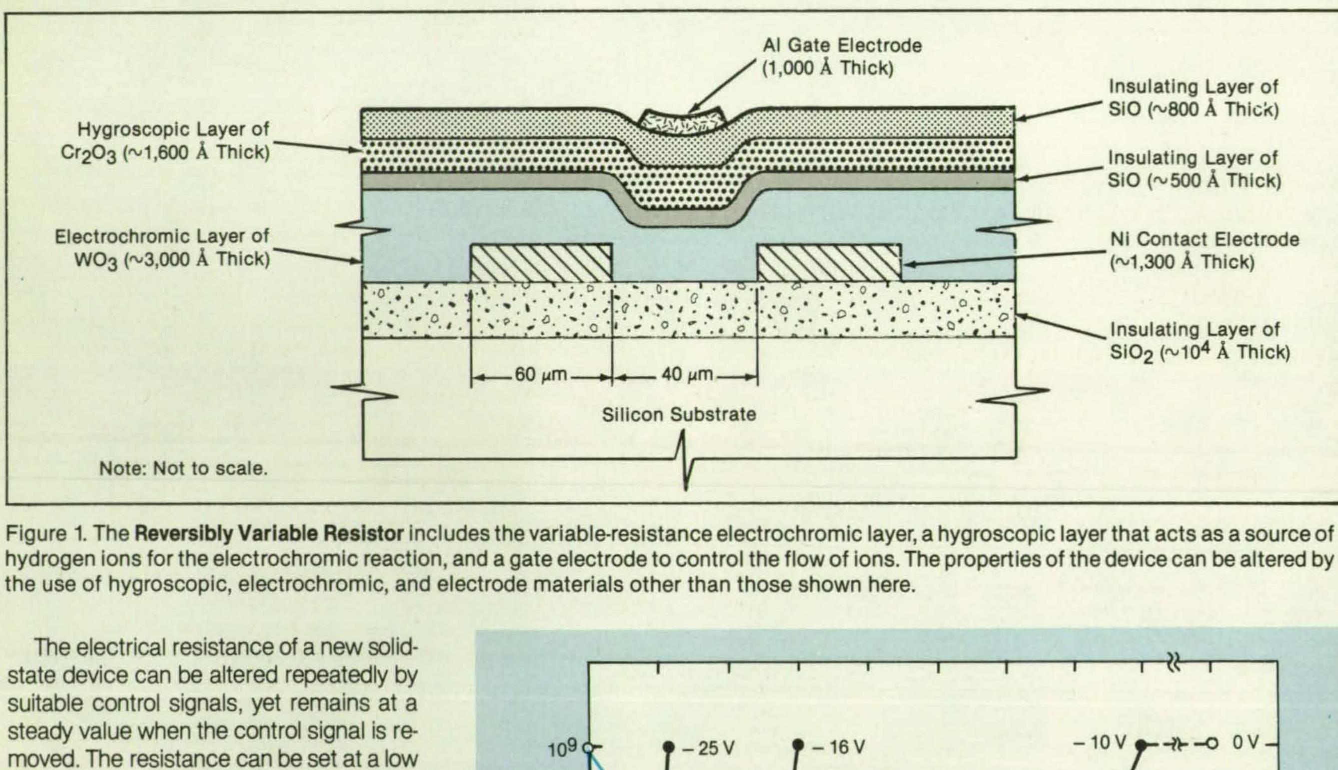

Figure 1. The **Reversibly Variable Resistor** includes the variable-resistance electrochromic layer, a hygroscopic layer that acts as a source of hydrogen ions for the electrochromic reaction, and a gate electrode to control the flow of ions. The properties of the device can be altered by the use of hygroscopic, electrochromic, and electrode materials other than those shown here.

The electrical resistance of a new solid-state device can be altered repeatedly by suitable control signals, yet remains at a steady value when the control signal is removed. The resistance can be set at a low value ("on" state), a high value ("off" state), or at any convenient intermediate value and left there until a new value is desired. The device can serve as an element of an electrically erasable, programmable read-only memory integrated circuit. Circuits of this type are particularly useful in nonvolatile, associative electronic memories based on models of neural networks. Furthermore, such programmable analog memory resistors are ideally suited as synaptic interconnects in "self-learning" neural nets.

The operation of the device depends on the electrochromic property of WO_3, which when pure is an insulator. This material undergoes the reversible electrochemical reaction

$$WO_3 + xH^+ + xe^- \rightleftarrows H_xWO_3$$

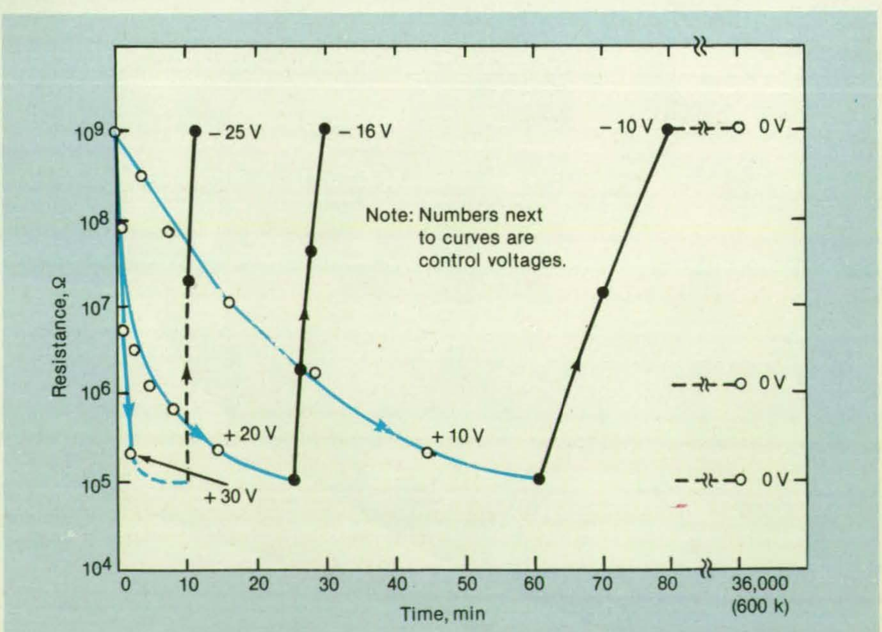

Figure 2. The **Resistance Increases or Decreases With Time** according to the magnitude and sign of the control voltage applied to the gate electrode. When no voltage is applied, the resistance remains at the value set by the most recently applied voltage.

THE SHAPE OF THE FUTURE

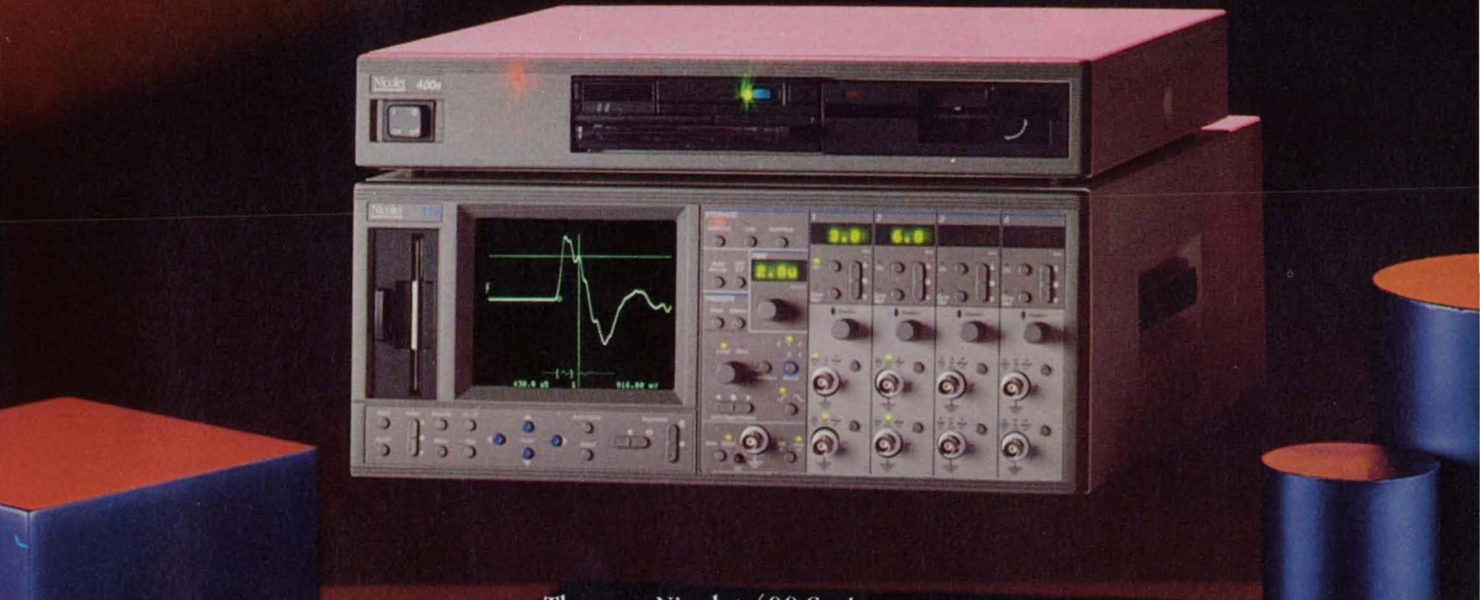

The new Nicolet 400 Series. Complete with 64K-256K expandable memory. Easy upgradability. Even removable hard drive.

Facts are facts.

Only one digital oscilloscope provides 64K-256K expandability. Software that upgrades your unit instantly. And a 44 Megabyte removable disk providing fast, easy data retrieval.

That's the new Nicolet 400 Series—a rare combination of power and speed, flexibility and convenience. It gives you all this *today* . . . so you'll be in better shape *tomorrow.*

Its expandable memory multiplies your ability to record transients over time. And along with on-board calculations, its 32-bit CPU provides waveform processing ten to 100 times faster than a PC.

The 400 takes a fresh look at data collection, too. Disk-downloadable sequences and programs help you transfer and archive data with new-found speed and accuracy. You can even cascade together four channels for memory as long as one MegaSample. And programs can be loaded with the simple touch of a button.

See how much Nicolet has done to improve your future. Send for a new 400 brochure now.

Nicolet

INSTRUMENTS OF DISCOVERY

Nicolet Test Instruments Division

5225-2 Verona Road, Madison, WI 53711, 608/273-5008 or 800/356-3090

Circle Reader Action No. 696

As the WO_3 combines with or releases hydrogen ions, its electrical resistivity decreases or increases, respectively.

The device (see Figure 1) includes two Ni contact electrodes in a layer of WO_3. The resistance of the device is sensed between these electrodes. The source of hydrogen ions is a hygroscopic layer of Cr_2O_3, which is separated from the WO_3 by an insulating layer of SiO. (This SiO layer also donates some H^+ ions, but is not as rich a source as is the Cr_2O_3.) A second, insulating layer of SiO separates the Cr_2O_3 from an aluminum gate electrode.

When a positive control voltage is applied to the gate electrode with respect to one of the contact electrodes the electric field ionizes the H_2O present in the Cr_2O_3 and drives the H^+ ions through the inner SiO layer, into the WO_3, toward the negative contact. The H^+ ions are neutralized in the WO_3 via the reversible electrochemical reaction, and the electrical resistivity of the WO_3 is thus reduced. When a negative control voltage is applied to the gate electrode, the H_xWO_3 is dissociated and the hydrogen ions are pulled back into the Cr_2O_3, thus increasing the electrical resistivity of the WO_3. The amount of H_xWO_3 and, therefore, the electrical resistance of the device remains constant when the control signal is removed. The control signal can be applied again to change the amount of H_xWO_3, and hence the resistance, to a new steady level.

The inner layer of SiO helps to control the flow of ions as well as to prevent shorting of WO_3 by the less resistive Cr_2O_3 layer. Both layers of SiO serve as blocking contacts that allow only the desired ionic or electronic current to pass and then only when a sufficient control signal is applied to the gate electrode. The switching speed of the device depends on the magnitude of the control signal (see Figure 2); for example, a control signal of 30 V changes the resistance by a factor of 1,000 in less than 1 min.

This work was done by Rajeshuni Ramesham, Sarita Thakoor, Taher Daud, and Anilkumar P. Thakoor of Caltech for **NASA's Jet Propulsion Laboratory**. *For further information, Circle 96 on the TSP Request Card.*

In accordance with Public Law 96-517, the contractor has elected to retain title to this invention. Inquiries concerning rights for its commercial use should be addressed to

Edward Ansell
Director of Patents and Licensing
Mail Stop 305-6
California Institute of Technology
1201 East California Boulevard
Pasadena, CA 91125

Refer to NPO-17398, volume and number of this NASA Tech Briefs *issue, and the page number.*

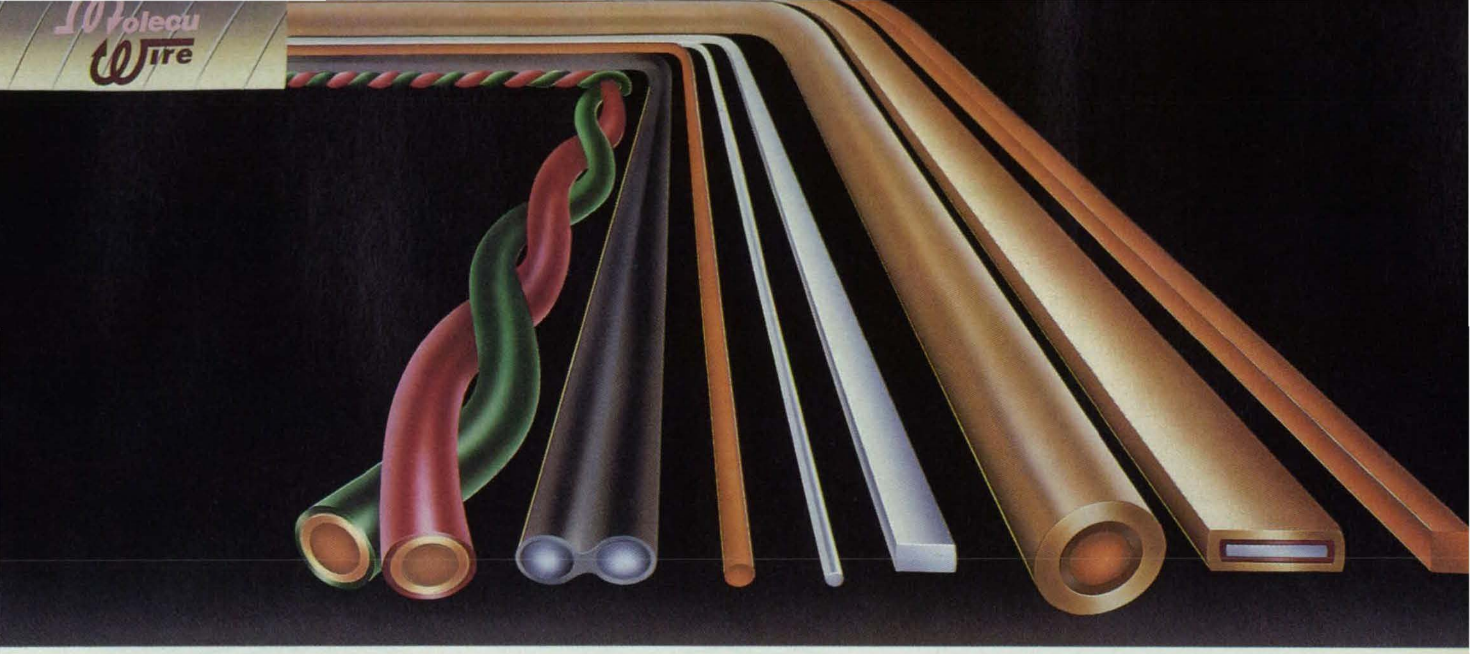

Mechanically-Steered, Mobile Satellite-Tracking Antenna

The signal from a satellite can be tracked in a moving vehicle.

NASA's Jet Propulsion Laboratory, Pasadena, California

An L-band, mechanically-steered, medium-gain antenna is part of the prototype radio equipment mounted in a vehicle to demonstrate the concept of a land-mobile/satellite communication system. The system will provide such services as mobile telephone, voice or alphanumeric dispatch, paging, position-location information, and low-rate data transmission, for users within the continental United States and Alaska.

The radiating part is a linear array of four square microstrip patches tilted with respect to the ground plane to provide coverage of the range of elevation angles from 20° to 60°. The minimum gain over the ranges of transmitting frequencies from 1646.5 to 1660.5 MHz and receiving frequencies from 1545.0 to 1559.0 MHz is 10 dB with respect to a circularly polarized isotropic source. In addition to providing a gain up to 6 dB better than that of a low-gain, omnidirectional antenna, and thus reducing the required power and/or size of the antenna aboard the satellite, the narrower beam provides much higher rejection of multipath signals and can be made to provide enough isolation for operation in the presence of two satellites.

The rotating antenna platform is mounted on a fixed platform that includes a motor drive and rotation-rate sensors. The initial pointing toward the satellite (acquisition) is achieved by seeking the direction from which maximum power is received from a pilot signal transmitted by the satellite. The tracking is performed by a single-channel phase-comparison monopulse scheme in which the difference between the level of the signals received by the two identical halves of the antenna array is used as an error signal to drive the stepping motor that rotates the antenna platform.

The antenna has been mounted on the test van (see Figure 2) that serves as a mobile platform for evaluation of the evolving ground equipment, including the steerable antenna, transceiver equipment, modulation, and coding schemes. The antenna system is covered by a cylindrical polyester-and-glass radome that has a diameter of 20 in. (51 cm) and a height of 9 in. (23 cm), and has little effect on the radiation pattern of the antenna.

The antenna has been tested in conjunction with the 1,000-ft (305-m) National Oceanic and Atmospheric Administration tower in Erie, Co. and with the INMARSAT satellite. The antenna has acquired and maintained tracking in a variety of field conditions and at vehicle speeds up to 60 mph (27 m/s). Plans call for further tests, a higher degree of integration of the discrete radio-frequency components with the array, and reduction of the overall height of the antenna to about 4.5 in. (11.4 cm) by removal of the pointing electronics from the fixed lower platform to behind the tilted array on the rotating platform, or to a separate compartment inside the vehicle.

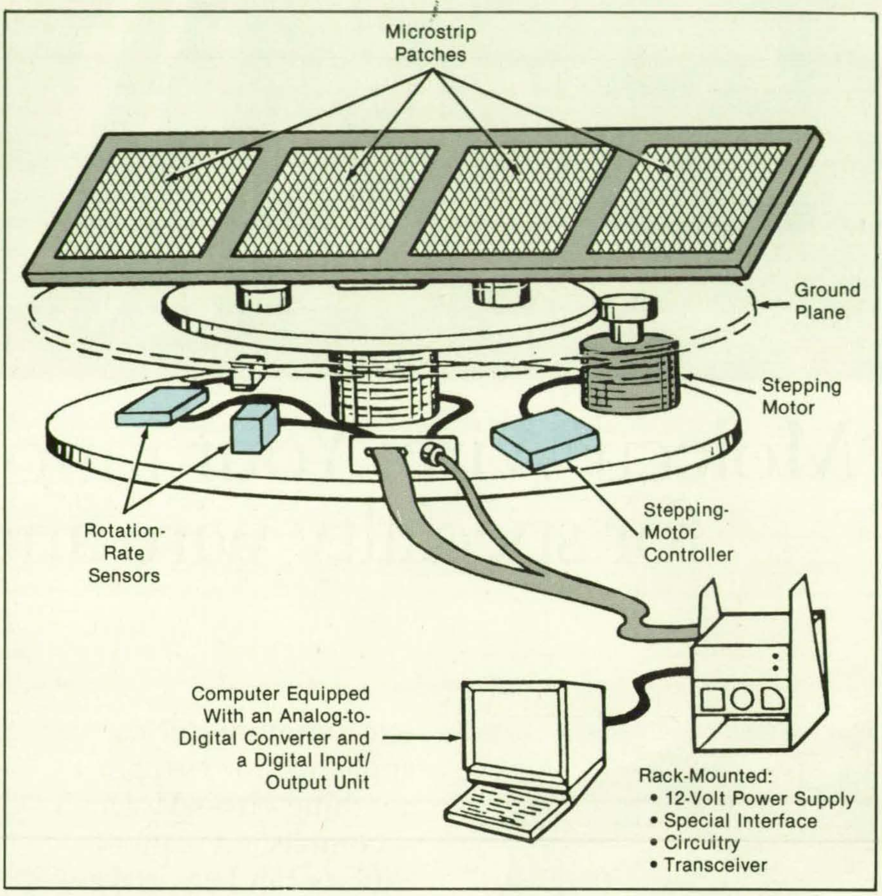

Figure 1. The **Antenna Is Rotated Mechanically** until it finds the direction from which the maximum signal comes. The rate sensors provide an inertial frame of reference during acquisition, so that the antenna can lock onto the signal even when the vehicle is turning.

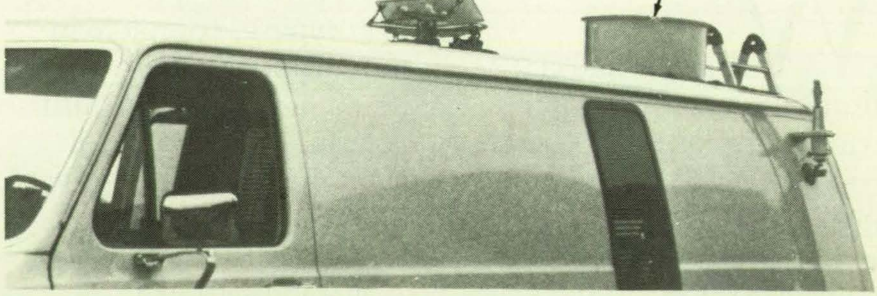

Figure 2. The **Antenna Is Mounted** on top of a van that serves as a test vehicle for the land-mobile/satellite communication system now undergoing development.

This work was done by D. J. Bell, J. B. Berner, V. Jamnejad, and K. E. Woo of Caltech for **NASA's Jet Propulsion Laboratory**. *For further information, Circle 42 on the TSP Request Card.*
NPO-17607

MATLAB™ Version 3.5

Introducing the Signal Processing Toolbox

- **Faster Matrix Computation**
- **Digital Filter Design**
- **Spectrum Estimation**
- **Parametric Modelling**
- **Time Series Analysis**
- **New 2-D and 3-D Graph Types**

MATLAB v3.5 is the latest version of the premier interactive system for numerical analysis and signal processing. Problems and solutions are expressed just as they are written mathematically — ***without traditional programming***.

MATLAB has rapidly become an industry standard for digital signal processing research. Its unique interactive interface, algorithmic foundation, easy extensibility, and speed make MATLAB the software system of choice for ***high productivity*** and ***high creativity*** research at thousands of universities, laboratories, and companies.

Over 200 Built-in Functions

• eigenvalues	• 1-D and 2-D FFTs
• least squares	• matrix arithmetic
• cubic splines	• multivariate statistics
• convolution	• polynomial arithmetic
• complex arithmetic	• nonlinear optimization
• IIR and FIR filters	• linear equation solving
• curve fitting	• differential equations
• singular value decomposition, ***and more***	

Version 3.5 adds new 2-D and 3-D plot types, including feather plots, error bars, automatic contour labelling, and optimized VGA support.

Family of step responses

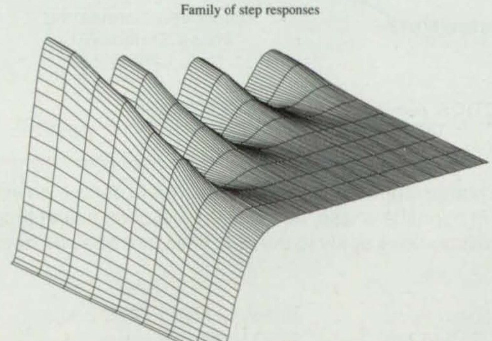

The company and product names mentioned above are trademarks of their respective holders.

Computers

- ✓ PC and AT Compatibles
- ✓ 80386 Computers
- ✓ Macintosh
- ✓ Sun Workstations
- *NEW!* ✓ HP 9000 Workstations
- ✓ Apollo Workstations
- ✓ VAX/VMS and Unix
- ✓ Ardent Titan
- *NEW!* ✓ Convex C-Series
- *NEW!* ✓ Alliant FX/Series
- ✓ Other Computers

Open and Extensible

Create functions and programs rapidly — without the time-consuming compiling, linking, and complex syntax of traditional languages. Our open-system philosophy gives you access to algorithms so you can edit functions or add your own.

Optional Toolboxes extend MATLAB with application-specific capabilities, such as control system design, parametric modelling, and chemometrics.

Benchmarks (20 MHz 386-based PC)

50 x 50 matrix multiply	0.71 sec
50 x 50 matrix inverse	1.32 sec
50 x 50 eigenvalues	1.21 sec
4096-point complex FFT	1.16 sec

Fast, Accurate, and Reliable

MATLAB can handle lots of data and do it fast, fully utilizing all available floating point hardware for maximum performance. You won't have to question the results either — the algorithms have been programmed by leading experts in mathematical software and are used by leading researchers around the world.

Please provide additional information!

Name ____________
Company ____________
Dept. ____________
Address ____________
City, State, Zip ____________
Country ____________
Telephone ____________
Computer ____________

The MATH WORKS Inc.
21 Eliot Street
South Natick, MA 01760
Tele: (508) 653-1415
FAX: (508) 653-2997

NASA 2/90

Printed-Circuit Cross-Slot Antenna

Coupling between the perpendicular slots is suppressed.

NASA's Jet Propulsion Laboratory, Pasadena, California

A balanced feed configuration minimizes the coupling between the slots of a printed-circuit cross-slot antenna unit. Units of this type could be elements of phased-array antennas for radar, mobile/satellite communications, and other applications that require flush mounting and/or rapid steering of beams with circular polarization.

In most respects, the unit and array have a conventional cavity-backed-printed-circuit, crossed-slot antenna design. The novelty lies in the type of symmetry and phasing of the strip-line feeders. The figure shows, partly schematically, the feed configuration for one of the slots. A strip-line feeder below the plane of the slotted conductive antenna element brings power from a power-divider/phase-shifter to the left member of the horizontal slot at point *a*, where the relative phase is 0°. A similar strip-line feeder brings power to the right member of the slot at point *b*; the power-divider/phase-shifter is configured so that position *b* is fed 180° out of phase with position *a*.

In the figure, the pattern of arrows indicates the electric field resulting from this feed configuration. As they show, the signals propagating around the corners at the intersection into the vertical slot from the two feed points cancel each other because they are of opposite phase. The vertical slot is fed by similarly configured strip lines to yield phases of 90° and 270° at points *c* and *d*, respectively. In this case, the 180° difference in phase between these two feed points results in the cancellation of signals propagating around the corners into the horizontal slot. Overall, the 90° increments of phase at sequential feed points around the center result in circularly polarized radiation.

The power-divider/phase-shifter includes a network of strip lines below the plane of the slotted conductive antenna element. The ground plane and the conductive antenna element are two boundaries of the antenna waveguide cavity. The edges of the square antenna unit and the other four boundaries are defined by fences of plated through-holes, screws, or pins that electrically connect the conductive antenna element with the ground plane.

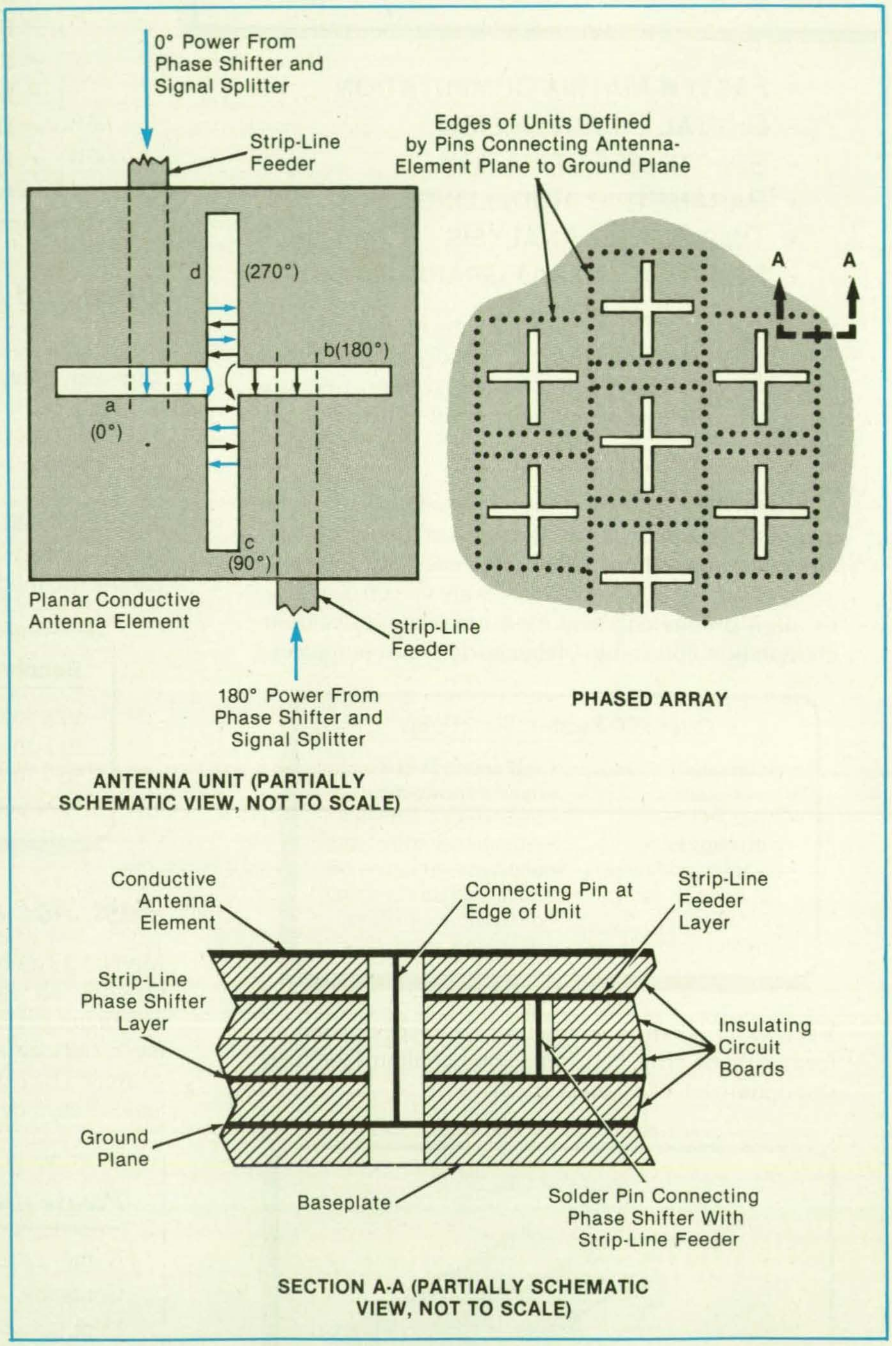

Strip-Line Feeders behind the planar conductive antenna element deliver power to the horizontal slot at points *a* and *b* in opposite phase. As a result, little or no power propagates into the vertical slot. Similar considerations apply to the strip lines (not shown) that feed the vertical slot at points *c* and *d*.

This work was done by Wong Foy, Hsien-Hsien Chung, and Sheng Y. Peng of Teledyne Ryan Electronics for **NASA's Jet Propulsion Laboratory**. *For further information, Circle 4 on the TSP Request Card.*

Title to this invention has been waived under the provisions of the National Aeronautics and Space Act [42 U.S.C. 2457(f)]. Inquiries concerning licenses for its commercial development should be addressed to

G. A. Cooley
Senior Vice President
Teledyne Ryan Electronics
8650 Balboa Avenue
San Diego, CA 92123

Refer to NPO-17706, volume and number of this NASA Tech Briefs *issue, and the page number.*


TEAM WORK
ARIANE PUTS SATELLITES INTO SPACE THAT SPEAK 27 LANGUAGES. AS INDUSTRIAL ARCHITECT AEROSPATIALE COOPERATES WITH 11 EUROPEAN COUNTRIES PROVIDING SPACE-AGE TECHNOLOGY AND MANAGEMENT SKILLS. WITH THE NUMBER OF SATELLITES LAUNCHED FOR AMERICAN COMPANIES, WE PROVE OUR CAPABILITY OF WORKING TOGETHER. AND AEROSPATIALE HAS BUILT MORE THAN 40 TECHNICALLY DIVERSIFIED SATELLITES, MANY OF THEM WITH AMERICAN PARTNERS. WORKING AND CREATING TOGETHER KEEPS US UP THERE. MEET THE TEAM.
aerospatiale
AEROSPATIALE INC. 1101, 15TH STREET N.W. WASHINGTON DC 20005
PHONE: 202 293 0650
Circle Reader Action No. 661
© PUBLICIS ZB-A2

Electronic Systems

Hardware, Techniques, and Processes

Books and Reports

Graphical Display of Test-Flight Trajectories

Trajectories are displayed directly on maps.

Ames Research Center, Moffett Field, California

A computer graphical system shows the trajectories of experimental aircraft in real time during flight tests. The system enables an operator to choose a variety of display modes and to issue course corrections to the pilot. The principle of the system can be adapted to a variety of civil, military, and commercial uses in which the paths of vehicles are overlaid on maps — for example, in dispatching delivery vans.

The graphical system is housed in a computer workstation. It accepts processed data from telemetry and radar systems. It employs a 32-bit processor and the UNIX operating system. Its software package, RIM (for real-time interactive map), consists of about 7,000 lines of code in C language. Its data base is derived from maps from the U.S. Geological Survey and the Defense Mapping Agency.

The operator can select the level of detail in the map. By eliminating certain map features, the operator makes the map less cluttered and can concentrate on points of special interest. At any time, the operator can zoom toward or away from the map and can translate the map in any direction. By pressing a button near the display screen, the operator can order a color print of any image. In 35 to 45 seconds, the workstation prints a paper copy of the display.

*This work was done by Robert G. Comperini and Donald C. Rhea of **Ames Research Center**. Further information may be found in NASA TM-100429 [N88-20344], "Development of an Interactive Real-Time Graphics System for the Display of Vehicle Space Positioning."*

Copies may be purchased [prepayment required] from the National Technical Information Service, Springfield, Virginia 22161, Telephone No. (703) 487-4650. Rush orders may be placed for an extra fee by calling (800) 336-4700.

Inquiries concerning rights for the commercial use of this invention should be addressed to the Patent Counsel, Ames Research Center [see page 16]. Refer to ARC-12211

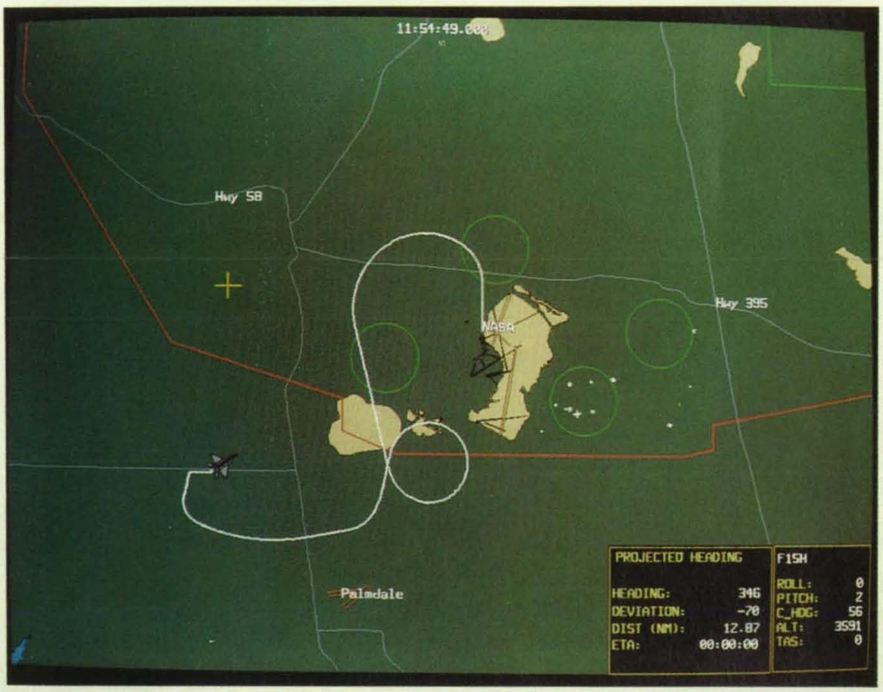

The **Basic Display Shows the Path** traveled by an aircraft as a white line on a map. Alphanumeric data on the aircraft can be called up in a window display like that at lower right.

VLSI Reed-Solomon Encoder With Interleaver

Size, weight, and susceptibility to burst errors are reduced.

NASA's Jet Propulsion Laboratory, Pasadena, California

An encoding system built on a single very-large-scale integrated (VLSI) circuit chip produces a (255, 223) Reed-Solomon (RS) code with programmable interleaving up to a depth of 5. The new encoder weighs less and consumes less power than the prior encoder of this type, which contains at least 32 chips and has interleaving capability up to a depth of 2 only.

The numbers 255 and 223 denote the total number of symbols and the number of information symbols, respectively, in each code word (each symbol contains 8 bits). The RS code can correct up to 16 symbol errors in each word. The RS code is meant

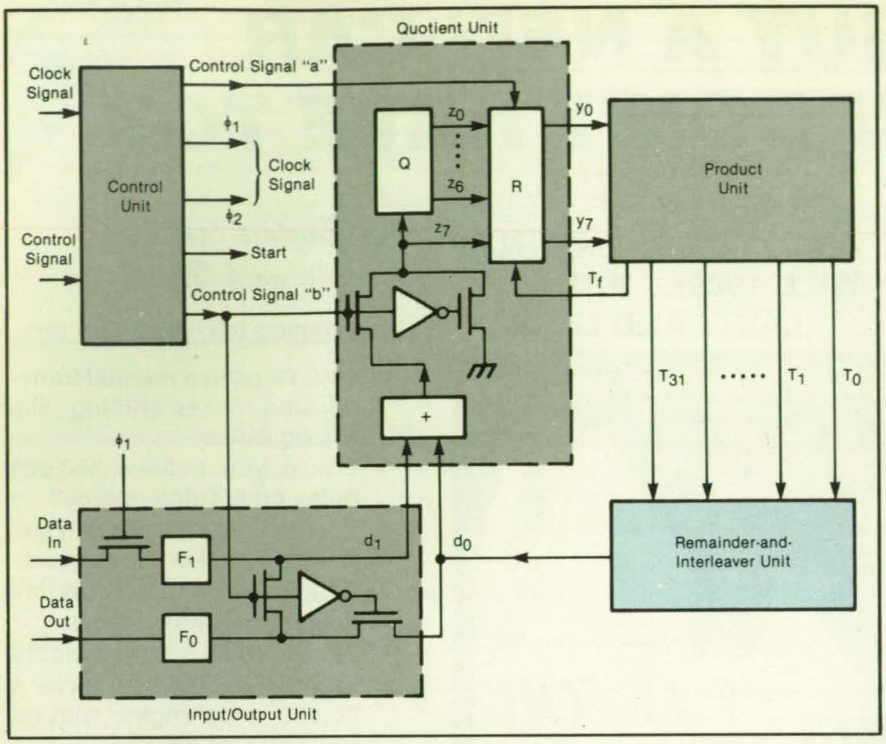

Figure 1. The **(255, 223) RS Encoder** includes a new remainder-and-interleaver unit that provides programmable interleaving of code words.

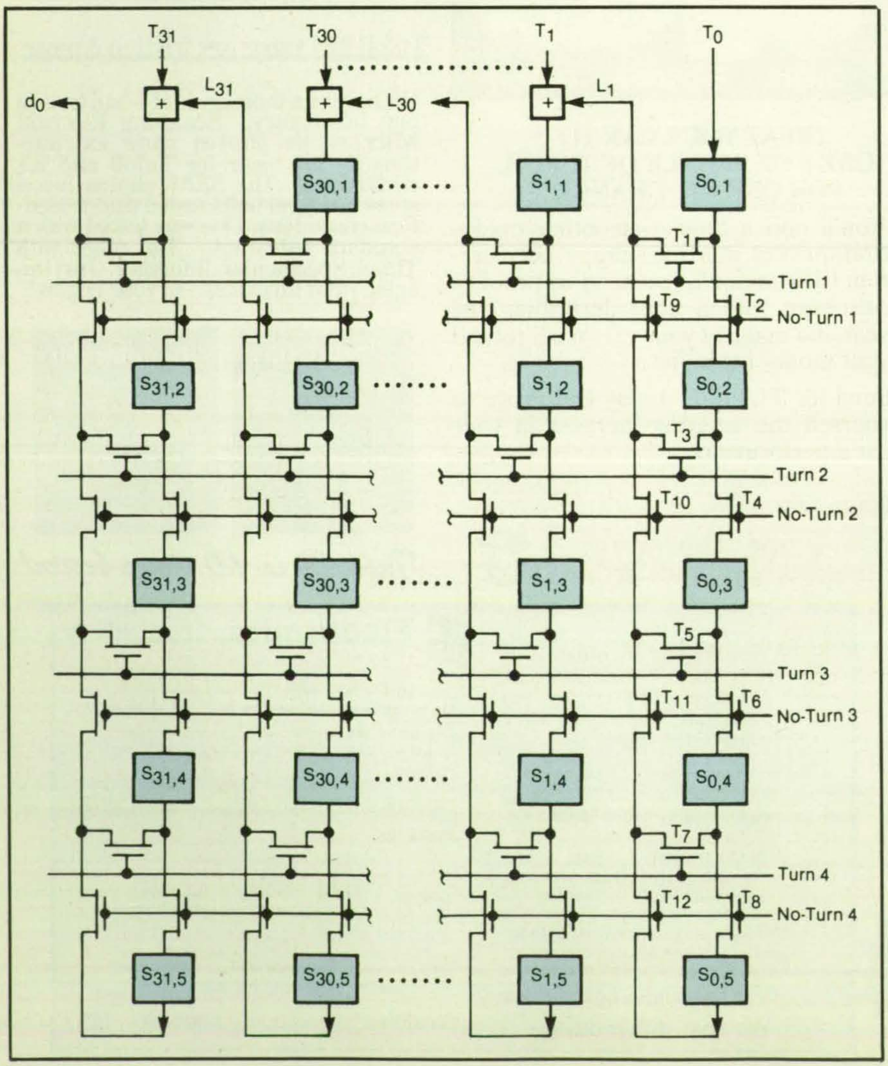

Figure 2. The **Remainder-and-Interleaver Unit** contains shift registers and modulo-2 adders. Signals on the "turn" and "no-turn" lines control the depth of interleaving.

to be used as an outer code concatenated with an inner convolutional Viterbi code of rate 1/2 and constraint length 7. Interleaving at the RS encoder (at the input of the overall coding/decoding system) helps to reduce the vulnerability of the RS decoder (at the output of the overall coding/decoding system) to sequences of erroneous symbols in the inner transmission channel or in the Viterbi decoder. With a sufficient depth of interleaving, a burst of errors in the Viterbi decoder affects only one symbol in an RS code word.

An RS encoder is essentially a circuit that performs polynomial division in a finite field — an operation that requires finite-field multiplication. The new encoder is based on E. R. Berlekamp's bit-serial multiplication algorithm for a (255, 223) RS encoder over the Galois Field (2^8). This algorithm requires only shifting and exclusive-OR operations and makes possible a VLSI architecture that can be realized on a single VLSI chip by use of negatively-doped-channel metal oxide/semiconductor (NMOS) technology.

The circuit (see Figure 1) is divided into five major parts: the product, remainder-and-interleaver, quotient, input/output, and control units. All except the remainder-and-interleaver unit are similar to those of a prior (255, 223) RS encoder based on the Berlekamp algorithm. The remainder-and-interleaver unit is used to store the coefficients of the remainder during the division process and performs the interleaving operation.

The units denoted $S_{i,j}$ ($0 \leqslant i \leqslant 30$ and $1 \leqslant j \leqslant 5$) in Figure 2 are 8-bit shift registers that use modulo-2 addition (exclusive-OR operation). The outputs of the registers are sent to the inputs of modulo-2 adders by buslines L_i through transistors controlled by the "turn" and "no-turn" signals, which set the depth of interleaving.

The circuit chip, which comprises about 10,000 transistors, was fabricated in 4-μm NMOS. The chip was tested successfully. The maximum clock frequency is about 1.5 MHz. The operating speed is limited mainly by the long clock lines associated with the two-phase clocks used in the dynamic shift registers, and there are more than 1,250 dynamic registers. The area of the chip is estimated to be 4,800 by 3,220 μm.

This work was done by In-Shek Hsu, L. J. Deutsch, and Trieu-Kie Truong of Caltech and I. S. Reed of the University of Southern California for **NASA's Jet Propulsion Laboratory**. *For further information, Circle 66 on the TSP Request Card.*

This invention is owned by NASA, and a patent application has been filed. Inquiries concerning nonexclusive or exclusive license for its commercial development should be addressed to the Patent Counsel, NASA Resident Office-JPL [see page 16]. Refer to NPO-17280.

Carrying Synchronous Voice Data on Asynchronous Networks

Buffers restore synchronism for internal use and permit asynchronism in external transmission.

NASA's Jet Propulsion Laboratory, Pasadena, California

A proposed asynchronous local-area digital communication network (LAN) would carry synchronous voice, data, or video signals, or non-real-time asynchronous data signals. The network would use a double buffering scheme that reestablishes phase and frequency references at each node in the network. The concept has been demonstrated in a token-ring network operating at 80 Mb/s, pending development of equipment that can operate at the planned data rate of 200 Mb/s. However, the technique is generic and can be used with any LAN as long as the protocol offers deterministic (or bonded) access delays and sufficient capacity.

In the network, signals are transmitted along fibers as discrete packets of data. At each node in the network, an input buffer queues the packets for synchronous delivery to the node equipment, while an output buffer queues synchronous signals from the equipment for transmission over the network in asynchronous packets. This approach is called "double elastic buffering." The buffers are elastic in that the lengths of the queues can vary as the rates of arrival or departure of packets vary. Of course, if the overall packet rate for the network is fairly constant, the mean queue length for all nodes also remains constant.

The scheme is analogous to a bucket brigade between two barrels of water (see figure). The input and output barrels are continuously filled and emptied, respectively, by identical pipes. As long as the net volume of water (bits) passing through the system remains constant, no information is lost. In a real system, the steady flows at the nodes may not be precisely the same, corresponding to local timing frequencies that are slightly different. The barrels (buffers) would then overflow or empty eventually. Therefore, the input/output frequencies should be matched closely (< 1 ppm). An input/output buffer skew can be corrected by either discarding or duplicating a packet. Typically, this only affects a few voice samples every few hours and is largely undetectable.

The size and average rate of packets, the size of the buffer, and the synchronous output and input rates of the buffers (corresponding to the sizes of the buckets, the rate of delivery of buckets, size of the barrel, and the rates of flow in the pipes) are set by design according to the requirements of the blend of traffic on the network. For example, small packets at high rates reduce the latency through the network — the time it takes a signal to pass from a transmitting to a receiving node, including queue time and transmission time, but are vulnerable to loss when traffic becomes congested. Low latency is important in feedback control systems, parallel processors, and many human/machine interfaces that require fast responses.

For another example, large packets enable the use of lower rates and increase the tolerance of the network to fluctuations in traffic. However, they increase queuing time. The latency of the system may then be too great for fast-response nodes. The delay may not necessarily be too great for voice traffic however, provided that it does not cause echoes.

The size of a buffer should be at least 4.5 Kbits for voice signals. This size is based on an input/output rate of 1.544 Mb/s in a nine-station, 1-km ring operating at 80 Mb/s with 2-Kbyte packets. The technique will allow up to 26 T1 circuits (an equivalent of 624 voice channels) to be transmitted over an 80 Mb/s LAN.

This work was done by Larry A. Bergman of Caltech for **NASA's Jet Propulsion Laboratory**. *For further information, Circle 53 on the TSP Request Card.*

In accordance with Public Law 96-517, the contractor has elected to retain title to this invention. Inquiries concerning rights for its commercial use should be addressed to

Edward Ansell
Director of Patents and Licensing
Mail Stop 305-6
California Institute of Technology
1201 East California Boulevard
Pasadena, CA 91125

Refer to NPO-17431, volume and number of this NASA Tech Briefs *issue, and the page number.*

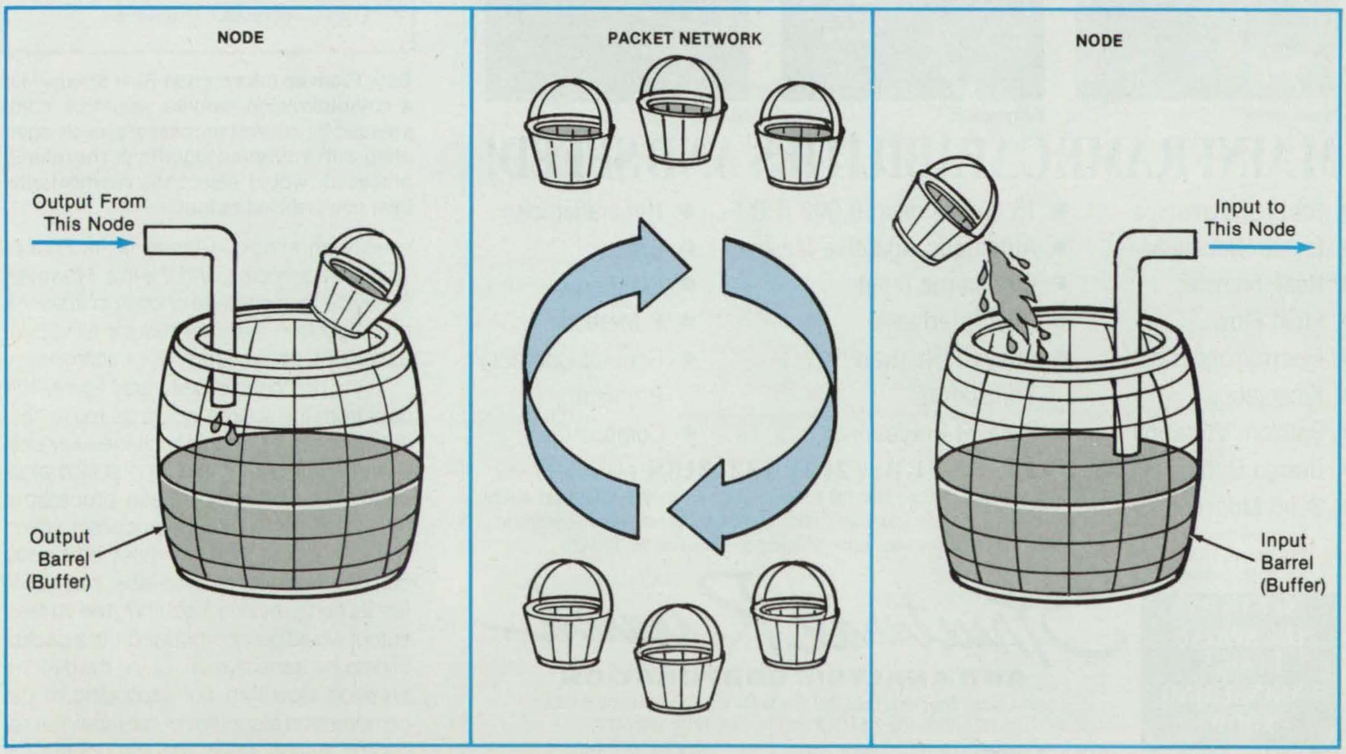

The **Bucket-Brigade Analogy** illustrates the flow of synchronous digital data from node to node through the asynchronous network.

Competitive Parallel Processing for Compression of Data

The momentarily-best compression algorithm would be selected.

NASA's Jet Propulsion Laboratory, Pasadena, California

A proposed competitive-parallel-processing system would compress data for transmission in a channel of limited bandwidth. There will be an increasing need for compression of data as broadcasting and other services that involve large volumes of data proliferate while the available frequencies remain limited. A likely application for compression may lie in high-resolution, stereoscopic color-television broadcasting.

There are already many compression algorithms, each of which reduces the number of data bits that have to be transmitted by coding the data in a way that avoids the repetitive transmission of some redundant portions. For example, one algorithm could transmit only information on picture elements that have changed since the last transmission, another algorithm could specify an image in terms of its Fourier spatial frequencies, and the like. However, it may be impossible to choose in advance one algorithm that can reduce all sets of data to the proper length for transmission.

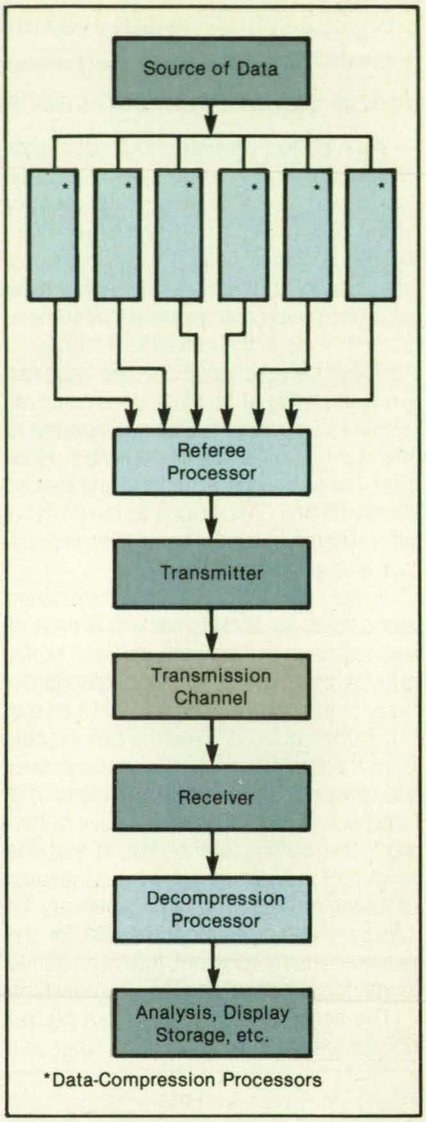

Data From an Information-Rich Source like a color-television camera would be compressed by several processors, each operating with a different algorithm. The referee processor would select the momentarily-best compressed output.

In the proposed system (see figure), the data from the source would be fed to several processors, each simultaneously executing a different data-compression algorithm. The outputs of these processors would be fed to a referee processor, which would choose the one most efficiently compressed. Along with a label that identifies its compression algorithm, the chosen output would be incorporated into a packet of data for transmission. Using the decompression algorithm corresponding to the compression algorithm of the label, the receiving station would reconstruct the full stream of data.

When the data could not be compressed to within the limited bandwidth of the transmission channel, the referee processor would choose whichever incomplete compressed output could be utilized best by the receiving station. (This may not always be the compressed output with the fewest bits.) The chosen output would be transmitted with an additional label warning that the data are not accurate. This would inform the processing equipment and user as to which was the most-recent accurate set of data and whether the present data can be trusted.

This work was done by Daniel B. Diner of Caltech and Antony R. H. Fender of Lama Engineering for **NASA's Jet Propulsion Laboratory**. *For further information, Circle 44 on the TSP Request Card.* *NPO-17445*

Integrated Optoelectronic Interface

A "universal" interface would be easily adaptable to specific equipment.

NASA's Jet Propulsion Laboratory, Pasadena, California

A proposed optoelectronic integrated-circuit device would serve as a "universal" or standard interface for the transmission and reception of digital and analog signals in communication, data-processing, and control systems. The device would eliminate the need for the custom design of interface circuitry in the sense that it would embody a "master-chip" design that would be easily adaptable to use with specific equipment.

The device would include a directly modulated semiconductor laser to generate light signals for transmission along an optical fiber; a positive/intrinsic/negative, avalanche, or other photodiode to detect light signals received along another optical fiber; and driving, synchronizing, preamplifying, and signal-regenerating circuitry. The device would be able to multiplex the electronic signals before transmission and/or demultiplex the electronic signals after reception.

The various configurations and modes of operation of the interface would include the following (see figure):

- Simplex Transmitter: In this mode, the device would transmit an optical signal amplitude-modulated in proportion to the input electronic signal.
- Simplex Receiver: In this mode, the device would receive optical signals, detect them, and shape them so that they could directly drive digital electronic circuitry.
- Duplex Transceiver: This mode would be a combination of the two simplex modes.
- Digital Repeater: This mode would be useful in an application in which the link is too long to maintain repeaterless transmission. In this case, the output of the receiver circuit would be connected directly to the laser driver.
- Analog Repeater: In this mode, the detected signal would not be fed into the digital shaping circuitry, but directly routed to the laser driver. This configuration would be most appropriate for the highest operating speed.

The configuration for a specific case could be selected at one of the last steps of fabrication of the device, by use of specialized metallization masks. Alternatively, the interconnections could be made via transistor switches, which could be controlled by external logic circuitry, internal logic circuitry, software supplied by the user, or some combination of these.

The concept of the interface is based on the level of integration achievable in current technology. It also provides for anticipated technological progress; e.g., the replacement of AlGaAs integrated circuitry with InGaAsP circuitry. In addition, the "master-chip" concept can be extended to

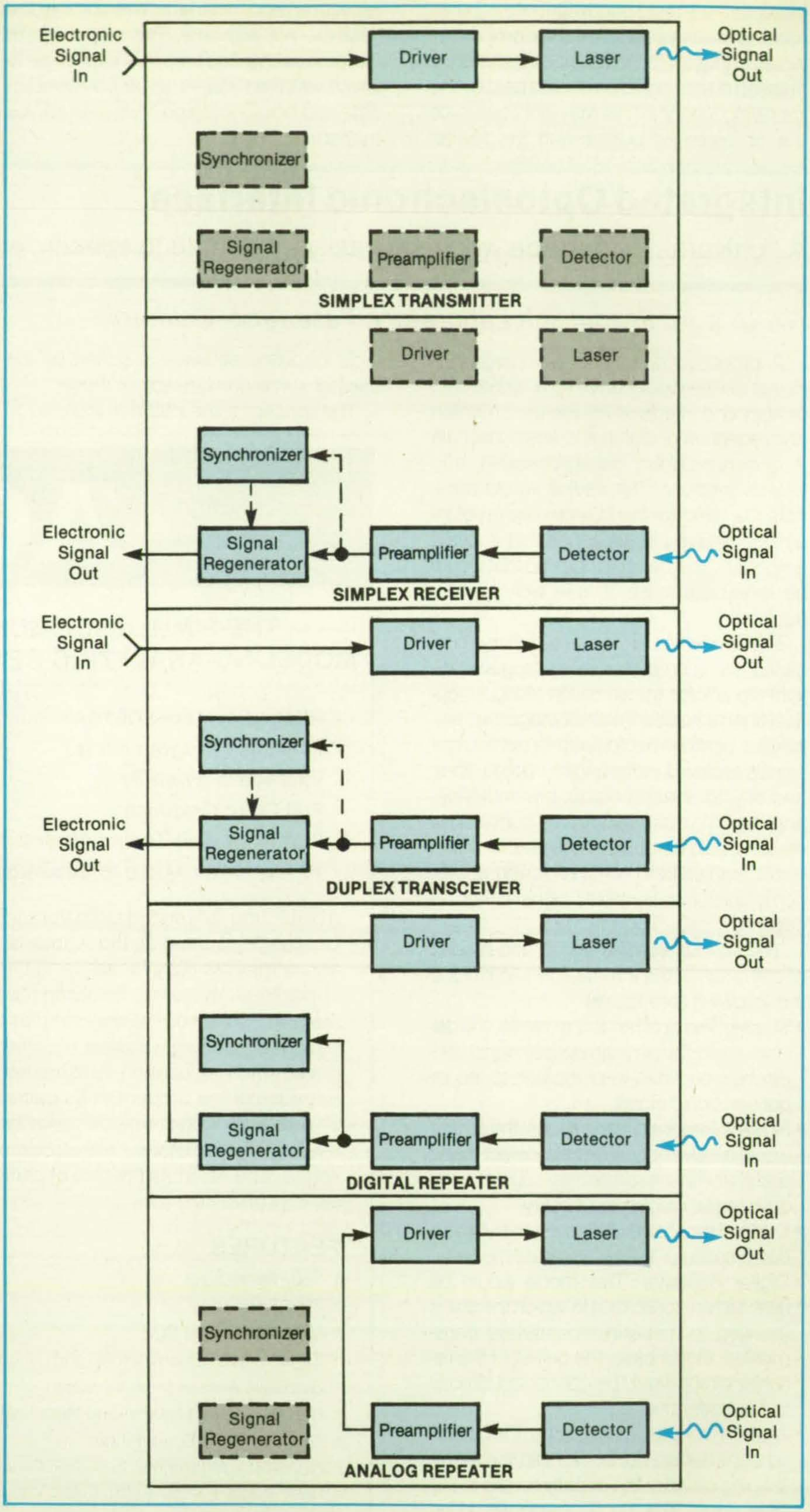

The **Integrated Optoelectronic Interface** would be made as a "master" integrated-circuit chip. The interconnections between the component circuits on the chip could be selected to choose any of the operating modes and configurations shown here.

optoelectronic circuitry of greater complexity to address more-general issues in the optoelectronic processing of signals.

This work was done by Joseph Katz of Caltech for **NASA's Jet Propulsion Laboratory**. *For further information, Circle 9 on the TSP Request Card.*

Inquiries concerning rights for the commercial use of this invention should be addressed to the Patent Counsel, NASA Resident Office-JPL [see page 16]. Refer to NPO-17650

Books and Reports

These reports, studies, handbooks are available from NASA as Technical Support Packages (TSP's) when a Request Card number is cited; otherwise they are available from the National Technical Information Service.

Laser Doppler and Range Systems for Spacecraft

Active transponders would be used to measure delays and shifts in frequencies.

A report discusses two types of proposed laser systems containing active transponders that would measure the distance (range) and line-of-sight velocity (via the Doppler effect) between a deep space vehicle and an earth-orbiting satellite. A laser system offers a diffraction advantage over a microwave system. It can deliver comparable power to a distant receiver while using smaller transmitting and receiving antennas and a less-powerful transmitter. Furthermore, laser beams are less subject to phase scintillations caused by passage through such inhomogeneous media as the solar corona.

One type of system is called "incoherent" because the range and Doppler measurements would not require coherence with the laser carrier signals. In a system of this type, a radio-frequency subcarrier, the two-way Doppler shift of which is to be measured, and a range code, the two-way time delay of which is to be measured, would be combined at the near (master) transmitter to modulate the intensity of a laser carrier, thereby generating the forward-link optical signal. Each optical receiver would consist of only a telescope and a photodetector. The sensitive phase-locked tracking functions would be performed after photodetection at radio frequencies, where the technology is mature.

At the distant receiver, a phase-locked-loop subsystem would serve as a narrowband frequency-tracking filter for the detected radio-frequency subcarrier, while a code-tracking subsystem would track the range code. The outputs of these subsystems would be combined to modulate the intensity of transponder laser for the return link. Back at the master terminal, the photodetected return subcarrier and range code would again be tracked and used for two-way range and Doppler measurements.

The other type of system is called "coherent" because successful operation would require coherent tracking of the laser signals. This type of system would require larger and more-complicated receivers. Like an incoherent system, a coherent system would use a ranging code on a radio-frequency subcarrier. However, it would use phase modulation instead of intensity modulation. The system would employ homodyne optical receivers in which the range would be extracted from the modulation and the Doppler measurement would be extracted from the carrier. The advantage of this concept is that the Doppler shift in the frequency of the carrier is much greater than that of the subcarrier, enabling more precise measurement of velocity.

The distant terminal would use an optical Costas loop to track the forward-link laser carrier and to reconstruct the forward-link range code on the subcarrier. The tuned laser output from the optical Costas loop would serve as the laser carrier for the return link, which would be modulated by the range code. At the master terminal, an optical Costas loop would track the return-link laser carrier, using a heterodyne principle to compare the frequencies of the forward and return links.

This work was done by P. W. Kinman of Caltech and R. M. Gagliardi of the University of Southern California for **NASA's Jet Propulsion Laboratory**. *To obtain a copy of the report, "Doppler and Range Determination for Deep Space Vehicles Using Active Optical Transponders," Circle 26 on the TSP Request Card.*
NPO-17486

Output Control Using Feedforward and Cascade Controllers

Open-loop solutions to the output-control problem are studied.

A report presents a theoretical study of open-loop control elements in a single-input, single-output linear system. The focus is on the output-control (servomechanism) problem, in which the objective is to find the control scheme that causes the output to track certain command inputs and to reject certain disturbance inputs in the steady state.

The output $y(t)$ of the system to be controlled (where t = time) is expressed as a weighted sum of the control input $u(t)$, the disturbance input $w(t)$, and the state of the system $x(t)$. The internal dynamics of the system are described by expressing the rate of change of $x(t)$ as a weighted sum of $x(t)$, $u(t)$, and $w(t)$. A disturbance-feedforward controller (called simply the "feedforward" controller) provides a filtered version of $w(t)$ to the input terminal, where it constitutes an additive component of $u(t)$. A command-feedforward controller (called the "cascade" controller) provides a filtered version of the command signal $v(t)$ that also is an additive component of $u(t)$.

The equations that describe the foregoing are Laplace-transformed into transfer-function form. The problem then becomes one of finding the Laplace transforms $P(s)$ of the feedforward controller and $Q(s)$ of the cascade controller (where s = the Laplace-transform complex frequency) that make $y(t)$ track $v(t)$ and suppress the influence of $w(t)$ on the output in the steady state.

Assuming that the system is stable, it is shown that a necessary and sufficient condition for the $P(s)$ that rejects $w(t)$ in the steady state is that the poles of $W(s)$ [the Laplace transform of $w(t)$] not coincide with the zeros of the control component of the transfer function of the system. The ideal $P(s)$ can be calculated as a ratio of the control component to the disturbance component of the transfer function of the system, evaluated at the poles of $W(s)$. The zeros of $W(s)$ need not be known.

Similarly, it is shown that a necessary and sufficient condition for the $Q(s)$ that makes $y(t)$ track $v(t)$ in the steady state is that the poles of $V(s)$ [the Laplace transform of $v(t)$] also not coincide with the zeros of the control component of the transfer function of the system. The ideal $Q(s)$ can be calculated as a reciprocal of the control component of the transfer function of the system, evaluated at the poles of $V(s)$.

Next, it is shown that if the system is unstable, it can be stabilized by the addition of a feedback controller $K(s)$, the form of which is determined by using standard procedures. The selection of $K(s)$ has no effect on $Q(s)$ and $P(s)$; that is, the feedback controller can be designed independently of the feedforward and cascade controllers.

The report closes with a brief discussion of the characteristics and relative merits of feedforward, cascade, and feedback controllers and combinations thereof. The main points can be summarized as follows:

- Where the time constants of a system are appreciable, a feedback controller is inefficient for the rejection of disturbances, but a feedforward controller can counteract the effects of disturbances quite well.
- In principle, feedforward controllers can track commands and reject disturbances perfectly, but, to do so, they require exact knowledge of the parameters of the system and cannot accommodate changes in these parameters.
- Feedforward and cascade controllers are generally simpler and of lower order than are feedback controllers.
- Feedforward control can reject only measurable disturbances.

This work was done by Homayoun Seraji of Caltech for **NASA's Jet Propulsion Laboratory**. *To obtain a copy of the report, "Output Control Using Feedforward and Cascade Controllers," Circle 43 on the TSP Request Card.*
NPO-17420

High-Sensitivity Ionization Trace-Species Detector

Features include high ion-extraction efficiency, compactness, and light weight.

NASA's Jet Propulsion Laboratory, Pasadena, California

An ionization/mass-spectrometer detector of trace molecular species features space-charge-limited reversal electron optics that provide controllability for the generation of positive or negative ions. The detector, an improved version of a previous ionization detector, features an in-line geometry that enables the extraction of almost every ion from the region of formation. The in-line feature also makes the instrument compact and light in weight.

In the instrument, a jet of gas containing the trace molecular species of interest is ionized by a beam of electrons. To generate negative ions by attachment of electrons, one would normally use electrons with a kinetic energy of 0 to 20 eV; to generate positive ions, one would normally strike the molecules with electrons of about 40 to 70 eV.

The electrons are generated at a filament and focused by electron optics to a space-charge-limited reversal region (see figure), where the gas to be analyzed is introduced. At the point of reversal, the lateral and longitudinal components of the velocity of the electrons are very nearly zero. By suitable adjustments of the electric potentials applied to the electron-optics-lens electrodes 1 through 7, the point of reversal can be moved to the left or right between electrodes 6 and 7.

If the point of reversal coincides with the jet of gas, then the directed kinetic energy of the bombarding electrons is nominally zero. If the point of reversal is moved to the right, then the kinetic energy of the electrons at the point of bombardment is greater because at that point they have not yet been reversed. Because the electrons are reflected back to the filament along the path of the incoming electron beam, each electron crosses the gas twice, thus doubling the detection sensitivity by doubling the effective density of ionizing electrons.

The design of the instrument is simplified by using some of the same electrodes for both the electron-focusing and ion-focusing operations. Fast electronics switch between these two operations with a duty cycle of one-half and nearly 100 percent extraction of ions during the ion portion of the cycle. First, a pulse of electrons is generated by applying suitable pulsed voltages to electrodes 1 through 7. Within 2 μs after turning off the electrons, the ions are extracted by the application of suitable pulsed voltages to electrodes 5 through 7. The ions travel out toward the right, into a time-of-flight or quadrupole mass analyzer.

This work was done by Mark T. Bernius and Ara Chutjian of Caltech for **NASA's Jet Propulsion Laboratory**. *For further information, Circle 48 on the TSP Request Card.*

Inquiries concerning rights for the commercial use of this invention should be addressed to the Patent Counsel, NASA Resident Office-JPL [see page 16]. Refer to NPO-17596

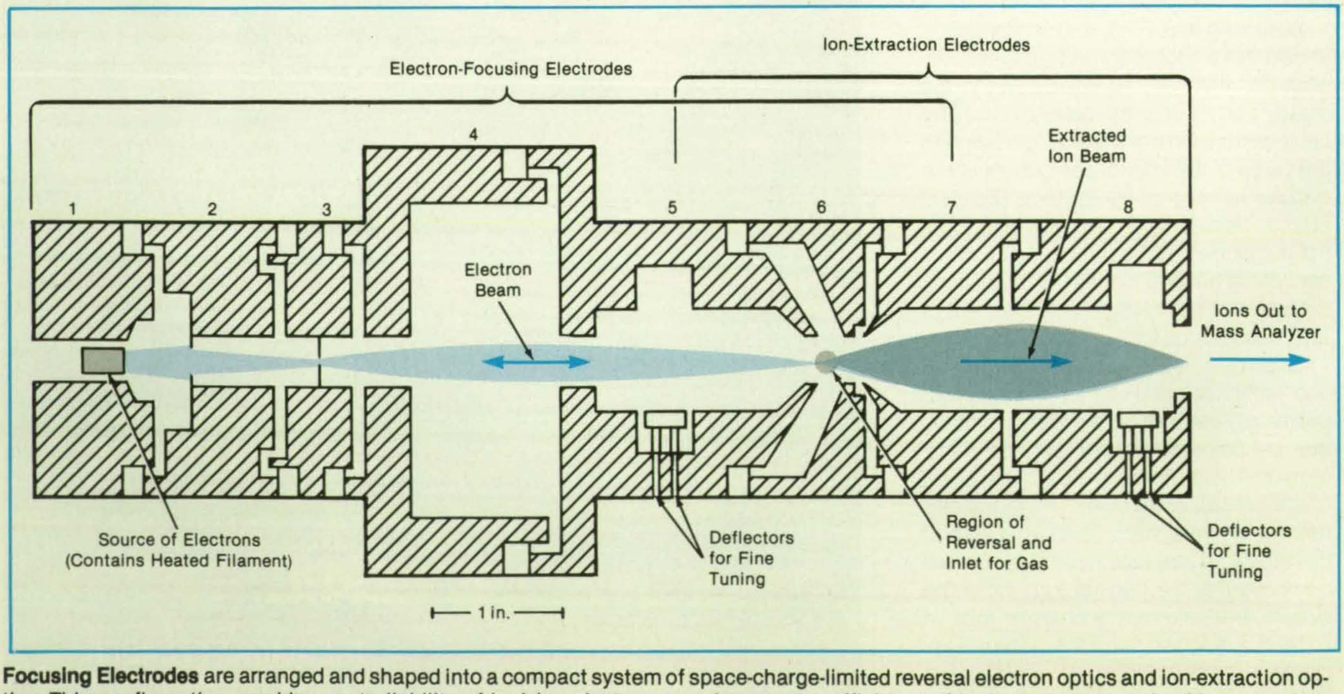

Focusing Electrodes are arranged and shaped into a compact system of space-charge-limited reversal electron optics and ion-extraction optics. This configuration provides controllability of ionizing electron energies, greater efficiency of ionization, and nearly 100 percent ion-collection efficiency.

Books and Reports

These reports, studies, handbooks are available from NASA as Technical Support Packages (TSP's) when a Request Card number is cited; otherwise they are available from the National Technical Information Service.

Two Tethered Balloon Systems

These systems take meteorological measurements for a variety of research projects.

A report describes work done by NASA Langley Research Center in atmospheric research using tethered balloon systems composed of commercially available equipment. Two separate tethered balloon systems described in the report have payloads and configurations tailored to the requirements of specific projects. Each system is capable of measuring an atmospheric parameter or species in situ and then telemetering this data in real time to a ground station. Meteorological data and the concentration of ozone are typically measured with these systems.

The two systems are distinguishable by their sizes among other characteristics. There are two versions of the large system, in which the balloons differ in the number of dilation panels. The balloons of the larger version of the large system are aerodynamically-shaped, nonrigid structures conforming to a modified class "C" shape with a fineness ratio of 2.75 to 1.

The small balloon system is capable of lifting 2.75 kg of payload to a height of 800 m. Four channels of data can be serially telemetered to the ground for real-time or postexperiment analysis. The larger balloon system can lift 45 kg to 775 m or 30 kg to 2,500 m. The telemetry system has six channels for the acquisition of data, which are stored for subsequent analysis. Any four of the channels can be displayed in real time. The tethered balloons can be stationed at a set altitude or moved up and down at a rate changing from 0 to 45 m/min.

The small balloon system, used primarily to obtain meteorological and ozone data in the field, consists of a blimp-shaped balloon, a sensor package, an electric winch with 800 m of 50-kg test line, and a ground station with a modified HP-97 (or equivalent) calculator. The entire system is portable and designed to be set up and operated by two people. Profiles of the atmosphere from ground to 800 m and return can be taken in about 55 min. Full-scale synchronization and zero references are included in the recorded data to simplify interpretation in real time and to ensure the quality of data. All data are linear

and scaled for quick interpretation on charts.

The report indicates that instrumented tethered balloon systems have distinct advantages over other systems for gathering data on the troposphere. For example, the balloon systems provide both vertical and horizontal variability that cannot be achieved with ground-based systems and do not suffer from sampling problems caused by lack of instrument response and by difficulties in reconciliation of probe losses found in aircraft-based systems. In addition, the frequency-modulation sideband configuration used for telemetry provides for simultaneous multiple-parameter measurements, and the real-time capability enables researchers to make decisions in the field during experiments.

This work was done by Otto Youngbluth, Thomas L. Owens, and Richard W. Storey of **Langley Research Center**. *Further information may be found in NASA TM-83260 [N87-18936], "NASA Langley Research Center Tethered Balloon Systems."*

Copies may be purchased [prepayment required] from the National Technical Information Service, Springfield, Virginia 22161, Telephone No. (703) 487-4650. Rush orders may be placed for an extra fee by calling (800) 336-4700.

This invention is owned by NASA, and a patent application has been filed. Inquiries concerning nonexclusive or exclusive license for its commercial development should be addressed to the Patent Counsel, Langley Research Center [see page 16]. Refer to LAR-13837.

Cell Model of a Disordered Solid

Elastic properties are predicted from first principles.

A paper discusses a generalization of the cell theory of a disordered (that is, noncrystalline) solid to include anisotropic stresses. This study is part of the continuing effort to understand the macroscopic stress-and-strain properties of solid materials in terms of microscopic physical phenomena. The emphasis here is on the derivation, from first principles, of the bulk, shear, and Young's moduli of a glassy material at zero absolute temperature.

According to the cell theory developed previously, the solid material is treated as a collection of interacting spherical cells. A mean-field-theory approximation is used to derive a simple algebraic expression for the Helmholtz free energy, F, an integral over the surface of one cell for the energy E required to displace a reference particle in that cell, and an integral over the volume of the cell to obtain the free volume v_f of the cell for thermodynamic purposes. The two integral equations, together with the rela-

tion between the radius of a cell and the volume of a molecule, yield the equation of state and the bulk modulus, K, in the undeformed state.

The authors indicate the following general approach: Each cell is considered subject to identical strains, which are specified macroscopically. The strains transform a spherical cell into an ellipsoid, and the reference particle is displaced in its cell proportionately. The equations for F, E, and v_f are used to find the change in F due to the strain, and the change in F is used to find K. Poisson's ratio, μ, is introduced, and the Young's modulus, Y, is calculated from K.

The calculations are simplified in the limits of zero absolute temperature and low pressure [of the order of 1 atm (about 0.1 MPa)]. The Lennard-Jones potential $U(R) = -AR^{-n} + BR^{-m}$ (where A, B, m, and n are constants) is used for the energy of interaction between the reference particle and a particle on the surface of the cell at distance R. After extensive algebraic manipulations and the invocation of the zero-temperature condition and the low-temperature approximation, the equations for the elastic constants become

$$K = -(Nz/18)U_{min}nm/V_{00}$$
$$\mu = 1/4$$
$$Y = 1.5K$$
$$G = 0.6K$$

where N is the number of spherical cells, z is the number of nearest neighbor cells, U_{min} is the minimum value of U, V_{00} is the volume of the undeformed solid, and G is the shear modulus.

These results were obtained by including interactions between nearest neighbor cells only. Computations have also been done for interactions out to a third layer of cells for a potential with $m = 12$, $n = 6$, with the result that K is multiplied by 1.435, μ changes to 0.271, and the factor 0.6 decreases to 0.54. Although the numerical values appear to agree reasonably with observations of glassy materials, the observations were made at higher temperatures. Consequently, future efforts are expected to focus on the change of the elastic constants with temperature.

This work was done by Steven T. J. Peng, Robert F. Landel, and Jovan Moacanin of Caltech and Robert Simha and Elizabeth Papazoglou of Case Western Reserve University for **NASA's Jet Propulsion Laboratory**. *To obtain a copy of the report, "Cell Model and Elastic Moduli of Disordered Solids: Low Temperature Limit," Circle 31 on the TSP Request Card.*

Inquiries concerning rights for the commercial use of this invention should be addressed to the Patent Counsel, NASA Resident Office-JPL [see page 16]. Refer to NPO-17217.

Convective Evaporation of Clusters of Drops

Effects in sprayed liquid fuels are studied theoretically.

A report presents the results of continuing theoretical research in the behaviors of sprayed liquid fuels at temperatures characteristic of furnaces. Two earlier papers arising from this investigation were described in "Evaporation of Dense Fuel Sprays" (NPO-16954), *NASA Tech Briefs*, Vol. 12 No. 6 page 66.

As in the previous studies, the mathematical model of the spray includes a spherical cluster of droplets of a single-component fuel. The droplets all have the same diameter, are uniformly distributed throughout the cluster, and move together at the same velocity through the convective flow of air, evaporated fuel, and combustion products. Classical equations for the flow of heat, conservation laws, and the ideal-gas law are used to calculate the temperature in, and the evaporation from, each droplet. The rate of evaporation is expressed by a generalized, more realistic version of the Clausius-Clapeyron equation.

Also as in the previous studies, the important aspects of the interaction between the cluster of droplets and the surrounding flow are considered to be the following:

1. The extent of penetration of the cluster at each instant (which droplets "feel" the flow);
2. The instantaneous relative speed between the cluster and the flow; and
3. The relationship between the rates of evaporation with and without flow.

A comparison is made between the flow of gases evaporated from the drops and the flow of gases from the outer flow at the surface of the cluster. This yields a dynamic criterion to determine whether the external flow penetrates the cluster. An expression is also derived for the radius of partial penetration.

Again, as in the previous studies, the mathematical model was found to perform well for low penetration distances in dense clusters in hot environments with low relative speeds. The model predicts that, for the same initial velocity, the evaporation time is less for more-dilute clusters. For dilute clusters and large penetration distances, the model predicts that the evaporation time increases with dilution; however, this result is questionable inasmuch as the model is not considered to be valid in this regime.

The evaporation time was found to be a weak function of the initial relative speed and a strong function of the initial temperature of the droplets. The initial temperature of the surrounding gas has a strong influence in the lower-temperature (750 to

1,000 K) regime and a weak influence in the higher-temperature regime. The vitiation of the ambient gas by the fuel vapor was found to have a very small influence on the evaporation time of a rich mixture when the cluster is introduced into hot, strongly convective surroundings. In all cases, the interior temperatures of the drops were transient throughout the lifetimes of the drops, but nonuniformities of these temperatures persisted at most during the first third of the evaporation time.

This work was done by Josette Bellan and Kenneth G. Harstad of Caltech for **NASA's Jet Propulsion Laboratory**. *To obtain a copy of the report, "Analysis of the Convective Evaporation of Non-Dilute Clusters of Drops," Circle 38 on the TSP Request Card.*
NPO-17171

Survey of Gas-Correlation Spectroradiometry

The principal application is remote sensing of atmospheres.

A brief report discusses the use of gas-correlation spectroradiometry in remote measurements of the atmosphere of the Earth and other planets. It summarizes the history of the technique from the first such instrument flown aboard the Nimbus 4 Satellite in 1970 to one that is to fly on the Mars Observer Spacecraft to measure the vertical distribution of water vapor and temperature.

The major advantages of gas-correlation spectroradiometry — high spectral discrimination coupled with the ability to work with weak signals — can be realized only when the widths of the observed spectral lines are small compared with the spaces between the lines. For this reason, on Earth the technique is applied mostly to the upper atmosphere and only infrequently to the troposphere, where pressure broadening tends to blend spectral lines.

The Nimbus 4 Selective Chopper Radiometer made nadir-viewing emission-radiometery measurements of stratospheric temperatures via the 15-μm band of CO_2. In a selective chopper, two optical paths that contain different amounts of the gas of interest are sampled alternately by a detector, and the radiometric difference between them is a measure of the radiation originating in the atmosphere within the spectral lines of the reference gas. Although the technique presents difficulties in calibration, the Nimbus 4 and succeeding Nimbus 5 investigations provided the first global maps of temperature in the upper atmosphere.

The development of pressure-modulator radiometers provided a solution to the calibration problem. In this approach, there is only one optical path through the reference gas. A piston driven at reso-

nance modulates the amount of gas in a cell. The correlation signal is derived from the phase-sensitive detection of the modulation of radiation transmitted by the cell. An instrument of this type was first flown in 1975 for limb measurements of stratospheric and mesospheric temperatures and abundances of CO, CH_4, NO, N_2O, and H_2O. Another such instrument measured temperatures on the Pioneer Venus mission, and others are under development for use on future Earth-orbiting and outer-planetary missions.

The newest version of the technique — electro-optical phase-modulation gas-correlation spectroradiometry — has been developed with a view toward the measurement of winds in the upper atmosphere from a satellite moving much faster than the winds. This technique involves the use of an electro-optical modulator instead of a pressure modulator. In addition, the frequency distribution of the observed spectrum is under the control of the instrument, making it possible to perform the frequency-correlation measurements needed to sense winds.

This work was done by Daniel J. McCleese of Caltech for **NASA's Jet Propulsion Laboratory**. *To obtain a copy of the report, "Remote Sensing of Earth and Planetary Atmospheres Using Gas Correlation Spectroradiometry," Circle 34 on the TSP Request Card. NPO-17345*

Interpolation and FFT of Near-Field Antenna Measurements

The bivariate Lagrange interpolation is applied to plane-polar measurement scans.

A report discusses some recent advances in the application of fast-Fourier-transform (FFT) techniques to measurements of the near radiation fields of antennas on a plane-polar grid. Attention is focused mainly on the use of such measurements to calculate far radiation fields. There is also some discussion of the use of FFT's in the holographic diagnosis of distortions of antenna reflectors.

To apply the FFT, it is necessary to obtain measurements at points spaced regularly on a rectangular grid in a plane. However, it is often more practical to measure at equal radial and angular intervals on a plane-polar grid. The authors use the bivariate Lagrangian interpolation scheme to estimate the field quantities at each point on the rectangular grid from the field quantities measured at, and the coordinates of, the four nearest points on the polar grid. The advantage of this scheme is that it speeds the calculations because it requires fewer data and manipulations of data than do other schemes used for this purpose.

The interpolation is carried out at points on the rectangular grid, the outermost lines of which are tangent to the outermost measurement circle. At points on the rectangular grid outside this circle, the measured field is arbitrarily assigned the value of zero, as is often done in such cases. The horizontal grid interval Δx may differ from the vertical interval Δy as long as these intervals satisfy the requirements for the FFT and define the measurement plane fully. The data on the amplitude and phase of the field are converted to, and interpolated as, complex numbers; this is not mathematically equivalent to interpolation of the amplitude and phase themselves. However, the results of the FFT are nearly the same in both cases, and the complex-number representation is better suited to the FORTRAN computing routines used by the authors.

To compute the far field from the measured near field, the near-field quantities are first converted to an apparent induced current in the measurement plane. The far field is related to this apparent induced current via a radiation integral, which can be written as a Fourier transform. The integration is computed as an FFT, with transform variables u, v [$u = \sin(\theta)\cos(\phi)$; $v = \sin(\theta)\sin(\phi)$, where θ and ϕ are the polar and azimuthal angles of the observation vector

to the far-field point in a spherical coordinate system, and u and v are thus proportional to the rectangular far-field coordinates].

With respect to holographic diagnosis, the previous literature describes the deduction of distortions of reflector surfaces from far-field measurements. In this study, the authors bypass the measurements and calculations of the far field and instead diagnose the distortion by applying FFT's to the near-field measurements. The effects due to the focusing of the radiation emerging from the reflector and the effects of the information in the wide-angle regions of the far field upon the computed distortion are examined. The authors recommend further study in this area.

This work was done by Mark S. Gatti and Yahya Rahmat-Samii of Caltech for **NASA's Jet Propulsion Laboratory**. *To obtain a copy of the report, "FFT Applications to Plane-Polar Near-Field Antenna Measurement," Circle 78 on the TSP Request Card.*
NPO-17597

Absorption of Gases by Glassy Polymers

Infinite-dilution partial molar volumes are calculated from pressure, volume, and temperature data.

A report discusses the solubility of a gas in a glassy polymer, both above and below the glass-transition temperature (T_g). Thermodynamic arguments are brought to bear on previously-developed mathematical models, the result being a new model that enables the calculation of the infinite-dilution partial molar volume of the solvent in the glass or liquid solvent from data on the pressure, volume, and temperature of the solute in equilibrium with the solvent.

The text begins with a review of previous experimental and theoretical investigations. It describes the dual sorption model, in which Henry's law is corrected by the addition of terms to account for absorption in fixed sites or microvoids. The concentration of the microvoids is assumed to be proportional to the difference between the specific volume of the glass and the specific volume of the liquid extrapolated down to the temperature of the glass. Previous studies pertaining to the dual sorption model, including a model that expresses its relationship to the partial molar volume of the solute, are also described.

A chemical-potential model is introduced to analyze the situation at equilibrium and infinite dilution. The chemical potential of the solute in the vapor or gaseous phase is assumed to equal that in the glass. Similarly, the chemical potential of the solute in the gas or vapor is taken to equal that of the solute in the liquid. As a result, the equations for the chemical potentials can be manipulated to yield an equation for the ratio between the equilibrium concentrations of solute in the glass and liquid, in terms of the difference between the chemical potentials of the gas and liquid in standard states.

The equation for the change in chemical potential of a substance at constant temperature is used to obtain additional equations for this difference between chemical potentials, in terms of the infinite-dilution specific volumes of the solute in the liquid and in the glass, and of the pressure or negative pressure that would convert the glass to a liquid or the liquid to a glass, respectively, at the given temperature.

Various equations are then derived to facilitate the comparison of the theory with data on pressures, volumes, and temperatures. It is shown that the theory basically agrees with experimental data; i.e., that it is possible to estimate the partial molar volumes of the solute in both the glass and liquid states of the polymer. Furthermore, the analysis predicts that the partial molar volume in the liquid exceeds that in the glass.

This work was done by Robert F. Fedors of Caltech for **NASA's Jet Propulsion Laboratory**. *To obtain a copy of the report, "Absorption of Fluids by Glassy Polymers," Circle 70 on the TSP Request Card.*
NPO-17636

Materials

Finding Platinum-Coating Gaps on Titanium Anodes

A simple procedure makes gaps visible to the eye.

Marshall Space Flight Center, Alabama

Gaps in platinum coats (more precisely, platinum plate with rhodium overplate) on titanium electroplating electrodes can be found by a simple method. Such electrodes are used as anodes to plate copper on electrical and mechanical parts; they produce uniform plate of controlled thickness and bond strength. If, however, the platinum does not cover the titanium anode completely, titanium oxide forms on the unprotected titanium. Plating current cannot pass through the oxide, and the resulting copper plate tends to blister and to vary in thickness in areas near the gaps.

Gaps in titanium coverage cannot be detected visually. Until now, the presence of gaps could be detected only via the poor quality of the resulting plate. The anode had to be stripped and replated with platinum before it could be used successfully to plate copper onto other objects.

The new gap-detection method consists of plating a thin layer of a non-silver-colored metal like copper or gold on the anode. The contrast in color between the plated metal and the bare anode material makes gaps stand out. If the anode passes inspection, the copper or gold plate should be removable by reversal of the test-plating current. It remains to be determined whether the test plating and removal can damage the anode.

The new method is simpler and more economical than previous attempts to identify gaps in the platinum. For example, spot checks by emission spectroscopy proved to be inconclusive and destroyed the platinum coating in the immediate area. Another method — examining a charged anode in a sulfuric activation electrolyte to see whether gas bubbles are generated uniformly over the surface — was awkward and defined uncoated areas poorly.

This work was done by Ronnald Bodemeijer and Cecil E. Flowers of Rockwell International Corp. for **Marshall Space Flight Center**. *No further documentation is available.*

Inquiries concerning rights for the commercial use of this invention should be addressed to the Patent Counsel, Marshall Space Flight Center [see page 16]. Refer to MFS-29389.

Filling Porous Microspheres With Magnetic Material

Magnetic properties and particle sizes are controllable.

NASA's Jet Propulsion Laboratory, Pasadena, California

A new process produces magnetic microspheres with controllable sizes, compositions, and properties for use in medical diagnostic tests, biological research, and chemical processes. Paramagnetic microspheres can also be made with the process. Other processes for making magnetic microspheres require that magnetic particles be prepared first and then be encapsulated in a polymer. With such processes, the magnetic material is not uniformly distributed in the spheres, and the size and size distribution of the spheres are difficult to control.

In the new process, porous plastic microspheres are prepared by polymerization of a monomer in a diluent by a cross-linking agent. When the diluent is removed, it leaves tiny pores throughout the polymerized spheres. The size and distribution of the pores are determined by the amount and type of diluent and cross-linking agent.

The plastic microspheres are soaked in a solution of equimolar amounts of ferrous and ferric chlorides, which diffuse into the pores. Finally, sodium hydroxide is added to the solution, and the ferrous and ferric ions precipitate from the solution to form fine-grained magnetite evenly dispersed throughout the pores. The magnetite can be oxidized to adjust its magnetic properties; for example, to impart super-paramagnetism.

The process was demonstrated with polyhydroxyethylmethacrylate (polyHEMA) microspheres prepared by gamma radiation of a HEMA/trimethylol-propane trimethacrylate (TEMPA) mixture in the presence of stabilizers. Approximately 0.1 g of the polyHEMA microspheres, 1 μm in diameter, were swelled in 20 mL of a saturated equimolar mixture of ferrous and ferric chlorides. After the system had reached equilibrium, the suspension was spun and the supernatant solution was discarded. A sodium hydroxide solution was added to the microspheres. They turned black immediately and could be attracted by a magnet.

The addition of ethylenediaminetetraacetic acid (EDTA) to the monomer produces microspheres with higher iron content. The EDTA acts as a complexing agent for ferrous and ferric ions. The process was also tested successfully on microspheres composed of polystyrene and divinyl benzene.

This work was done by Manchium Chang and Michael S. Colvin of Caltech for **NASA's Jet Propulsion Laboratory.** *For further information, Circle 76 on the TSP Request Card.*

In accordance with Public Law 96-517, the contractor has elected to retain title to this invention. Inquiries concerning rights for its commercial use should be addressed to

Edward Ansell
Director of Patents and Licensing
Mail Stop 305-6
California Institute of Technology
1201 East California Boulevard
Pasadena, CA 91125

Refer to NPO-17044, volume and number of this NASA Tech Briefs *issue, and the page number.*

Computer Programs

COSMIC: Transferring NASA Software

COSMIC, NASA's Computer Software Management and Information Center, distributes software developed with NASA funding to industry, other government agencies and academia.

COSMIC's inventory is updated regularly; new programs are reported in *Tech Briefs*. For additional information on any of the programs described here, circle the appropriate TSP number.

If you don't find a program in this issue that meets your needs, call COSMIC directly for a free review of programs in your area of interest. You can also purchase the annual *COSMIC Software Catalog*, containing descriptions and ordering information for available software.

COSMIC is part of NASA's Technology Utilization Network

COSMIC® — *John A. Gibson, Director,*
(404) 542-3265
The University of Georgia, 382 East Broad Street, Athens, Georgia 30602

Computer Programs

These programs may be obtained at a very reasonable cost from COSMIC, a facility sponsored by NASA to make computer programs available to the public. For information on program price, size, and availability, circle the reference number on the TSP and COSMIC Request Card in this issue.

Physical Sciences

Model of Orbital Density of Air for Computing Drag

The new, simple model reduces computation time.

The Simple, Orbital Density Model for Drag Equations program is useful for computing the effect of drag over one or more orbits. The mathematical model embodied in the program incorporates the major changes in density due to solar activity and the magnetic activity of the Earth. The diurnal (day/night) effects on an orbit are averaged out. Inputs to the simplified model are the geomagnetic index, the 10.7-cm solar-flux constant, and the geometric altitude in meters. The range of the geometric altitude is from 100,000 to 1,000,000 m.

A simplified version of the 1970 Jacchia model of density was used to develop the new, simplified model. The Jacchia model also accounts for diurnal variations, monthly variations, and latitudinal variations and requires a solar ephemeris. The new, simplified model is based on the Jacchia daily-average density, evaluated at an average time of year. The advantages of the new, simple model are that the right ascension and the declination of the Sun are not needed and that the computation time is much reduced. The density in the new, simple model agrees with the average Jacchia density to about 5 percent.

The Simple, Orbital Density Model for Drag Equations program was written in FORTRAN 77 for execution on an HP-9000 series computer. It has also been run on a Sun 3/280 under SUNOS (UNIX bsd 4.3). This program was developed in 1986.

This program was written by W. M. Lear, of TRW, Inc., for **Johnson Space Center**. *For further information, Circle 18 on the TSP Request Card.*
MSC-21154

Mechanics

Simulating Orbiting Spacecraft

A user-friendly, menu-driven program facilitates mathematical modeling of complicated spacecraft.

SPASIS is a computer program for the simulation of orbits around the Earth in six degrees of freedom. It was developed to investigate the orbital dynamics of spacecraft designed by users. SPASIS is a user-friendly, menu-driven program and contains many features relevant to current and advanced space systems.

The program accepts inputs in the form of files of data representing parameters of orbits, mass properties, the sizes and placements of components of the reaction control system, specifications of control-moment gyros, docking parameters, definitions of propellant tanks and liquids, characteristics of jets, requirements for maneuvers, and specifications of articulating components. In addition to these, a matrix of grid points and a surface-area model are entered to describe the configuration of the spacecraft.

SPASIS advances the spacecraft along its orbit by integrating equations of translational motion. Set in an inertial frame of reference, these equations are driven by gravitational, environmental, propellant-slosh, docking, plume-impingement, and control-system forces. The accelerations from the equations of motion, the orientation quaternion rates, and the control-moment-gyro gimbal rates are integrated with a fourth-order Runge-Kutta-Gill integrator. Simultaneously, the attitude of the spacecraft is monitored via rotational equations of motion. Environmental torques, articulation of panels, motions of propellants and mobile masses, and torques resulting from the impingement of plumes provide the spacecraft disturbances while the control systems supply the reaction moments.

SPASIS has a number of advanced modeling capabilities. A state-of-the-art Jacchia model is used to obtain atmospheric density. There are two mathematical models of the large-amplitude dynamics of propellants: LAMPS3 for exacting calculation and the simplified rolling-ball-slosh model. Three-dimensional articulating panels in the forms of Sun-tracking solar arrays and anti-Sun-tracking radiators can be designed. Also, the effects of a mobile remote-manipulator system or even an astronaut moving along a section of truss can be investigated through the mobile-mass model.

During each orbit an assortment of data is available for output, all under the control of the user. This output includes the following: parameters of orbits; responses of and to the attitude-control system; activities of the solar and radiator panels; mass properties of the spacecraft; forces and moments caused by the impingement of plumes; data for plotting the impingement of plumes; the effects of movable jets; the history of the centers of mass of the propellants (LAMPS3); histories of the location, force, and acceleration of propellants (rolling-ball model); data on the locations, velocities, and accelerations of mobile masses; and binary plotting data selected by the user.

SPASIS was designed to run interactively or in batch mode on a DEC VAX 8650 computer under VMS 3.4. The package is written entirely in FORTRAN 77 with approximately 1 percent being VAX-dependent extensions. A stand-alone plotting package that makes use of the DI3000 graphics-library and software is included. Methods for establishing interfaces with other graphics-library packages are presented in the documentation. The program was developed in 1988.

This program was written by J. M. Stecklein, C. Plowman, A. Lewis, B. Drake, and K. Leahy of Lockheed Engineering & Management Service Co. for **Johnson Space Center**. *For Further information, Circle 104 on the TSP Request Card.*
MSC-21462

Mechanics

Two-Fault-Tolerant Release Mechanism

Failure of two out of three pyrotechnic devices will not prevent operation.

Lyndon B. Johnson Space Center, Houston, Texas

A remotely-operated, compact quick-release mechanism will still function in the event that one or even two attempts to actuate it fail. The mechanism contains three independent pyrotechnic devices. Firing of any one of the devices is sufficient to actuate the mechanism.

The item to be released is secured to the upper end of a toggle (see figure). The toggle seats in a spherical bearing, and three symmetrically spaced pins secure the lower end of the toggle to the base structure.

Each pin retracts under pressure from hot gases when its associated pyrotechnic cartridge is ignited. If all three cartridges fire, all three pins retract and the toggle floats free. If only one or two cartridges fire, the toggle becomes asymmetrically loaded and rotates in its bearing so that it frees itself from the remaining one or two pins. Thus, it can still float free of the base structure.

Besides allowing rotation after retraction, the bearing also aligns the toggle during assembly. A screw thread on the outside surface of the bearing provides for the adjustment of preload tension on the toggle during assembly. The pins remain in the base structure after the toggle has been operated. No debris are released during operation.

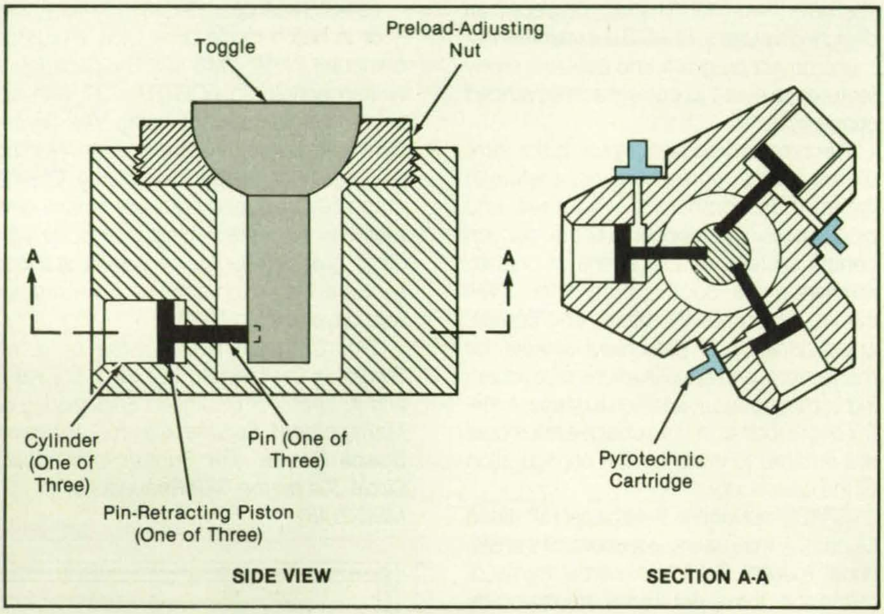

Three Pins Hold the Toggle at its base. The retraction of any one of the pins allows the toggle head to rotate in the spherical bearing to free itself from the remaining pin or pins.

This work was done by Thomas J. Graves and Robert A. Yang of **Johnson Space Center**. *For further information, Circle 23 on the TSP Request Card.*

This invention is owned by NASA, and a patent application has been filed. Inquiries concerning nonexclusive or exclusive license for its commercial development should be addressed to the Patent Counsel, Johnson Space Center [see page 16]. Refer to MSC-21354.

Pressure Gauges Monitor Leakage Past Seals

A statistical technique extracts additional information from measurements.

Lyndon B. Johnson Space Center, Houston, Texas

A method has been devised to measure the leakage of gas past each of two sets of primary and secondary seals into a common volume from which the aggregate flow can be measured. Although the method is applicable only to a specific combination of flow configuration and thermal conditions, it serves as an example of a more general approach that involves the use of statistical analysis to extract additional information from measurements.

As shown in the figure, gas at pressure P_{11} leaks past primary seal a_1 into an interseal space where the pressure is P_{21}. From there, it leaks past secondary seal b_1 into a fixed volume V, where the pressure is P_3. Similarly, gas at pressure P_{21} leaks past primary seal a_2 to intermediate pressure P_{22}, then past secondary seal b_2 to join the other leaked gas in volume V. The gas then flows from V through flowmeter c into a reservoir, vacuum, or the atmosphere at pressure P_4. All of the pressures are measured. In the case of P_3, the rate of change is also measured.

The system is assumed to be isothermal with absolute temperature T, and the flow past each seal and the flowmeter is assumed to obey the law of laminar, steady flow between closely-spaced parallel plates. It is also assumed that nowhere in the system does the gas condense into liquid. Under these conditions, the mass-flow rates w_i indicated on the figure are given by

$$w_1 = a_1(P_{11}^2 - P_{12}^2) = b_1(P_{12}^2 - P_3^2)$$

$$w_2 = a_2(P_{21}^2 - P_{22}^2) = b_2(P_{22}^2 - P_3^2)$$

$$w_3 = c(P_3^2 - P_4^2)$$

$$\frac{dm}{dt} = w_1 + w_2 - w_3$$

$$\frac{dm}{dt} = \frac{V}{RT}\frac{dP_3}{dt}$$

where a_1, a_2, b_1, and b_2 are the unknown laminar-flow resistance coefficients of the seals so labeled; c is the laminar-flow resistance coefficient of the flowmeter, which is known from the calibration; R is the ideal-gas constant; m is the mass of gas in volume V; and t = time.

Because there are six unknowns and only five equations, a complete solution cannot be obtained from a single set of pressure measurements. However, the solution can be completed by applying the method of multiple linear regression to sets of measurements taken at different pressures. For the ith set of measurements, the following quantities are defined:

$$x_1(i) = P_{12}^2(i) - P_3^2(i),\ x_2(i) = P_{22}^2(i) - P_3^2(i), \text{ and } y(i) = c[P_3^2(i) - P_4^2(i)] + (V/RT)\frac{dP_3(i)}{dt}$$

The following additional quantities are then defined:

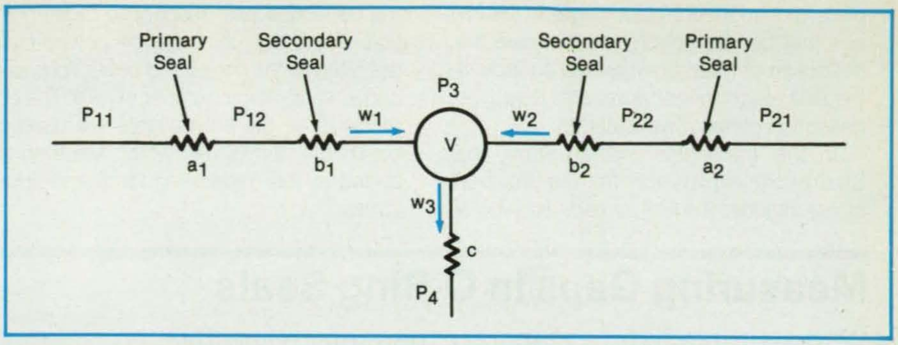

The **Pressures Are Measured** on both sides of each primary and secondary seal and on both sides of the calibrated restriction c. In addition, the rate of change of pressure in the common volume V is measured. From several sets of these measurements, one can determine the resistances of the seals and the rates of leakage.

$$c_{jk} = \sum_{i=1}^{m} x_j(i)\,x_k(i) \text{ and } z_j = \sum_{i=1}^{m} x_j(i)\,y(i)$$

where j and k can each equal 1 or 2 and m equals the number of sets of measurements. Then the result of the linear-regression analysis is

$$b_1 = (c_{22}z_1 - c_{12}z_2)/(c_{11}c_{22} - c_{12}c_{21})$$
$$b_2 = (c_{11}z_2 - c_{21}z_1)/(c_{11}c_{22} - c_{12}c_{21})$$

These estimates of b_1 and b_2, together with the equations for the mass-flow rates, can be used to determine the remaining unknowns a_1, a_2, w_1, and w_2.

This work was done by Steven A. Smith of Boeing Aerospace Co. for **Johnson Space Center**. *For further information, Circle 2 on the TSP Request Card.*
MSC-21385

Interferometric Measurement of Residual Stress

The stress averaged through the thickness of a plate can be measured nondestructively.

NASA's Jet Propulsion Laboratory, Pasadena, California

The theory of elasticity has been combined with a laser interferometric technique into a technique for the measurement of residual stresses in solid objects — usually in thin, nominally-flat plates. Unlike some prior techniques that measure stresses only near the surface or require destruction of part of each specimen, the new technique is nondestructive and measures the stress averaged through the thickness underlying each point of interest on the surface. Such measurements will be particularly useful in the inspection of wafers of single-crystal silicon for making solar cells or integrated circuits, because stresses that remain after the crystal-growing process can cause buckling or fracture.

The theory of elasticity of thin plates can be used to predict deflections of the plates caused by known applied loads under specified boundary condition, or to infer the applied loads that cause known deflections. Similarly, the theory can be used to relate known deflections to residual stresses equivalent to stresses that would be produced by fictitious applied loads. In the new technique, the deflection of a specimen is measured under a known load (or no load) and compared with the corresponding deflection predicted for the specimen in the absence of residual stress. The difference between the predicted and measured deflections is then attributed to the residual stress.

The figure illustrates a measurement of

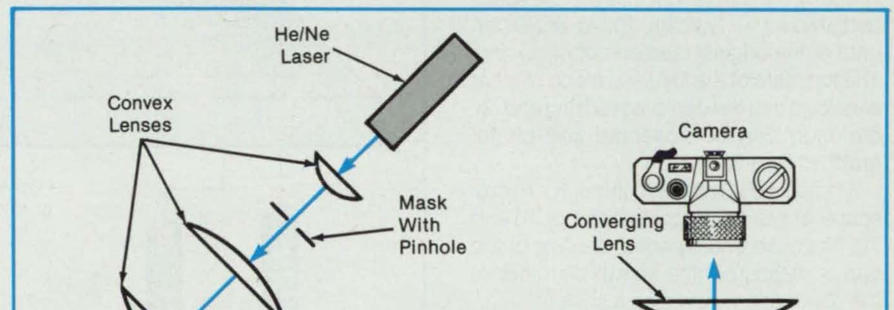

The **Deflection of a Circular Wafer of Silicon** is measured interferometrically. The pattern of deflection is used to infer the pattern of stress within the wafer.

a circular wafer of silicon. A beam of light from a helium/neon laser is spatially filtered in a pinhole, expanded by lenses, collimated by a paraboloidal mirror, and then reflected by a beam splitter through an optical flat onto the wafer. The wafer is supported at its edge and loaded at its center by a known force.

The light reflected from the wafer and the bottom of the optical flat passes through the beam splitter and is focused by a lens to form an image of the wafer in the camera. The interference between these two components of reflected light forms a

pattern of bright and dark fringes in the image that can be counted to measure the deflection at each point on the surface of the disk (each fringe represents a vertical deflection of half a wavelength).

In this particular configuration, the theoretical expression for the residual stress includes the first three derivatives of the deflection with respect to radial position. Therefore, third-degree polynomials are fitted to the measured deflections at a conveniently large number of radii. The coefficients of the polynomials are used to obtain the derivatives, which are then inserted in the expression for the residual stress.

This work was done by Steven Danyluk and A. T. Andonian of The University of Illinois at Chicago for **NASA's Jet Propulsion Laboratory**. *For further information, Circle 138 on the TSP Request Card. NPO-17440*

Measuring Gaps in O-Ring Seals

With a simple fixture, gaps are measured directly.

Marshall Space Flight Center, Alabama

A simple technique enables the measurement of the leakage areas created by small obstructions in O-ring seals. The obstructions could be thread, lint, steel or nylon wire, or human hair, for example. They may be as small as 0.00025 in. (about 6 μm) in diameter. The new technique is faster, easier, and more accurate than is the conventional estimation of blow-by area from difficult measurements of leakage.

The technique involves the use of a fixture that compresses the O-ring onto a flat plate and a wire or other obstruction of known diameter and material. By use of spacers, the compression is set to a specified amount — typically 10, 20, or 30 percent of the original diameter of the O-ring. The top plate of the fixture is made of clear plastic so that the compressed ring and obstruction can be observed and photographed (see figure).

Photographs are taken through a microscope at typical magnifications of 10 and 70. From the photographs, the size of the gap is measured (the known diameter of the obstruction serves as a scale).

This work was done by Scott E. Johnson of Morton Thiokol, Inc., for **Marshall Space Flight Center**. *For further information, Circle 30 on the TSP Request Card. MFS-28332*

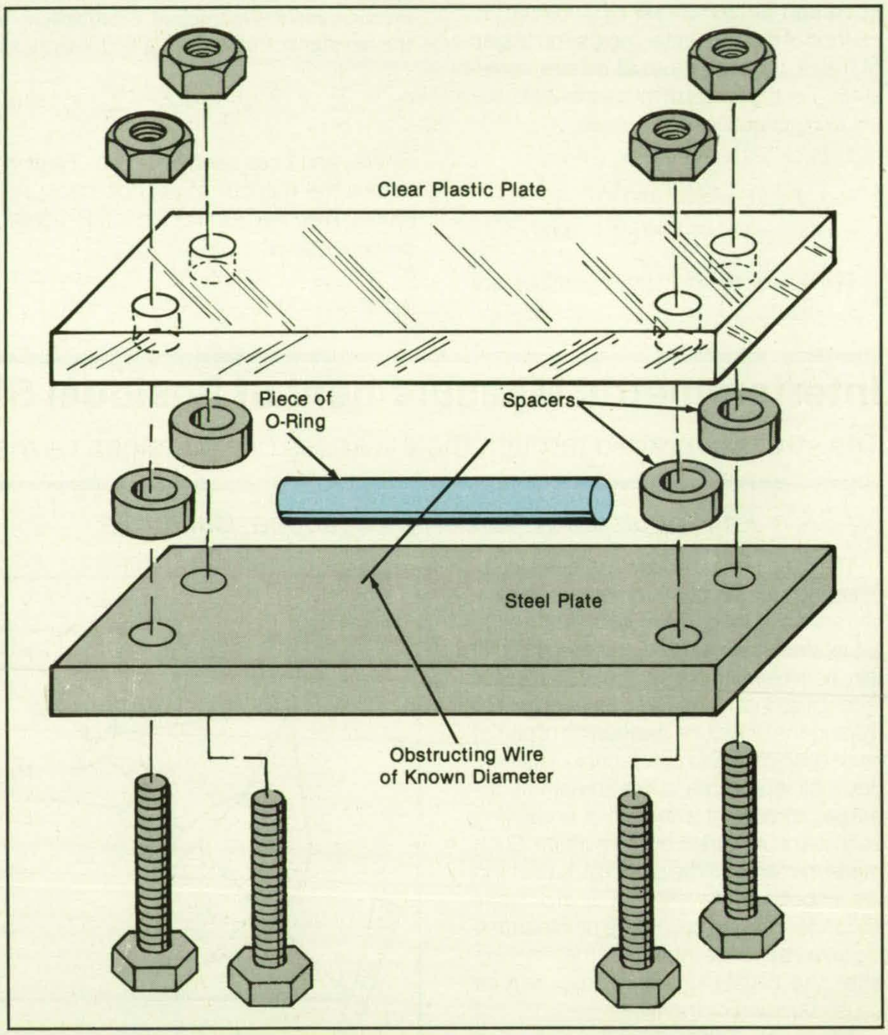

The **Fixture Compresses the Piece of O-Ring** by an amount determined by spacers. A camera aimed through the clear plastic top plate records the depression made in the O-ring by an obstruction.

Shape Gauge Measures Surfaces

Tedious measurements and calculations are performed quickly and accurately.

Marshall Space Flight Center, Alabama

An optical/mechanical/electronic system acts as a shape gauge by taking measurements of machine-tool motions or complicated contours of objects, then processing the measurement data into maps or profiles indicative of the shapes. Typical measurements include deviations from straightness in motions of positioning machinery, from roundness in machined cylinders or spheres, or from flatness in surface plates and optical flats.

The gauge can operate with input signals from a variety of displacement transducers. For example, in a determination of roundness, a combination of mechanical contact points can indicate against the surface while the position along a scanning path on the surface is measured via the rotation of a wheel. In a determination of flatness or straightness, any of several well-known interferometric systems can be

used to measure the local displacement of the surface perpendicular to the scanning path (nominally on the surface) or the local slope of the surface as a function of the displacement along the path (see figure).

The displacement along the path and the displacement and/or slope of the surface are measured automatically, under computer control, at prescribed points. Each displacement along the path serves as a position index to identify the measurement point and the perpendicular displacement or slope. In processing, the data taken along a path can be partitioned into subsets, within each of which the data points are separated by approximately the distance along the path between two contact points or an equivalent pair of measuring devices. Each subset is suitable for analysis by any of several methods analogous to the step method — a conventional method of determining the deviation of an edge from straightness by use of a sequence of measurements of slope at regularly spaced points along the edge.

Because the locations of the subsets relative to each other are measured accurately, many correlated stepped profiles of the surface are created. Straightforward least-squares techniques are then used to establish the unknown angular alignments of the subsets with each other. This process results in a surface profile of much-higher along-path resolution than is obtainable in the step method. Furthermore, because many correlated subsets are used to obtain the shape of the surface and the fitting technique allows only two degrees of freedom to each subset, there is a statistical improvement in the accuracy of the measurement in comparison with that of the step method.

Because of the ease and speed with which the shape gauge produces high-resolution profiles, many intersecting profiles can be measured on a surface. Then, by demanding closure at the intersection and using a generalization of conventional techniques for processing measurements of surface plates, a three-dimensional representation of the surface is generated.

This work was done by Ralph C. Veale, W. Tyler Estler, and Thomas Charlton, Jr., of **Marshall Space Flight Center**. *For further information, Circle 1 on the TSP Request Card.*

Inquiries concerning rights for the commercial use of this invention should be addressed to the Patent Counsel, Marshall Space Flight Center [see page 16]. Refer to MFS-28284.

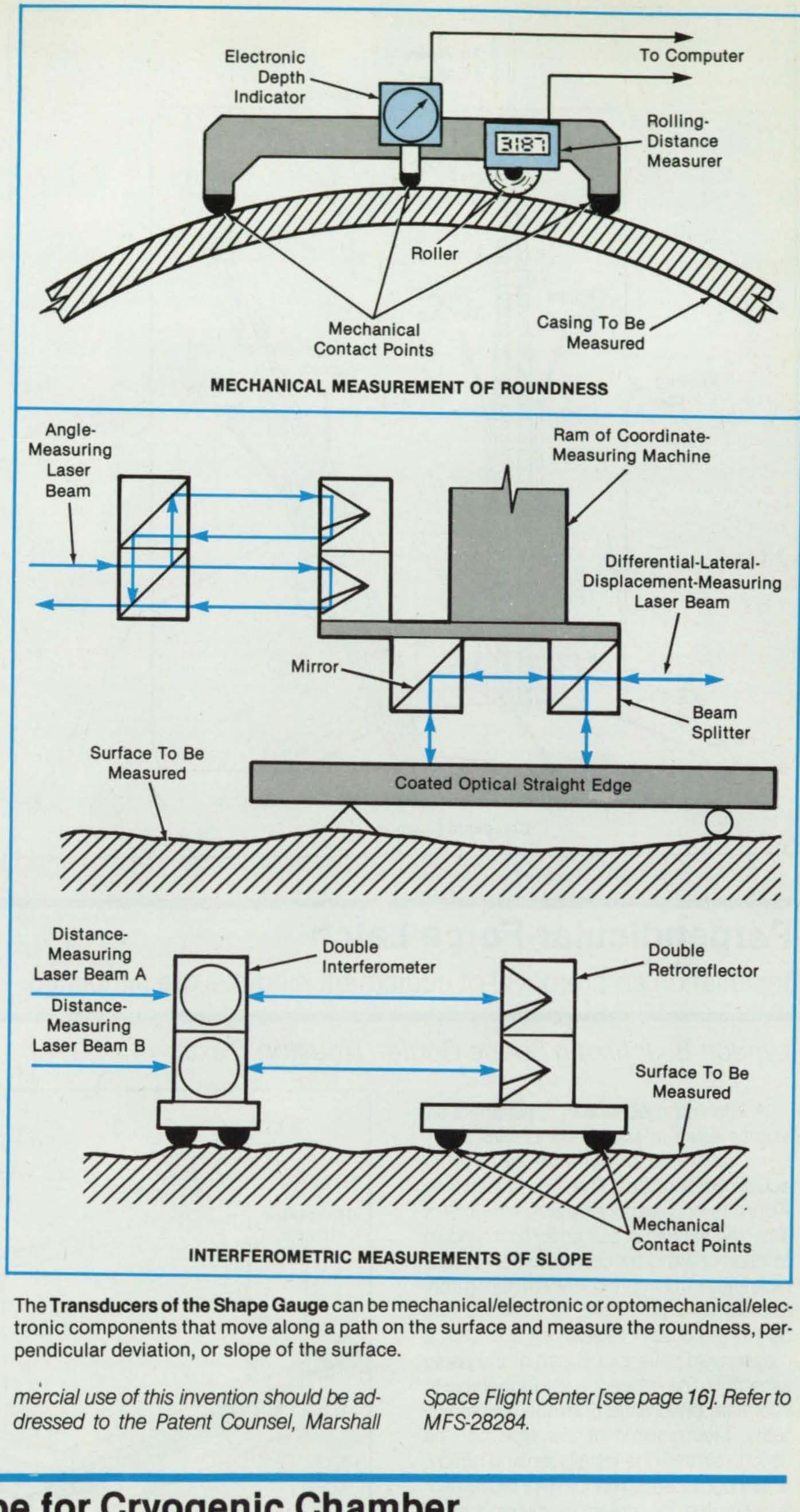

The **Transducers of the Shape Gauge** can be mechanical/electronic or optomechanical/electronic components that move along a path on the surface and measure the roundness, perpendicular deviation, or slope of the surface.

Visual-Inspection Probe for Cryogenic Chamber

Parts in cold environments can be observed from ambient temperature.

Lyndon B. Johnson Space Center, Houston, Texas

A visual-inspection probe that resembles a borescope enables an observer at ambient temperature to view objects immersed in a turbulent flow of liquid oxygen, liquid nitrogen, or other cryogenic fluid. The design of the probe is fairly conven-

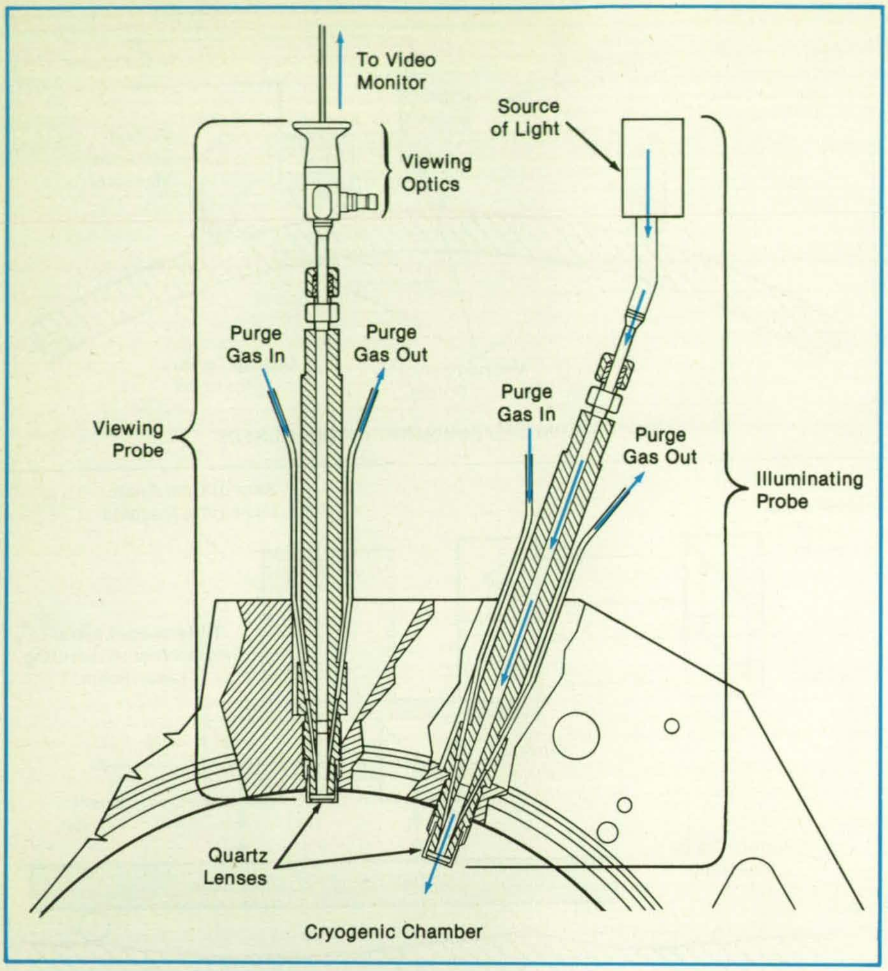

tional for such a device, except that special consideration is given to the selection of materials and to thermal expansion to provide for the expected range of operating temperatures.

As shown in the figure, the inspection probe is mounted in a hole through the wall of the cryogenic chamber, aimed at the object or region to be viewed. A similar probe, equipped with a source of light instead of viewing optics, is mounted in another hole to illuminate the field of view.

A quartz lens is sealed in the end of the probe that is inserted in the chamber. The side of the lens inside the probe is purged with a dry gas to prevent the accumulation of frost. The view is displayed on a video monitor.

This work was done by Steve Friend, James Valenzuela, and Jay Yoshinaga of Parker Hannifin Corp. for **Johnson Space Center**. *For further information, Circle 13 on the TSP Request Card.*
MSC-21444

The **Inspection Probe Penetrates the Wall** of a cryogenic chamber to provide a view of the interior. A similar probe illuminates the scene.

Perpendicular-Force Latch

Installation and removal of equipment modules are simplified.

Lyndon B. Johnson Space Center, Houston, Texas

A latching mechanism simultaneously applies force in two perpendicular directions to install or remove electronic-equipment modules. The mechanism (see Figure 1) requires only the simple motion of a handle to push or pull an avionic module to insert or withdraw connectors on its rear face into or from spring-loaded mating connectors on a panel and to force the box downward onto or release the box from a mating cold plate that is part of the panel assembly. The concept is also adaptable to hydraulic, pneumatic, and mechanical systems. Mechanisms of this type can be used to simplify the installation and removal of modular equipment where movement is restricted by protective clothing as in hazardous environments or where the installation and removal are to be performed by robots or remote manipulators.

Figure 2 shows an installation sequence. In step 1, the handle has been installed on the handle cam and turned downward. In step 2, the technician or

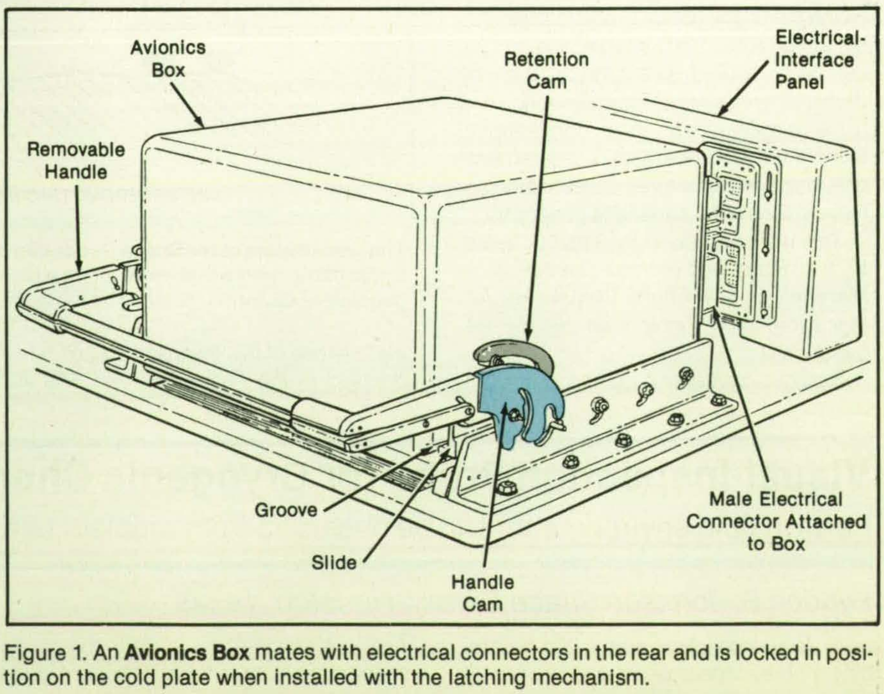

Figure 1. An **Avionics Box** mates with electrical connectors in the rear and is locked in position on the cold plate when installed with the latching mechanism.

robot pushes the box rearward as slides attached to the rails enter grooves near the bottom of the box. In step 3, as the box continues to move to the rear, the handle cam automatically aligns with the slot in the rail and engages the rail roller.

In step 4, the handle is rotated upward 75°, forcing the box rearward to mate with the electrical connectors. In step 5, the handle is pushed upward an additional 15°, locking the handle cam and the slide. In step 6, the handle is rotated an additional 30°, forcing the box and the mating spring-loaded electrical connectors downward so that the box engages the locking pin and becomes clamped to the cold plate. The sequence for removal is identical except that the motions are reversed.

This work was done by John P. Mattei, Peter A. Buck, and Michael D. Williams of Rockwell International Corp. for **Johnson Space Center**. *For further information, Circle 90 on the TSP Request Card.*
MSC-21406

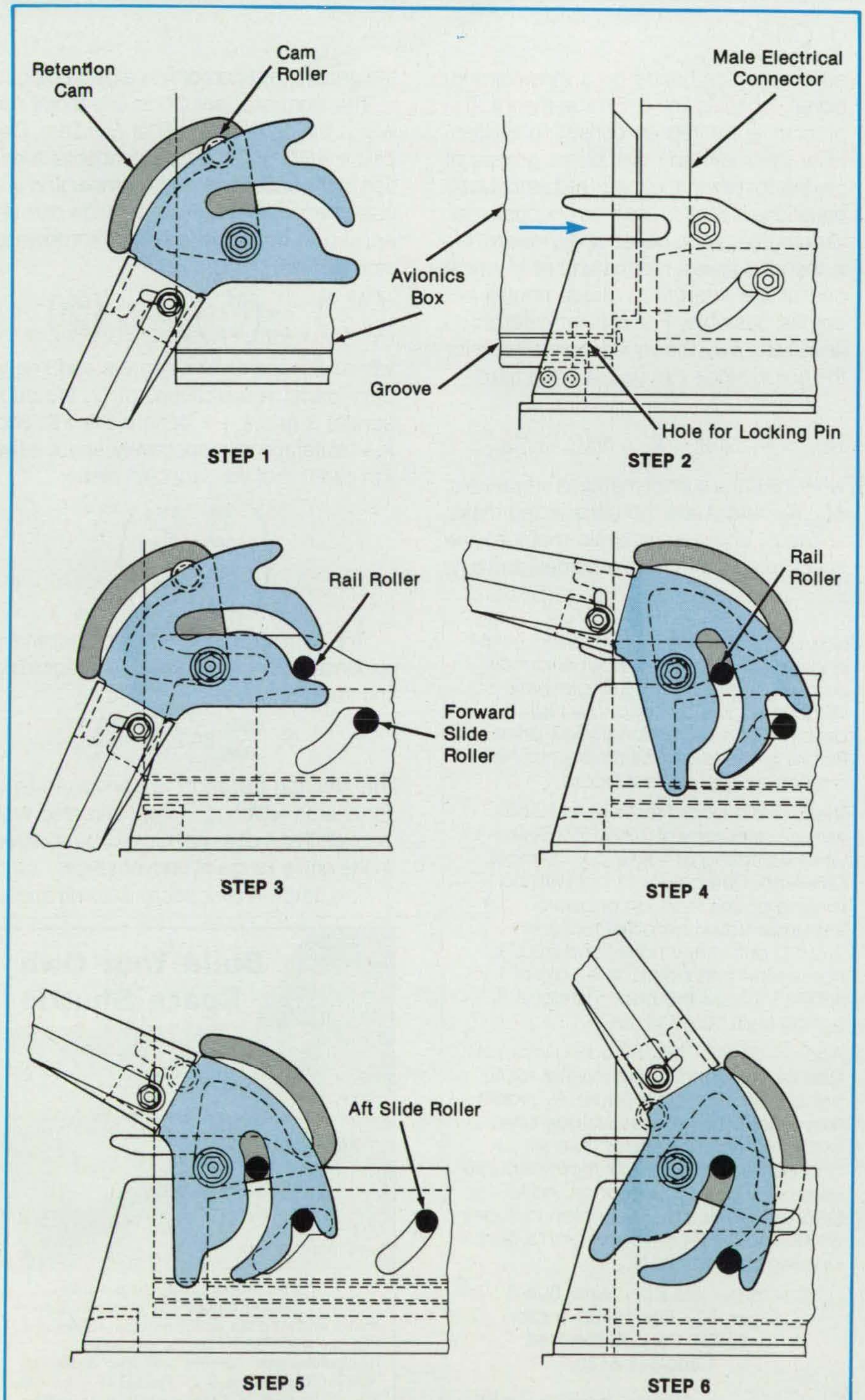

Figure 2. This **Installation Sequence** shows the positions of the handle and retention cams as the box is moved rearward and downward.

Machinery

Hardward, Techniques, and Processes

Computation of Flutter in Turbomachinery

A "direct" solution procedure supplants the conventional eigenmode analysis.

Lewis Research Center, Cleveland, Ohio

An iterative computational procedure yields the critical mach number, M_F, for the onset of flutter and the flutter angular frequency, ω_F, of a propfan, turbine with unshrouded blades, or other turbomachinery. Unlike the eigenmode analytical procedure used heretofore, the new procedure does not require the cumbersome tracking of eigenvalues and the computationally expensive use of inner and outer iteration loops for M_F and ω_F. In the new procedure, the flutter problem is treated as a complex, implicit double-eigenvalue problem that can be solved directly for M_F and ω_F by quasi-Newton iteration (see figure).

The procedure is applied to the aeroelastic analysis of a propfan, in which a finite-element model of the propfan structure is combined with a model of unsteady aerodynamics based on a three-dimensional subsonic-lifting-surface theory. The propfan is treated as consisting of identical, symmetrically distributed groups of blades, for which the linearized aeroelastic equations of motion are then uncoupled for various intergroup-phase-angle modes. M_F is then the lowest mach number at which one of the intergroup phase angles becomes unstable. For a given intergroup phase angle σ_F, the equations of motion for the group mode can be put in the form

$$B\mathbf{q}_0 = [-\omega_F^2 M_g + K_g - A(M_F, \omega_F)]\mathbf{q}_0 = 0$$

where B is the sum of matrices in brackets; M_g, K_g, and A are the generalized mass, stiffness, and aerodynamic matrices, respectively, for the group of blades; and $\mathbf{q}_0$ is the generalized-coordinate eigenvector.

The nontrivial solutions are those for which the determinant D of B is zero. Because $A(M_F, \sigma_F)$ is a transcendental function of the assumed mach number and angular frequency, Newton iteration can be applied to bring the determinant toward zero as follows:

$$\begin{pmatrix} M_F \\ \omega_F \end{pmatrix}_{(k+1)} = \begin{pmatrix} M_F \\ \omega_F \end{pmatrix}_{(k)} - J_k^{-1} \begin{pmatrix} D_R \\ D_I \end{pmatrix}_{(k)}$$

where D_R and D_I are the real and imaginary parts, respectively, of D; the subscripts k and $k+1$ denote the kth and $k+1$st iterations, respectively; and J_k is the kth iteration of the Jacobian matrix

$$\begin{pmatrix} \frac{\partial D_R}{\partial M_F} & \frac{\partial D_R}{\partial \omega_F} \\ \frac{\partial D_I}{\partial M_F} & \frac{\partial D_I}{\partial \omega_F} \end{pmatrix}$$

The evaluation of J_k is computationally expensive. By use of a theorem regarding the traces of

$$B_k^{-1}\frac{\partial B_k}{\partial M_F} \text{ and } B_k^{-1}\frac{\partial B_k}{\partial \omega_F}$$

the Newton iteration is converted to a formula in which J_k is approximated well enough that it does not have to be updated in the entire range of convergence.

The iterative procedure is summarized

as follows:
1. Obtain the initial estimates $M_{F(0)}$ and $\omega_{F(0)}$.
2. Estimate $\frac{\partial B_0}{\partial M_F}$ and $\frac{\partial B_0}{\partial \omega_F}$ by finite-difference approximations.
3. Compute the new estimates $M_{F(k+1)}$ and $\omega_{F(k+1)}$ $(k=0,1,2,\ldots)$ using the approximate iteration formula.
4. Test for convergence, and stop if the calculation has converged.
5. Increment $k(\text{new}) = k(\text{previous}) + 1$.
6. Compute updated derivatives $\frac{\partial B_k}{\partial M_F}$ and $\frac{\partial B_k}{\partial \omega_F}$ by an approximate formula.
7. Return to step 3.

The results of a test case show that the procedure converges well. The procedure is particularly suitable for optimization in design because as the optimal design evolves, the flutter solution is expected to change incrementally, so that the previous solution provides good estimates for the start of the current solution.

This work was done by Durbha V. Murthy of the University of Toledo for **Lewis Research Center**. *Further information may be found in NASA TM-100171 [N87-28058], "A Computational Procedure for Automated Flutter Analysis."*

Copies may be purchased [prepayment required] from the National Technical Information Service, Springfield, Virginia 22161, Telephone No. (703) 487-4650. Rush orders may be placed for an extra fee by calling (800) 336-4700.
LEW-14742

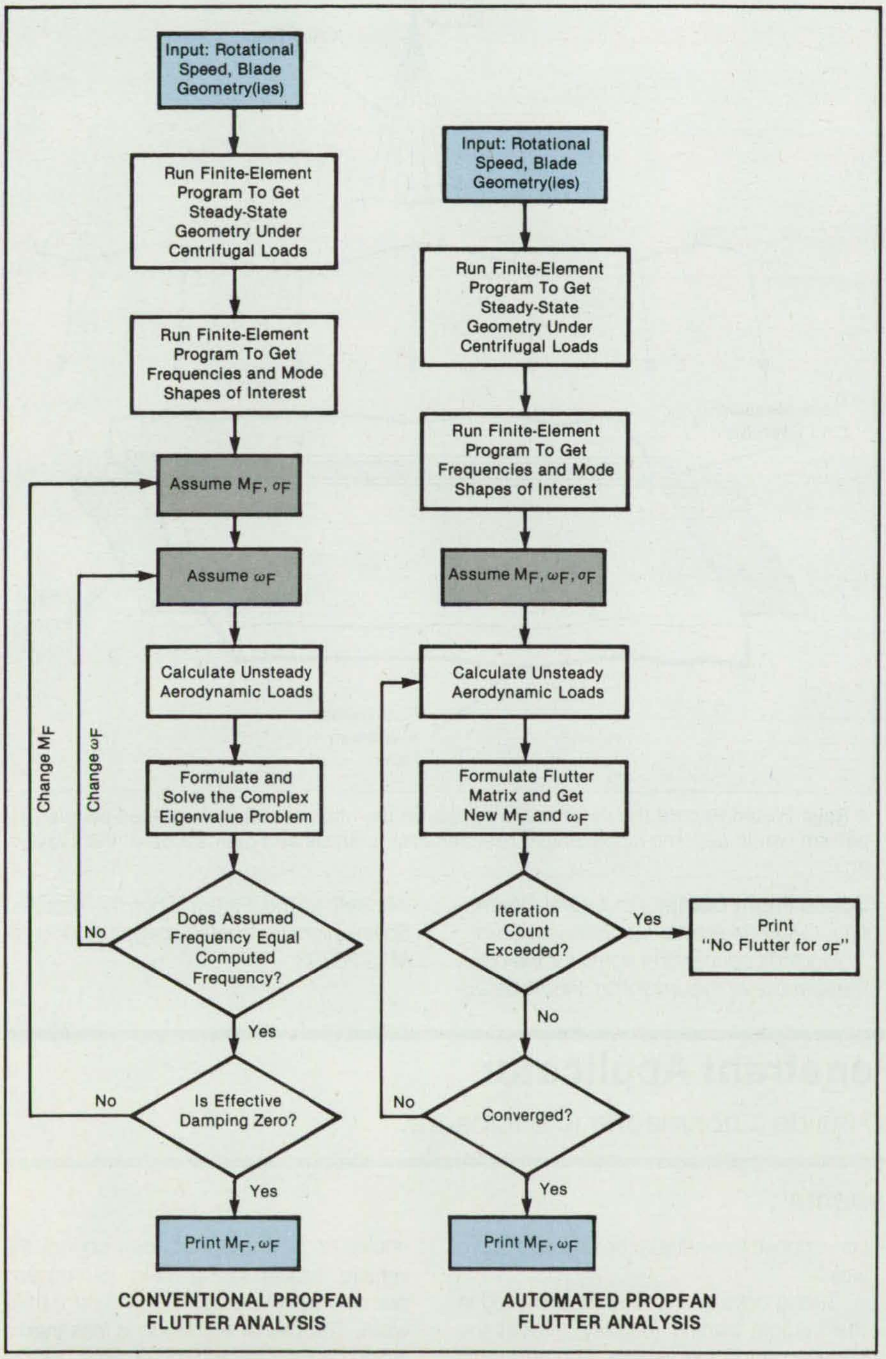

The **New Iterative Procedure** for the automated analysis of flutter in propfans is compared with the conventional double-loop iterative procedure.

Fabrication Technology

Hardware, Techniques, and Processes

Books and Reports

Printed-Circuit Tape Measures for X-Ray Inspections

A known pattern is impressed on the x-ray image for reference.

Marshall Space Flight Center, Alabama

Tapes made by flexible-printed-circuit technology would provide identification and position references for x-ray images of weld joints. The proposed tapes would consist of etched copper patterns on flexible substrates. Typically, a tape would be placed on the part to be inspected, on the side facing the x-ray source (see figure). Laid along a lengthy butt weld, for example, the tape would result in an x-ray image of its copper pattern on a continuous strip of 70-millimeter film as the weld was scanned by an x-ray source.

The recorded pattern would serve as a position reference for a report on the x-ray inspection, for reworking the weld if necessary, and for reinspecting it. It would furnish landmarks for digitally stored images, ensuring frame-to-frame continuity. By use of double-sided and/or stepped-thickness copper patterns, tapes could provide gray-scale references so that corrections could be made for variations of intensity in x-ray beams, and some of the minimum parameters of flaws in welds could be calibrated. Distance marks would enable the precise up- or down-scaling of images and correction for the various aspect ratios of cameras, scanners, and displays.

The substrate of the tape would be Kapton (or equivalent) polyimide. X-ray-absorbing copper would be plated on it in any of a variety of patterns. For example, numbered patterns in increments of length could be deposited so that human inspectors could read the marks directly. Such machine-readable patterns as bar codes could also be deposited.

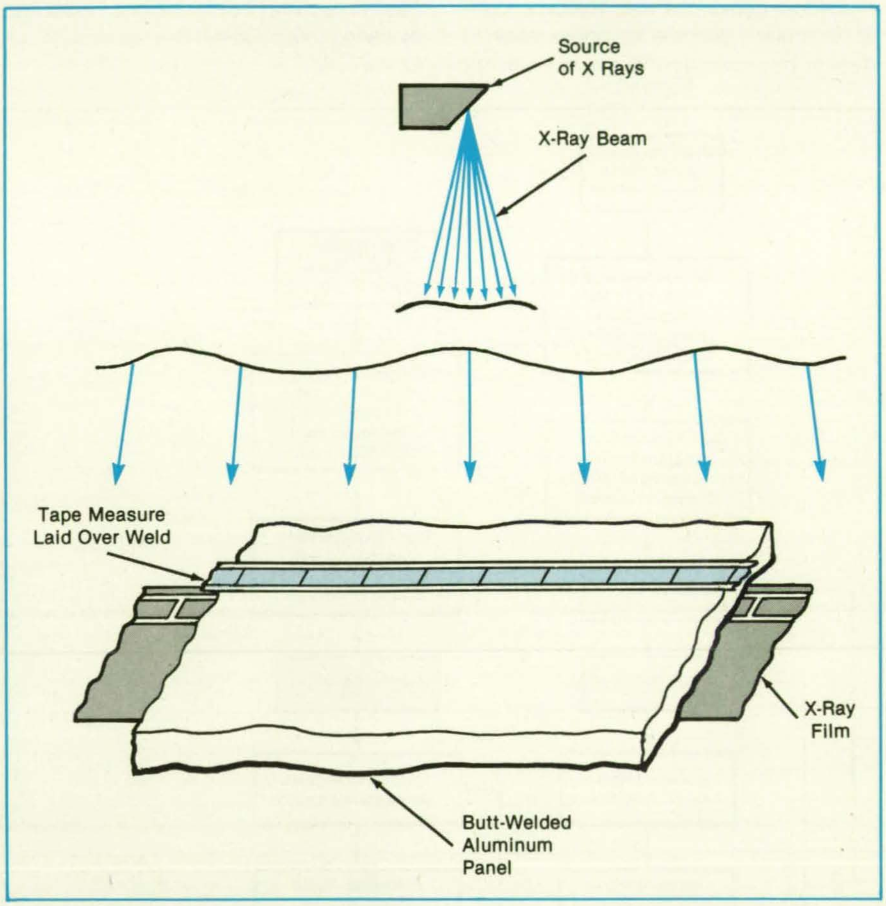

X Rays Would Record the pattern of the tape on the film beneath butt-welded panels. The pattern would become a convenient reference for analysis and digitization of the x-ray image.

This work was done by John E. Sullivan, Jr., of Martin Marietta Corp. for **Marshall Space Flight Center**. *For further information, Circle 64 on the TSP Request Card.*

*Inquiries concerning rights for the commercial use of this invention should be addressed to the Patent Counsel, Marshall Space Flight Center [see page **16**]. Refer to MFS-28388*

Magnetically-Guided Penetrant Applicator

A small wheeled vehicle is moved inside a nonmagnetic enclosure.

Marshall Space Flight Center, Alabama

A small, magnetically-controlled, wheeled vehicle (see figure) carries a replaceable foam-rubber pad to apply penetrant inspection fluid, developer, or etchant to welds on hidden surfaces of nonmagnetic tubes or other enclosures. The surfaces thus coated can then be inspected through borescopes to evaluate the qualities of the welds.

Strong cobalt magnets are mounted in the vehicle behind (usually, above) the sponge pad in the vehicle. The vehicle is guided by moving a similar set of magnets along the weld line on the outside of the enclosure. The magnets can control the vehicle through up to ¼-in. (6-mm) and perhaps as much as ½-in. (13-mm) thick walls. The risk of explosion is less than it would be if an electric motor were used to drive the vehicle.

The vehicle is relatively inexpensive to

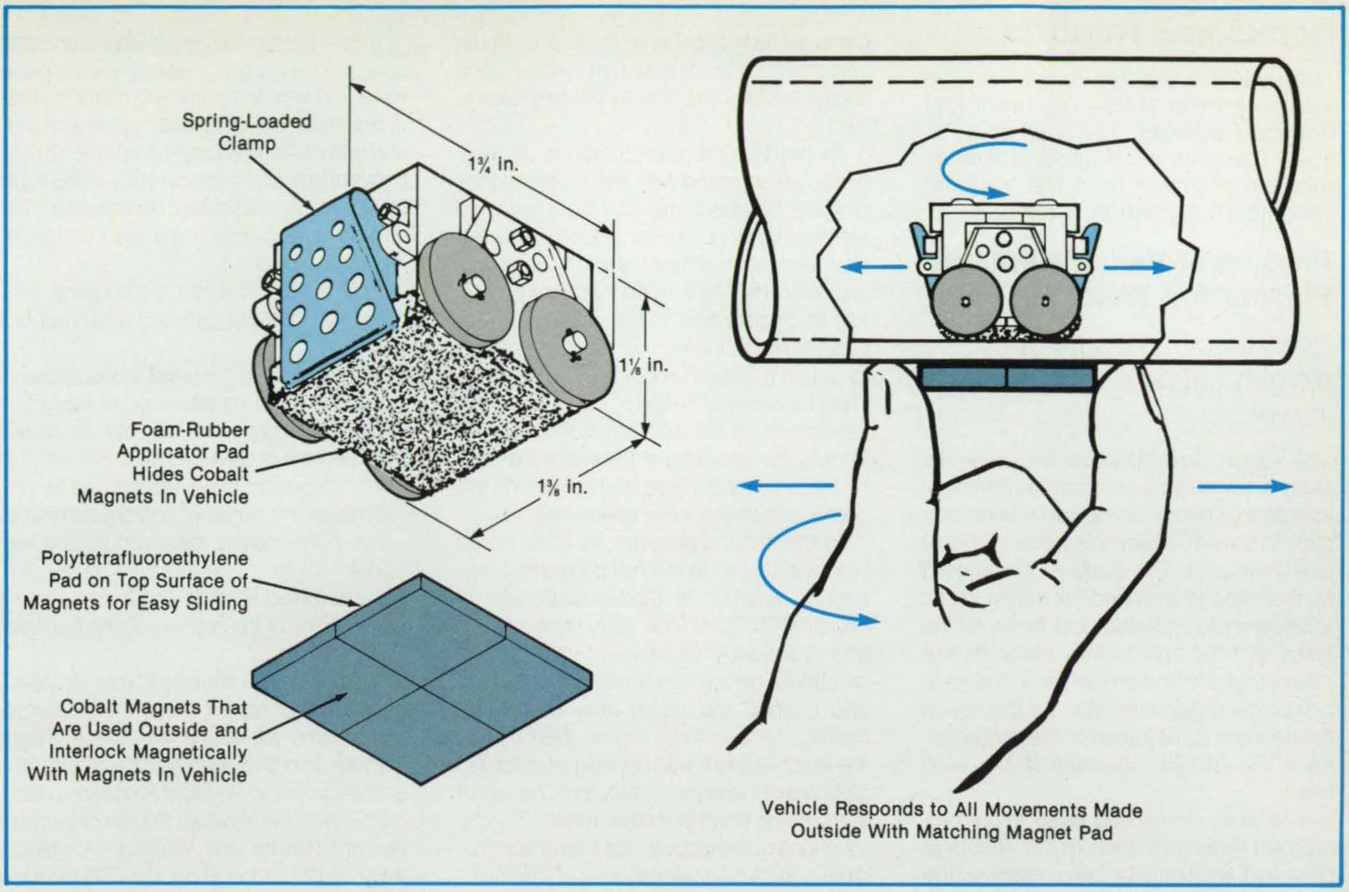

A **Miniature Magnetically Guided Truck** uses foam-rubber sponge pads to apply penetrant fluid for inspection of welds in hidden surfaces of nonmagnetic tubes.

make and could be made in a range of sizes. In the prototype, the wheels are made of polytetrafluoroethylene, and each is suspended independently to make the sponge pad maintain even contact with the surface. Spring-loaded clamps hold the sponge pad in place. A dry sponge pad can be used to mop up excess applied fluid.

This work was done by Orlando G. Molina of Rockwell International Corp. for **Marshall Space Flight Center**. *No further documentation is available.*
MFS-29358

Graphite/Thermoplastic-Pultrusion Die

An attachment to an extruder produces thermoplastic-impregnated graphite tape.

Langley Research Center, Hampton, Virginia

The thermoplastic-pultrusion die produces a hot-melt thermoplastic-impregnated graphite prepreg tape for subsequent use in lamination or molding. It consists of a profile die, a fiber/resin collimator, and a crosshead die body. The die is designed to be attached to a commercially available extrusion machine capable of extruding high-performance thermoplastics. The die is attached to the extruder similarly to a crosshead extrusion die; i.e., with the central axis of the die perpendicular to the central axis of the extruder barrel. The extrusion machine is used to heat the thermoplastic to its molten state and to extrude or inject the thermoplastic resin into the pultrusion die with some pressure.

The pultrusion die performs a variety of sequential processing functions while multiple tows of high-modulus graphite fiber are pulled continuously through its chamber, and a molten thermoplastic resin is simultaneously injected into its impregnation section. The die spreads and collimates the graphite fiber tows to form a thin ply as the tows enter the die. It heats the graphite fiber to the temperature of the molten thermoplastic as the graphite travels from the entrance of the die to the thermoplastic-impregnation section. The die impregnates the fiber with the molten resin, consolidating and compacting the impregnated fiber and metering the resin. Finally, it cools the composite to below the glass-transition temperature of the thermoplastic before the material leaves the die. The composite thus produced is a thin, one-ply, uniaxial sheet that can be coiled on a spool and stored for further laminating and molding.

This simple attachment to a commercial extruder should enable developers of composites to begin experimenting with large numbers of proprietary resins, fibers, and hybrid composite structures. No longer will they be limited to such combinations as graphite/epoxy. With this device, almost any possible fiber/resin combination can be fabricated.

This work was done by Maywood L. Wilson, Mark W. Frye, Gary S. Johnson, and Clarence E. Stanfield of **Langley Research Center**. *For further information, Circle 41 on the TSP Request Card.*

This invention is owned by NASA, and a patent application has been filed. Inquiries concerning nonexclusive or exclusive license for its commercial development should be addressed to the Patent Counsel, Langley Research Center [see page 16]. Refer to LAR-13719.

Books and Reports

These reports, studies, handbooks are available from NASA as Technical Support Packages (TSP's) when a Request Card number is cited; otherwise they are available from the National Technical Information Service.

Physics of Variable-Polarity Plasma Arc Welding

Even small amounts of oxygen cause damage in welds.

A report describes an experimental study of some of the physical and chemical effects that occur during variable-polarity plasma arc (VPPA) keyhole welding of 2219 aluminum alloy. The study was motivated by the need to gain understanding of the VPPA keyhole and weld pool, because the flows of heat and molten metal fix the microstructure and properties in the weld composite region and because the flow in the pool and static forces on the pool determine the ultimate structure of the weld bead.

The study comprised three major programs: (1) determination of the effects of chemical additions (i.e., impurities) on the structure and shape of the bead and keyhole; (2) determination of the flow in regions surrounding the keyhole; and (3) development of an analog that can be used easily to study the flow in the keyhole region.

In the first program, parts of Al 2219 plates were coated with chemicals (mostly oxides, halides, and sulfates) prior to welding. Each plate was welded in the vertical orientation while a view of its back side was recorded by a video system in an effort to discern flow in the weld pool. The welding operation was terminated abruptly to obtain a "fossil" record of the keyhole. Then the size and shape of the keyhole, the asymmetry of the weld bead, the depth of undercut or grooving at the toe of the weld on the anterior surface, and the sag on the posterior surface were measured.

In the second program, Al 2219 plates were welded as in the first program. However, in addition to (and occasionally in place of) Al 2319 filler wire, pure copper and nickel-alloy wires were inserted immediately before termination of the arc. The copper and nickel alloy both have melting temperatures higher than that of the Al 2219, and it was hoped that solidified globules of these materials would be swept along in the flows of molten metal. The distributions of the globules as seen in longitudinal and transverse sections of the terminal keyholes were used to determine the shapes of the weld pools.

In the third program, it was found that paraffin had the required low melting point, ease and safety of handling, verisimilitude to the hierarchy of forces (surface tension and gravitational/buoyant effects driving convection), and transparency in the liquid state, which facilitates observation. The paraffin analog specimens were welded by jets of hot argon.

The results of these experiments indicated the following (among other) conclusions:

- Oxygen, even in the small amounts due to contamination, moisture, or leakage of air into gas-supply hoses, can disrupt the stable keyhole and weld pool.
- The Marangoni effect (flow driven by gradients in the surface tension) dominates flow in the molten metal around the keyhole.
- The solidified keyhole does not have the true shape of the keyhole during the welding process.

This work was done by Daniel W. Walsh and Arthur C. Nunes, Jr., of the University of Alabama for **Marshall Space Flight Center**. *To obtain a copy of the report, "Examination of the Physical Processes Associated With the Keyhole Region of Variable Polarity Plasma Arc Welds in Aluminum Alloy 2219," Circle 6 on the TSP Request Card. MFS-27207*

Mathematics and Information Sciences

Finite-State Codes

A new class of codes with desirable properties can be constructed from block codes.

NASA's Jet Propulsion Laboratory, Pasadena, California

Finite-state codes constitute a new, more-general class of error-correcting codes that includes both convolutional and block codes. These codes are defined in terms of their encoders, which are machines that have parallel inputs and outputs and are capable of a finite number of internal states. Because any encoder made of real digital devices is necessarily a finite-state machine, the theory of finite-state codes can be used to study the properties of error-correcting codes in general and to design new codes to various specifications.

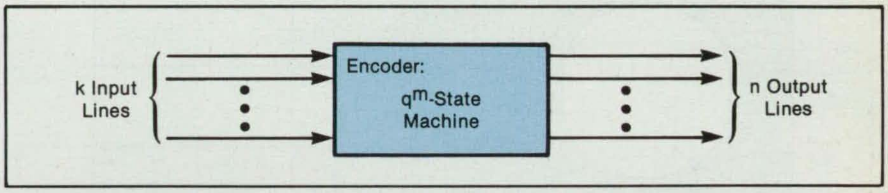

A **Finite-State Encoder** is a machine that has a finite number of internal states. It receives k parallel information symbols and transmits n parallel code symbols at each clock pulse. Finite-state codes include both block and convolutional codes.

A finite-state code is denoted by the parameters n, k, m. Its encoder (see figure) operates on a q-letter alphabet and has q^m possible states. The encoder starts from a fixed initial state, and at each clock pulse it receives k parallel information symbols, which change its state. In response to a sequence of such k-symbol input blocks, the encoder puts out a corresponding sequence of n-symbol output blocks, called a code sequence. If the encoder has only one state ($m = 0$), the finite-state code is an ordinary block code. If the encoder consists of a bank of parallel shift registers and each output symbol is a linear combination of the k input symbols plus the symbols stored in the shift registers, then the finite-state code is a linear convolutional code.

One of the important properties of these codes is the free distance, which is the minimum Hamming distance between two distinct, infinitely-long code sequences.

It is usually desirable to have as large a free distance as possible. The maximum attainable free distance is set by theoretical upper bounds in terms of the parameters n, k, and m. It is also important to define conditions ensuring that a finite-state code is noncatastrophic so that a bad burst of channel noise will never produce an infite number of decoder errors.

The general construction for finite-state codes is based on the partition of a block code into cosets of one of its subcodes. Such cosets will have larger minimum distance between their codewords than do the codewords of the original block code. These cosets are then assigned as labels to the branches of a state transition diagram, according to given rules to maximize the free distance and ensure that the resulting finite-state code is noncatastrophic. Theorems regarding noncatastrophic labeling have been proved and applied to the construction of finite-state codes. In many cases, the finite-state codes constructed this way have the largest possible free distances.

For example, for any & an optimal (2^j, $m+1$, m) finite-state code that has free distance 2^j can be constructed from a partition of the (2^j+1), minimum distance 2^{j-1}, first-order Reed-Muller code. In another example, a Reed-Solomon code can be used to construct an (n, k, m) finite-state code that has free distance $n-k+1+m$.

This work was done by F. Pollara, R. J. McEliece, and K. Abdel-Ghaffar of Caltech for **NASA's Jet Propulsion Laboratory**. *For further information, Circle 57 on the TSP Request Card.*
NPO-17285

Assignment of Finite Elements to Parallel Processors

Elements can be assigned approximately optimally to subdomains.

NASA's Jet Propulsion Laboratory, Pasadena, California

A mapping algorithm based on the simulated-annealing concept can be used to minimize approximately the time required to perform a finite-element computation on a hypercube computer or other network of parallel data processors. In general, a computational domain consists of n finite elements, each of which is to be assigned to a subdomain that is the responsibility of one of N processors. A mapping algorithm is needed when the shape of the domain is complicated (see figure) or it is otherwise not obvious what allocation of elements to subdomains will minimize the cost of computation.

The cost of using each processor depends not only on the cost of computation associated with the elements in its subdomain but also on the cost of transferring the subdomain-boundary information to other processors assigned to contiguous subdomains. The speed of the entire network of N processors is that of the slowest (most heavily loaded) processor. Therefore, an

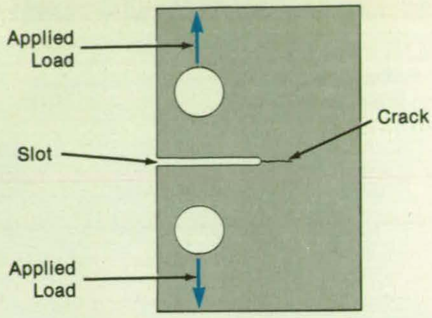

PLATE

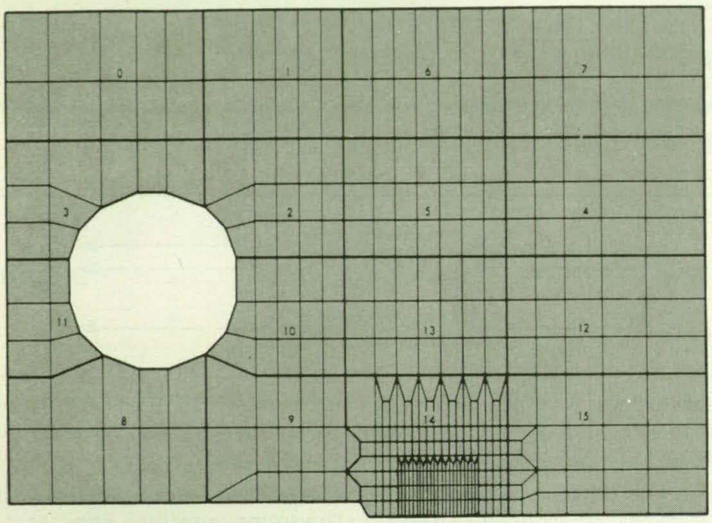

FINITE-ELEMENT MODEL OF UPPER HALF OF PLATE WITH INITIAL ALLOCATION OF ELEMENTS TO SUBDOMAINS

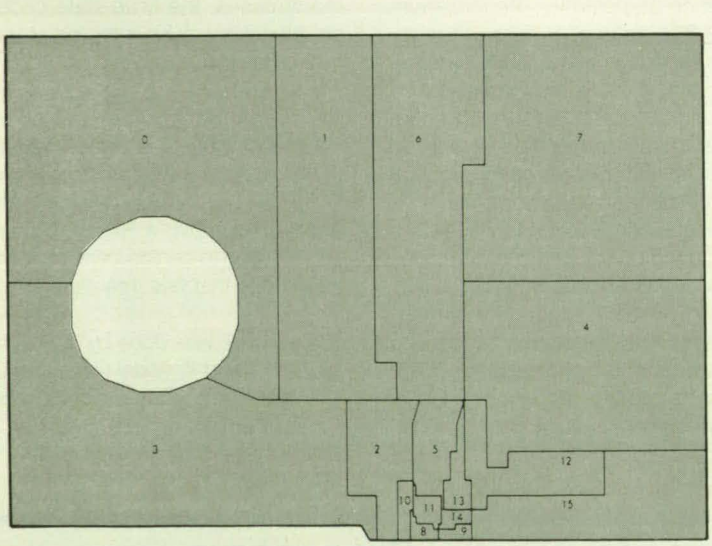

FINITE-ELEMENT MODEL OF UPPER HALF OF PLATE WITH OPTIMAL ALLOCATION OF ELEMENTS TO SUBDOMAINS

Half of a Plate that contains a slot and a crack is represented by a complicated finite-element model with extremely small elements around the tip of the crack. The 544 elements are allocated to subdomains, each of which is assigned to 1 of 16 processors in a hypercube computer.

optimal mapping strategy allocates elements to subdomains in a way that equalizes the total resources required by each processor. In practice, a suboptimal allocation that brings the total cost within 10 to 20 percent of the minimum value is usually acceptable.

The search for optimality is guided by a cost function *C* that penalizes an imbalance in the workload and represents the overall cost of computation within, and communication among, processors, as measured in multiples of an arbitrary standard unit of computation or communication time. To find the allocation that gives the exact global minimum of *C*, it would be necessary to compute and compare *C* for every allocation. Often, this is not practical because the number of possible allocations can be astronomically large.

A simulated-annealing algorithm provides an adequate suboptimal solution, without the need for an exhaustive search among all allocations. An initial, arbitrary allocation is made, then amended in an iterative approach to an approximate global minimum of *C*. So called because it involves equations similar to those that describe annealing in crystalline materials, a simulated-annealing algorithm probabilistically accepts allocations that temporarily increase *C*. This helps to prevent "trapping" in local minimums, enabling the system to continue moving toward the global minimum. *C* is analogous to the system energy in the annealing problem, and a fictitious temperature parameter is gradually decreased (analogously to cooling) so that the amounts of increase in *C* caused by nonimproving allocations are gradually reduced as the iterations proceed and the global minimum is presumably approached.

The initial value of the temperature parameter is critical to convergence to the true global minimum. Too high a temperature parameter causes the acceptance of too many nonimproving allocations. Too low a temperature parameter degrades the simulated-annealing strategy into a more-nearly-conventional iterative improvement strategy with little possibility of escape from local minima. Prior experience suggests that the initial temperature parameter should be selected to cause the acceptance of 30 to 80 percent of the non-improving solutions and that the temperature parameter should thereafter be reduced by a constant factor. Several allocations should be tried at each temperature parameter to assure the analog of thermal equilibrium.

This work was done by Moktar A. Salama, Jon W. Flower, and Steve W. Otto of Caltech for **NASA's Jet Propulsion Laboratory**. *For further information, Circle 81 on the TSP Request Card.*
NPO-17371

Algorithm for Control of Large Antenna

Alternative position-error feedback modes are provided.

NASA's Jet Propulsion Laboratory, Pasadena, California

Modern control theory is the basis for a computer algorithm used to control the two-axis positioning of a large antenna. The algorithm — incorporated into the software of a real-time control computer — enables rapid intertarget positioning as well as precise tracking (using one of two optional position-feedback modes) without the need of human operator intervention.

The position-control feedback loop is closed in the algorithm by the weighted feedback of the hardware-state variables. A linear estimator provides a measure of the rate, acceleration, and the other state variables that are not instrumented. The estimator produces the state variable estimates by repeated evaluation of the difference equations describing the antenna motion. Using feedback of the measured state variable (output of an axis-mounted angle encoder) as a reference for comparison with the estimated position, the estimator adjusts all the estimated states in a way to reduce the error between estimated and actual position (see figure). Overall, the algorithm differs from those algorithms based on classical feedback-control theory that rely on cascade networks, implemented in either hardware or software, to provide the necessary servo compensation.

This and other state-variable control algorithms have several advantages:

- They can incorporate compensation techniques that do not necessarily correspond to physically realizable networks.
- The state-variable approach facilitates discrete-time-domain design methods, resulting in efficient utilization of the control computer.
- The state estimator provides an accurate, low-noise measure of rate and acceleration.
- The estimator provides a powerful method of detection and correction of errors in encoder data, thereby enabling uninterrupted operation during brief intervals when the encoder data are unusable.
- The state-variable method involves a standardized matrix representation of the system, which is convenient for digital processing.

The antenna employs two different methods of angular-position feedback to accommodate different tracking requirements. A two-axis optical autocollimator generates error signals according to the deviation of an antenna-mounted mirror from the orientation of a precision-instrument mount located immediately behind the vertex of the antenna dish. The axis-mounted angle encoders enable tracking beyond the limiting elvation angle where the approaching geometric singularity renders the autocollimator unusable.

The shaft-angle encoder and the autocollimator are represented in the figure by two blocks, the input to which is the state vector **X**. The representative equation of the dynamics block is the generalized difference equation relating the state vector at the discrete times of the computer sampling to the previous value of the state vector and to the control input, **U**. The discrete transition matrix, Φ, and the input vector, Γ, describe the dynamic behavior of the physical system. The angle encoder and the autocollimator are represented by vectors $\mathbf{H_E}$ and $\mathbf{H_A}$, which operate on the state vector, **X**, and produce the scalar

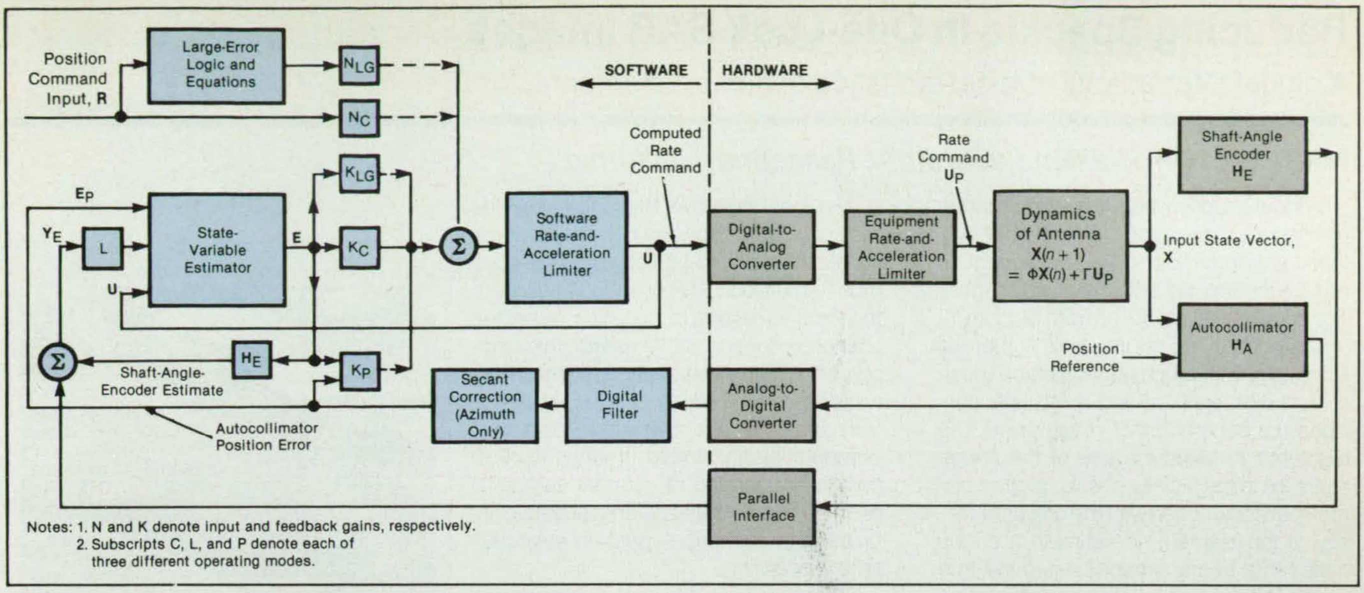

The **Control System** for one axis of a two-axis azimuth/elevation control system is embodied mostly in software based on advanced control theory. The system has the linear properties of a classical linear feedback controller. Its performance is described by bandwidth and linear error coefficients.

azimuth (or elevation) encoder angle and autocollimator angle error.

The software estimator computes the state variables for subsequent processing and feedback to the equipment control input. The estimator is essentially a dynamical simulation of the physical antenna and has the same input and difference equations as those of the equipment. Under ideal conditions, the estimator-output state vector, **E**, is identical to the antenna state vector, **X**. Errors in the estimated state vector, **E**, arise from errors in the mathematical model of the dynamics and from uncompensated disturbances. These errors are corrected by comparison of the estimated with the true values of the encoder angle, and feedback of the estimator error, $\mathbf{Y_E}$, with a feedback gain factor, **L**.

The feedback of the estimator error introduces a feedback loop around the estimator, with a dynamic response governed by the amount of correction (gain) in the loop. By proper selection of the estimator correction coefficient, **L**, the speed of correction of erroneous estimates (and the speed of response to transient invalid encoder data) can be adjusted. The coefficients are therefore designed to reach a compromise between rapid corrections of estimator errors and filtering of noise in encoder data.

The servofeedback loop is closed by multiplying the state estimate, **E**, by a feedback gain, **K**. Because the estimate, **E**, is approximately equal to the equipment output (state vector), **X**, the result is an effective feedback loop around the equipment. The dynamic properties of the closed servoloop are thus controlled by the value of **K**. The input to the software rate-and-acceleration limiter is given by

$$U = \mathbf{N} \cdot \mathbf{R} - \mathbf{K} \cdot \mathbf{E}$$

where **R** is the input command, **N** is the input gain constant, and **K•E** is the scalar product which, when expanded, yields

$$U = \mathbf{N} \cdot \mathbf{R} - \mathbf{K}_1 \cdot \mathbf{E}_1 - \mathbf{K}_2 \cdot \mathbf{E}_2 - \mathbf{K}_3 \cdot \mathbf{E}_3 - \cdots - \mathbf{K}_6 \mathbf{E}_6$$

The input gain, **N**, controls the overall gain of the servo and is assigned different values according to the mode of operation.

The elements K_i of gain vector **K** correspond to integral error, position, rate, acceleration, and other gains, and thus determine the closed-loop stiffness and dynamic response of the servo. The **K** values are assigned to impart the desired linear-system performance.

This work was done by Robert E. Hill of Caltech for **NASA's Jet Propulsion Laboratory**. *For further information, Circle 61 on the TSP Request Card.*
NPO-17482

Software for Clear-Air Doppler-Radar Display

Features include portability and maintainability.

John F. Kennedy Space Center, Florida

A system of software has been developed to present plan-position-indicator scans of a clear-air Doppler radar station on a color graphical cathode-ray-tube display. Interactive inputs enable the user to select the following:
- A field of either radar reflectivity or radial wind velocity;
- A particular scan from the directory of the data base by specification of the desired rate, time, and elevation angle;
- A maximum radar range from a set of ranges that cover the interval from 10 to 60 km; and
- A contour interval from a set of contour intervals that cover the interval from 2 to 15 units.

The software system was designed to incorporate the latest accepted standards for equipment, computer programs, and meteorological data bases. This includes the use of the Ada programming language, of a "Graphical-Kernel-System-like" graphics interface, and of the Common Doppler Radar Exchange Format (universal format). The software has a high degree of portability to other computing environments. The use of Ada makes the software more maintainable. In addition, the use of Ada software packages has produced a number of software modules that can be easily reused on other related projects.

This work was done by Bruce W. Johnston of the University of Wisconsin-Stout for **Kennedy Space Center**. *No further documentation is available.*
KSC-11427

Reducing Speckle in One-Look SAR Images

A digital filter adapts to local statistics of picture elements.

NASA's Jet Propulsion Laboratory, Pasadena, California

A local-adaptive-filter algorithm is incorporated into the digital processing of synthetic-aperture-radar (SAR) echo data to reduce the speckle in the resulting imagery. The speckle pattern arises from random interference among returns from numerous scatterers on a rough target surface within a resolution element and is typically considered a component of image noise. The algorithm involves the use of the image statistics in the vicinity of each picture element, in conjunction with the original intensity of the element, to estimate a brightness more nearly proportional to the true radar reflectance of the corresponding target.

The probability density of the speckle noise is assumed to vary from resolution cell to resolution cell as the negative exponential of a quantity proportional to the sum of the squares of the in-phase and quadrature amplitudes of the SAR response to a point target. It is also assumed that the signal is much stronger than the thermal noise, so that the brightness of a speckled picture element can be modeled as the product of the true local radar reflectance and the speckle noise. The statistics of the noise are found to depend on the signal and give rise to a signal-dependent correction formula.

This formula is applied to an $M \times M$ block of picture elements centered on the element for which the estimate is sought. The estimated brightness, x, of the central element is given by

$$x = \bar{y} + \tfrac{1}{2}\,[1 - (\bar{y}^2/2\sigma_y^2)](y - \bar{y})$$

where $\bar{y}$ = the average observed (that is, speckled) brightness of all the elements in the block, y = the observed brightness of the central element, and σ_y^2 = the variance of the brightnesses of the elements in the block.

The block has to be large enough to contain a statistically meaningful number of samples, but not so large as to cause unacceptable blurring and loss of resolution. The performances of local adaptive filters of various sizes were compared with each other and with those of other filters in terms of the resolution obtainable at a given equivalent number of looks (ENL), which is the ratio $\bar{x}^2/\sigma_x^2$ over a window of uniform backscatter in the final image (where $\bar{x}$ and σ_x are defined similarly to $\bar{y}$ and σ_y, respectively). In terms of these quantities, a filter of $M = 5$ seemed to yield the best results when applied to two SAR test images (see figure).

The local adaptive filter increases the ratio of signal to speckle noise without the substantial degradation of resolution common to multilook SAR images. It adapts to the local variations of statistics within the scene, preserving subtle details; for example, smoothing relatively uniform areas while preserving edges. Unlike the Kalman filter and other adaptive filters, this one is computationally simple. It lends itself to parallel processing of different segments of the image, thus making possible increased throughput — possibly even real-time processing.

This work was done by K. S. Nathan and J. C. Curlander of Caltech for **NASA's Jet Propulsion Laboratory**. *For further information, Circle 135 on the TSP Request Card.*
NPO-17254

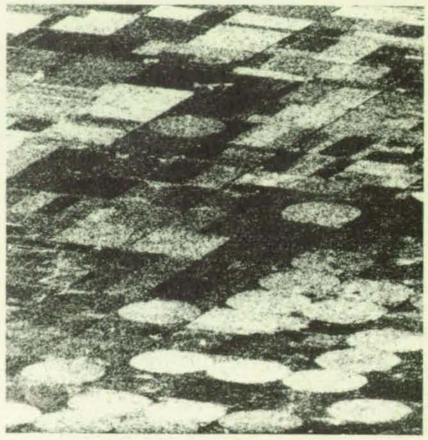

ORIGINAL ONE-LOOK IMAGE
ENL = 1.0

LOCAL ADAPTIVE FILTER (M = 5)
ENL = 11.4

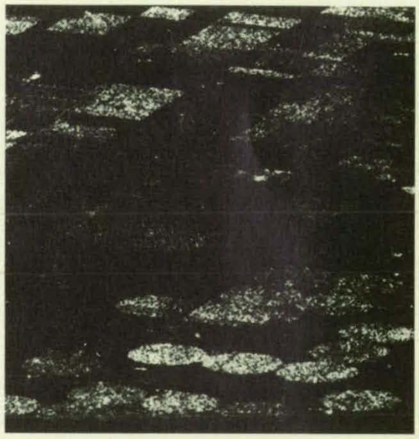

MEDIAN FILTER (M = 5)
ENL = 8.5

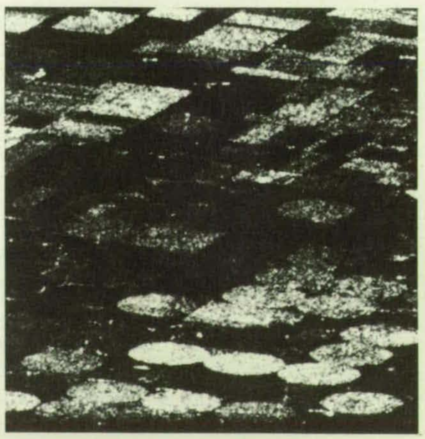

AVERAGING FILTER (M = 5)
ENL = 14.0

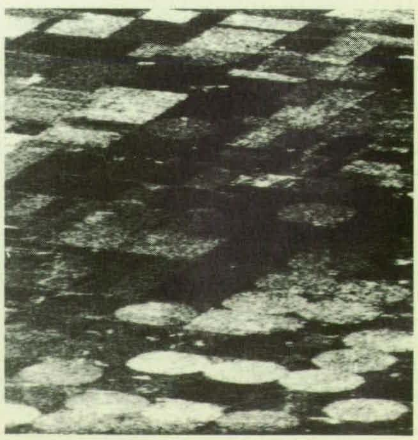

TRADITIONAL EIGHT-LOOK PROCESSING
ENL = 7.0

A **Raw SAR Image** (top) of agricultural fields was processed by various filtering techniques, including the new local-adaptive-filter algorithm.

Alsys Ada cross-compilers get you there in no time.

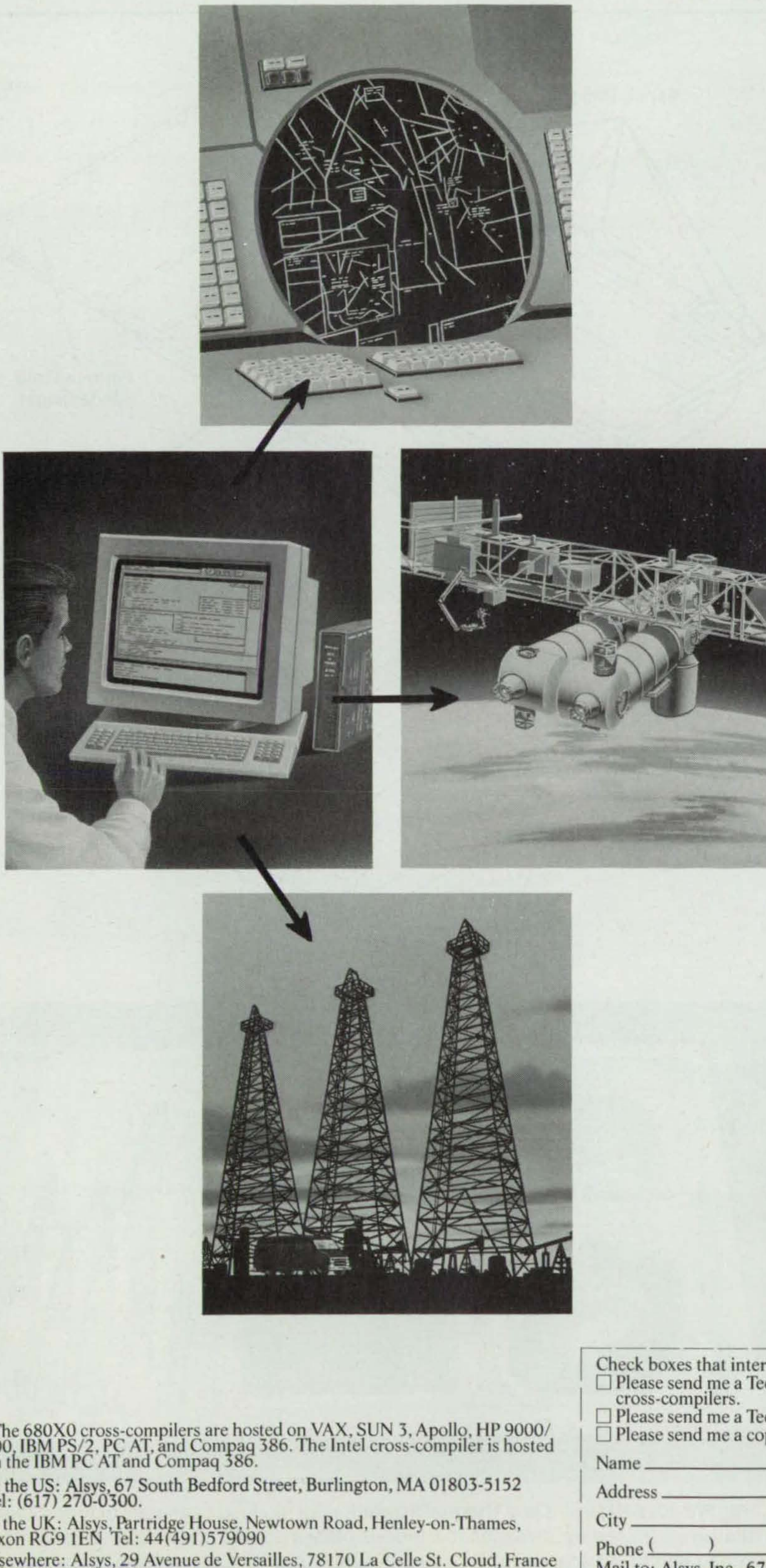

It's time you knew that Alsys, the premier Ada company, offers a range of powerful and flexible cross-compilers for all microprocessors in the Motorola MC680X0 and Intel i80X86 families* to get your applications up and running fast.

Part of the reason for this speed are powerful development tools such as AdaProbe, a source level debugger and program viewer providing facilities to address both the execution properties of a program and its static structure. In addition, there's support for placing program components into ROM, and the Alsys Multi-Library Environment allowing program units to be shared among libraries for team programming.

With Alsys' full line of cross-compilers you'll discover impressive flexibility and power. There's a configurable run-time system giving you full control over tasks, interrupts and all components of your application. The debugger and transfer utility are configurable. Best of all, it's easy to take advantage of all this power because there are only a few files to modify.

When you need to get from here to there without getting lost somewhere in between, use a cross-compiler that knows the shortest route.

alsys
AdaNow.

*The 680X0 cross-compilers are hosted on VAX, SUN 3, Apollo, HP 9000/300, IBM PS/2, PC AT, and Compaq 386. The Intel cross-compiler is hosted on the IBM PC AT and Compaq 386.

In the US: Alsys, 67 South Bedford Street, Burlington, MA 01803-5152
Tel: (617) 270-0300.

In the UK: Alsys, Partridge House, Newtown Road, Henley-on-Thames, Oxon RG9 1EN Tel: 44(491)579090

Elsewhere: Alsys, 29 Avenue de Versailles, 78170 La Celle St. Cloud, France
Tel: 33(1) 3918.12.44

Check boxes that interest you. NTB2/90

☐ Please send me a Technical Summary on the Motorola MC680X0 cross-compilers.
☐ Please send me a Technical Summary on the Intel i80X86 cross-compilers.
☐ Please send me a copy of your "Many Facets of Quality" brochure.

Name ______

Address ______

City ______ State ______ Zip ______

Phone ( )

Mail to: Alsys, Inc., 67 South Bedford Street, Burlington, MA 01803-5152

Circle Reader Action No. 341

Aerospace Food Tray

Utensils and packages of food are restrained.

Lyndon B. Johnson Space Center, Houston, Texas

A lightweight tray designed for use in microgravity has features that may also make it useful for serving meals in airplanes, boats, hospitals, and facilities that care for children. Despite its special design based on a modular-food-packaging concept, the tray is easy to use. The surfaces are made smooth to facilitate cleaning, and the number of cracks, crevices, and pits where food residues can collect is kept to a minimum.

The tray (see figure) consists mostly of a thermoformed sheet of polycarbonate. It includes two channels bounded by overhanging lips, which lock the packages of food in place. The packages are inserted or removed easily by pushing or pulling while twisting or bending the tray slightly. The packages are made shallower than the channels, so that the airspace between the bottoms of the packages and the bottoms of the channels provide some thermal insulation to keep the food warm and to prevent burning of the user's hands.

A ferrous plate is attached under the right side of the tray to restrain the eating utensils, which are magnetic. Beyond the utensil area on the right side are restraints for a pouch containing a beverage, consisting of two rows of small nylon spheres on stems. Two pairs of adjacent spheres grasp a pouch by pinching on an edge. Each restraint is molded as one piece integrally with a strap that can be easily snapped into the tray or removed to facilitate cleaning.

Spring clips provide additional points of attachment for pouches and miscellaneous objects. They are made from flat strips and have an open-frame configuration that facilitates cleaning. The handles of the clips fold down over the clips when not in use to allow the trays to nest together efficiently for storage.

This work was done by Maureen A. Aragon of Lockheed Engineering and Management Services Co., Inc., and Michael F. Fohey of KRUG International Technology for **Johnson Space Center**. *For further information, Circle 22 on the TSP Request Card.*
MSC-21412

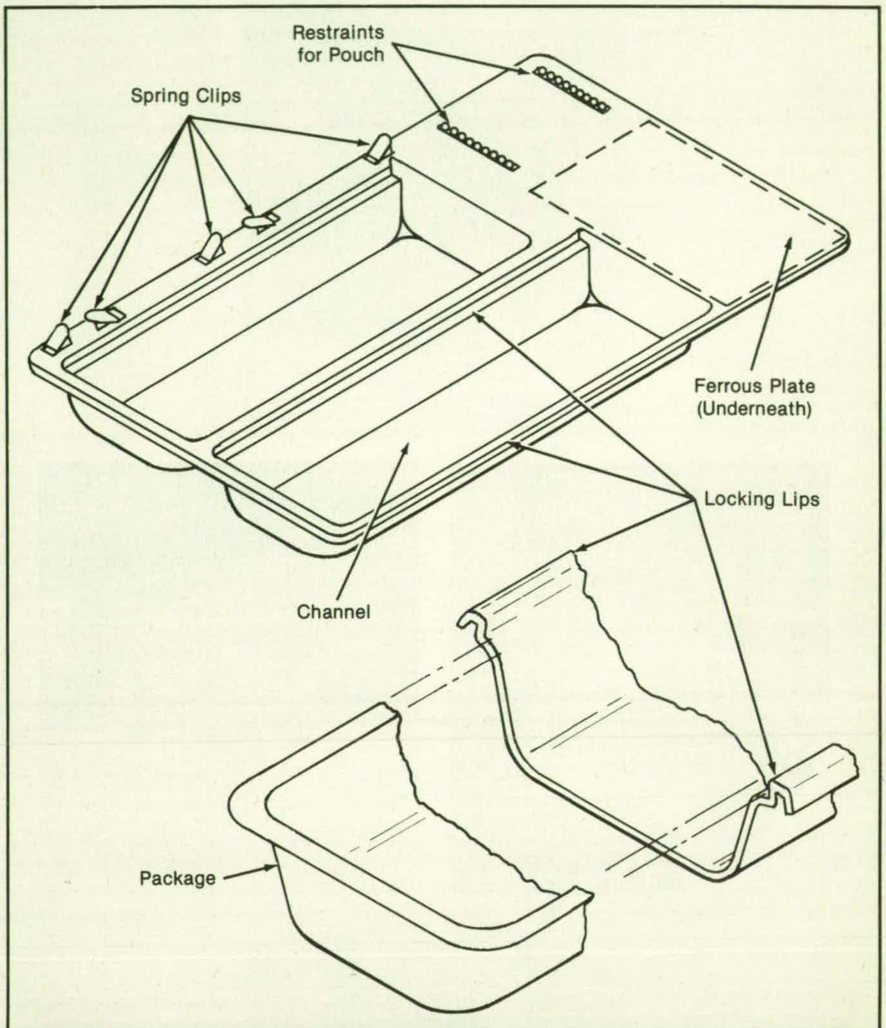

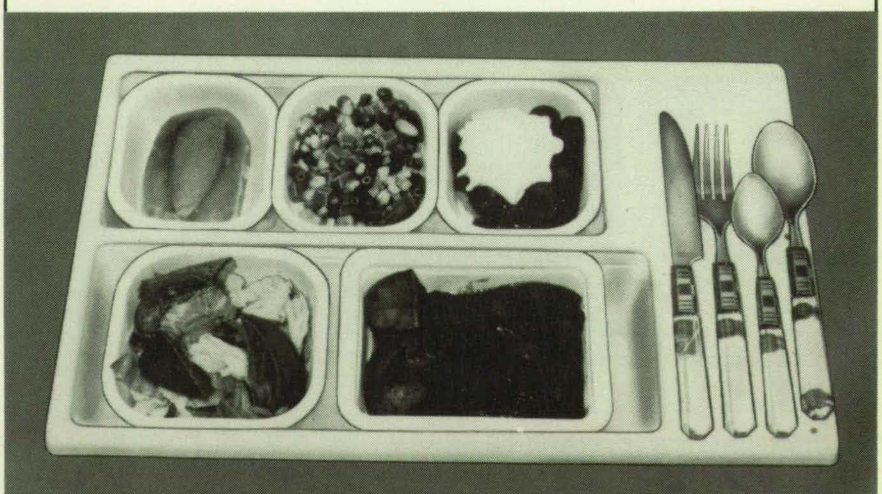

The **Tray Provides Restraint and Thermal Insulation** for modular packages of food. Magnetic utensils are restrained by attraction to a ferrous plate mounted underneath. Restraints for a pouch and spring clips are also provided but have not yet been added to the prototype shown in the photograph.

TEAC.
BECAUSE IT TAKES ALL KINDS.

If you need to measure the bumps, the shakes, the beats, the pressure, or the heat, TEAC makes a data recorder in the right size and format to meet your needs. In fact, we make so many different kinds of data recorders you almost need a data recorder to keep track of them all.

We made the first, and we offer the most extensive line of VHS data recorders. For ease of operation, economy, and convenience of media, the VHS format is the best.

We make the world's smallest 9-channel portable Philips cassette data recorder.

And we make a comprehensive line of reel-to-reel data recorders with extended recording times and up to 28 channels available.

We offer the widest selection of cassette data recorders from 1- to 9-channel models, from pocket-sized to sturdy laboratory and field systems.

Our new portable data recorders incorporating DAT technology are the leading edge in instrumentation recorders.

If you can't find the data recorder in the format you need from TEAC, then it doesn't exist.

And if it doesn't exist it's because TEAC hasn't built it yet.

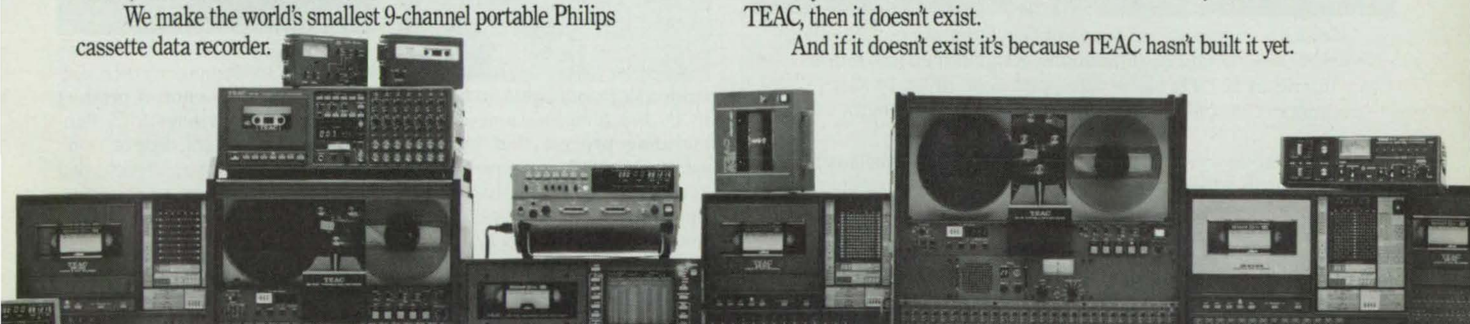

TEAC®

Instrumentation Data Recorder Division.

Circle Reader Action No. 344

New on the Market

Connector Plus, a new **connector treatment** developed by Miller-Stephenson Chemical Co., Danbury, CT, combines the surface conditioning qualities of Monsanto's Polyphenyl Ether with the cleaning power of a carrier solvent system to lubricate and protect connectors against corrosion, galling, and environmental contaminants. Its lubricant causes no electrical resistance and forms no residue, even at high temperatures. Connector Plus is available in aerosol or liquid form.
Circle Reader Action Number 796.

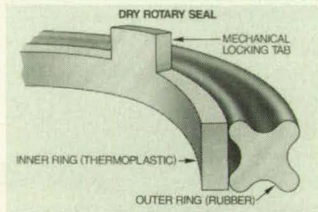

Minnesota Rubber, Minneapolis, MN, has created a **self-lubricating rotary seal** for applications where lubrication is not constant and an elastomeric seal would burn up. Dubbed the Quad PE Plus, the seal combines a thermoplastic bearing material with a rubber backing ring that forms an elastomeric spring. It is encased within a rotary shaft or a groove in the housing that allows it to move without rotating. A slit in the bearing ring enables the seal to compensate for thermal expansion of the shaft as it rotates.
Circle Reader Action Number 794.

Belden Wire and Cable, Indianapolis, IN, has developed a new **manufacturing process that improves safety standards for power supply cords.** PODSS™ (Process of Deterring Surface Stranding) reduces the risk of surface stranding by adding a second layer of insulation to the female connectors of power supply cords. This process encapsulates conductors in a uniform manner and traps any stray copper strands not captured in the crimp. Beyond maximizing the safety of plugs, PODSS ensures consistent dimensions in prong spacing and length.
Circle Reader Action Number 792.

Z-World Engineering, Davis, CA, has introduced Dynamic C™, **the first integrated C development environment for embedded systems.** It enables programmers to edit, compile, debug, and run in one environment. The C programming tool compiles at 25,000 lines per minute while simultaneously downloading to the target system. Dynamic C runs as a single program on the IBM PC.
Circle Reader Action Number 790.

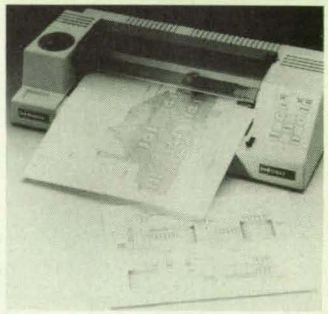

A new **desktop pen plotter** from Océ Graphics USA Inc., Mountain View, CA, produces A (8-1/2" x 11") and B (11" x 17") size plots at a speed of 22 inches per second and a noise level of 58 dB. The Océ G1022 uses six HP®-style pens to create plots in up to six colors or different line widths. It is fully compatible with HPGL® data formats and cables and operates with MacPlot®, AutoCAD®, VersaCAD™, CADKEY™, Harvard™, and Lotus 1-2-3® software packages. The Océ G1022 retails for $1195.
Circle Reader Action Number 798.

The Computerfone™, a two-way telephone to computer **voice digitizer and phone control product** from Suncoast Systems Inc., Pensacola, FL, can accept, digitize, store, and transfer incoming speech; dial phone numbers; answer incoming calls; and convert incoming tones to standard ASCII characters for processing. The intelligent stand-alone device operates with any computer or operating system using industry-standard RS-232/ASCII protocol. Applications include telephone ordering, monitoring and telephone reporting of system malfunctions, and remote control of other devices. Computerphone sells for $695.00.
Circle Reader Action Number 800.

New on the Market

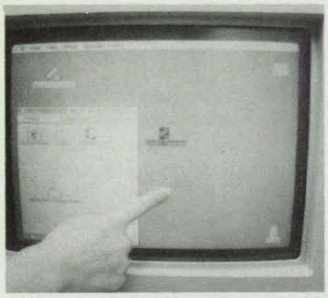

Information Strategies Inc., Richardson, TX, is marketing a new **touch monitor** that replaces mice in Macintosh and Microsoft window environments. Unlike other touch screens, the MouseTouch monitor does not require a special stylus and works even when users are wearing gloves. Point, click, double click, and drag functions are all supported in hardware. Priced at $1639, MouseTouch plugs directly into the existing serial mouse port on IBM compatibles or the Apple Desktop Bus port on Macintosh IIs.
Circle Reader Action Number 770.

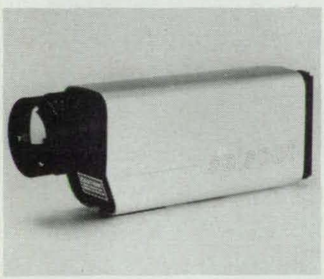

Selcom, Southfield, MI, has developed an optoelectronic **motion measurement camera** that withstands force accelerations and impact of more than 25 Gs with no effect on resolution. Designed for high-impact testing of automobiles, aircraft, spacecraft, and other vehicles, the Selspot High-Shock camera provides two- or three-dimensional real-time analysis up to 10,000 times a second within a 0.025% measuring range and with 0.1% accuracy. The camera comes fastened in a 1/3" thick aluminum case which is securely mounted on the moving object to prevent motion during impact.
Circle Reader Action Number 768.

DataCon Interconnect Sub-Systems, Horsham, PA, has introduced a 100 MHz monolithic **VME system** for military and commercial applications. The system consists of a one-piece monolithic backplane and low-profile daughter boards for use in standard 0.8" and high-density 0.6" spaced systems. The design accommodates such standard logic as TTL, CMOS, and ECL 10K and 100K.
Circle Reader Action Number 772.

Axum, a PC-based **technical graphics and data analysis package** from TriMetrix Inc., Seattle, WA, offers 2D technical plotting, 3D and contour plotting, and data analysis within a windowing and menuing environment. The software package features an extensive selection of 2D and 3D scientific graph types not available in business graphics packages. These include logarithmic axes, 3D mesh and line plots, and error bar plots. Advanced text features such as angling, subscripting, and scientific fonts are also available. Priced at $495, Axum requires an IBM PC, XT, AT, PS/2 or compatible with a hard disk, a computer graphics card, and DOS 2.0 or above.
Circle Reader Action Number 766.

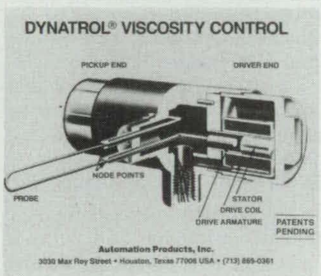

The Dynatrol® System from Automation Products Inc., Houston, TX is designed for continuous **measurement and/or control of viscosity** at process conditions. The detector is installed directly in process vessels or lines without the need for sampling or laboratory analysis. It responds to both Newtonian and non-Newtonian products, including coatings, paints, glues, oils, emulsions, polymers, and resins.
Circle Reader Action Number 774.

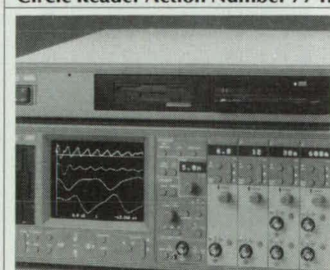

A new four-channel **digital oscilloscope** from Nicolet Instruments Inc., Madison WI, offers 8 bit speed in two channels and precise 10 MS/s, 12 bit resolution in the other two channels. The Nicolet 490 is equipped with FFT and features a dual timebase for observing both slow and fast events simultaneously. Options include a removable 44 megabyte hard disk for instant data recall and transfer.
Circle Reader Action Number 776.

Circle Reader Action No. 486

New Literature

The Evil Eye™, an eye-slaved **target acquisition system** which enables an operator to designate or control machine or cockpit functions simply by looking at the chosen target, is described in a brochure from Iscan Inc., Cambridge, MA. The system employs a video-based tracking technique to monitor the position of the subject's eye with respect to an imaging sensor. The sensor and associated optics can be mounted beneath a flight helmet visor, or embedded into a fixed sighting system. Applications include cockpit control, rapid weapons pointing, camera guidance, and human factors evaluation.

Circle Reader Action Number 708.

The High-Performance Amplifier Handbook, Volume IV, features a variety of **operational amplifiers**, including the first 1000 volt op amp, a 200 watt power op amp, and voltage/current boosters. Published by Apex Microtechnology Corp., the handbook contains application notes covering voltage-to-current conversion for grounded and ungrounded loads, as well as application tips for the Apex Power Booster series of amplifiers and WBO5 Wideband Current Buffer.

Circle Reader Action Number 712.

A four-page catalog from Itek Encoder, Newton, MA, provides complete listings, technical specifications, and resolutions/accuracies for Itek's DIGISEC® **rotary absolute and incremental encoders** in both solid shaft and thru-hole configurations. The catalog features sections on Itek's LSI MicroSeries® rotary absolute optical shaft angle encoders, which offer medium to high resolutions in solid shaft configurations, and the Series 40 Pancake encoders, which provide up to 17 bits resolution.

Circle Reader Action Number 704.

The Conductive Plastics Design Guide from Bekaert Corp., Marietta, GA, features a compilation of **conductive engineering plastics** used for electromagnetic interference (EMI) shielding and electrostatic discharge (ESD) protection of electronic circuitry. The publication lists suppliers for each product and includes performance data such as impact strength and shielding effectiveness.

Circle Reader Action Number 710.

A new catalog from Automation Gages, Rochester, NY, includes design features and technical details of 62 high-precision **ball and roller slides**. The catalog describes the company's patented preload adjusting wedge, which permits adjustment with a single screw. Also covered are AG positioning and measuring stages, accessories, and custom applications.

Circle Reader Action Number 778.

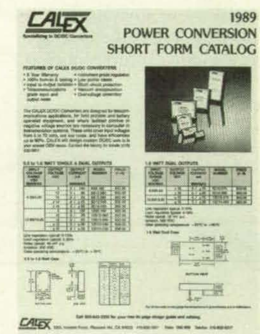

Calex Manufacturing Company Inc., Pleasant Hill, CA, is offering a free short-form catalog with electrical and mechanical specifications and case outline drawings for 116 **DC/DC converters** and 47 AC/DC encapsulated modular power supplies. The DC/DC converters cover input voltages from 5 to 72 volts, are low-noise, and have efficiencies up to 90%. They are designed for telecommunications applications, for field-portable and battery-operated equipment, and where isolated positive or negative voltage sources are needed in computer or instrumentation systems.

Circle Reader Action Number 706.

A free eight-page brochure from Technical Marketing Company, Inc., Eden Prairie, MN, describes **vacuum products** such as Krytox vacuum pump fluids and fluorinated greases, Kinney liquid ring and rotary vane pumps, Motorguard filtration systems, and Bransonic ultrasonic benchtop cleaners. The brochure also features HaloVac oils, which are widely used in plasma etching, LPCVD, and oxygen processes as a safeguard for personnel and equipment.

Circle Reader Action Number 714.

New Literature

The properties and applications of **ductile iron** are detailed in a new publication from QIT-Fer et Titane Inc., Montreal, Canada. Written for design engineers, the guide describes the three major types of ductile iron castings—ferritic, pearlitic, and pearlitic-ferritic—and highlights basic principles of ductile iron casting design such as designing for optimum economy, simplicity, and casting soundness.
Circle Reader Action Number 724.

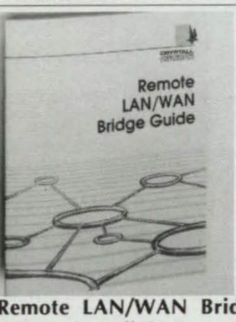

The Remote LAN/WAN Bridge Guide from Cryptall Communications Corp., Cranston, RI, describes ways to evaluate and improve Local Area Network (LAN) and Wide Area Network (WAN) performance. The guide explains when to use bridges versus routers, when and how filtering and routing algorithms affect performance, and how to select the best transmission media for a particular application.
Circle Reader Action Number 718.

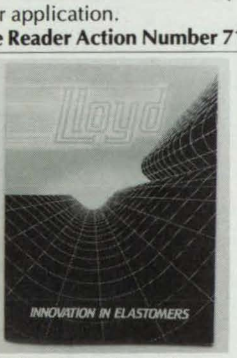

Lloyd Manufacturing, Warren, RI, has published a brochure on **industrial rubber sheeting** products for applications in the automotive, data entry, appliance, medical, and recreation fields. The brochure discusses Lloyd's custom sheeting services and describes special sheet configurations including fabric supported sheeting for increased tensile and dimensional stability.
Circle Reader Action Number 722.

The Derwent Guide to Patents describes the functions of patents, the patenting process, how to file a patent, and how to read a patent number. Available from Derwent Inc., McLean, VA, the guide features numerous real-world examples that illustrate the importance of patents.
Circle Reader Action Number 726.

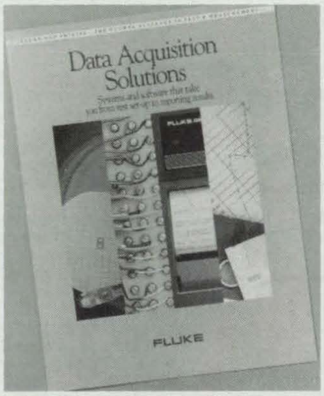

John Fluke Mfg. Co. is offering a full-color brochure on its complete line of **data acquisition equipment**, including PC-based data acquisition software, data acquisition front ends, stand-alone data loggers, and multipoint hybrid recorders. Available free of charge, the brochure highlights the new 2286A data logger, which offers a built-in MS-DOS compatible micro-floppy drive and expandability to 1500 channels, as well as the Helios Plus data acquisition front end, which features high measurement accuracy, noise rejection, and resolution.
Circle Reader Action Number 716.

A new line of miniature shell and tube **heat exchangers** is spotlighted in a free brochure from Exergy Inc., Hanson, MA. Designed for applications with fluid flow rates from <1 to 15 GPM, the stainless steel heat exchangers can withstand pressures up to 1200 psi. The brochure includes complete specifications and operating limitations.
Circle Reader Action Number 720.

Subject Index


DALLAS CONVENTION CENTER

MARKETPLACE

To Advertise—Call (212) 490-3999

Advertiser's Index

***RAC** stands for **Reader Action Card.** For further information on these advertisers, please circle the RAC number on the Reader Action Card elsewhere in this issue. This index has been compiled as a service to our readers and advertisers. Every precaution is taken to ensure its accuracy, but the publisher assumes no liability for errors or omissions.

NASA Tech Briefs, ISSN 0145-319X, USPS 750-070, copyright © 1990 in U.S., is published monthly by Associated Business Publications Co., Ltd. 41 E. 42nd St., New York, NY 10017-5391. The copyrighted information does not include the individual Tech Briefs which are supplied by NASA. Editorial, sales, production and circulation offices at 41 E. 42nd Street, New York, NY 10017-5391. Subscriptions for non-qualified subscribers in the U.S., Panama Canal Zone, and Puerto Rico, $75.00 for 1 year; $125.00 for 2 years; $200 for 3 years. Single copies $10.00. Remit by check, draft, postal or express orders. Other remittances at sender's risk. Address all communications for subscriptions or circulation to NASA Tech Briefs, 41 E. 42nd Street, New York, NY 10017-5391. Second-class postage paid at New York, NY and additional mailing offices.

POSTMASTER: please send address changes to NASA Tech Briefs, 41 E. 42nd Street, Suite 921, New York, NY 10017-5391.


esa
NASA
2
NASA